OPTIMIZATION AND IMPLEMENTATION OF MAINTENANCE SCHEDULES OF POWER SYSTEMS

BY

YANG FAN

(B. ENG.)

A THESIS SUBMITTED

IN PARTIAL FULFILLMENT OF THE REQUIRMENT

FOR THE DEGREE OF DOCTOR OF PHYLOSOPHY

DEPARTMENT OF ELECTRICAL & COMPUTER ENGINEERING

NATIONAL UNIVERSITY OF SINGAPORE

2011

ACKNOWLEDGEMENT

I would like to express my gratitude to A/P C.S. Chang as my PhD supervisor for his great enthusiasm, valuable discussions, and precious guidance throughout the course of this research work; which have fundamentally changed the way I think about and approach my research.

Great thanks are also expressed to Lab Officer, Mr. H.C, Seow, colleagues Dr. Z.X. Wang and Mr. C.M. Kwan, and all the other colleagues, who have helped me during the course of my PhD.

And finally, I am grateful to my parents and all my friends for their encouragement and moral support during the course of the study. Special thanks to Mr. Y. Liu for his unconditional love and support. Perhaps no one knows this difficulty more than him.

TABLE OF CONTENT

ABSTRACT

The growing economic pressure and complexity of power systems has necessitated the development of intelligent tools to seek a cost-effective maintenance strategy to keep substations operating both reliably and economically. This thesis investigates the application of multi-objective evolutionary algorithms and fuzzy logic techniques for optimization and implementation of preventive maintenance scheduling. The overall objective is the development of an adaptive condition-based maintenance scheme to achieve a balance between the reliability benefits and costs of preventive maintenance in the presence of uncertainty and constraints.

Preventive maintenance is performed to extend component lifetime in power systems, and at the same time, the maintenance cost is one of the main expenditure items. In order to evaluate and optimize preventive maintenance schedules, a two-level model for establishing a quantitative relationship between maintenance and reliability at the component level and overall system level has been developed. The strength of this reliability model lies in its ability to easily incorporate various failure modes, protection actions, and constraints in complex system.

Based on prediction of reliability, Pareto-optimal maintenance schedules are obtained using multi-objective evolutionary algorithms. This powerful technique identifies the existence of several objectives, operational cost, expected energy not served, and failure cost, all of which are mutually exclusive. A holistic view of relationship between the conflicting objectives of substations has been provided by Pareto front, and the most compromised schedule for achieving certain requirements has been identified for the decision maker. In cooperation with the two-level reliability model, an integrated maintenance optimizer suitable for substations and their connected power grid has been developed. It has been tested on different basic substation configurations and medium-size power system (Roy Billinton Reliability Test System and IEEE Reliability Test System) and impressive results were obtained.

Implementation of maintenance schedules according to actual operational variations and uncertainties is crucial for offshore substation because it is often remotely located and the information collected during implementation can rarely avoid uncertainties. Updating the reliability indices of key elements in offshore substations requires re-establish the Pareto-optimal maintenance schedules. A hierarchical fuzzy logic has been developed for effectively handling the operational variations and uncertainties. This approach avoids complex inference process, and it significantly reduces the computational complexity and rule base than conventional Type-1 fuzzy logic.

The adaptive condition-based maintenance scheme described in this thesis provides an explicit framework for analyzing system reliability and costs under different maintenance strategies, and produces the optimal maintenance schedules for power systems. Simulation carried on an offshore substation shows that this approach is effective in re-establishing the optimal maintenance schedules in presence of continually updated operational variations during implementation.

LIST OF RELEVANT PUBLICATIONS

Journal Papers:

[1] C.S. Chang, Z.X. Wang, F. Yang, and W.W. Tan, "Hierarchical Fuzzy Logic Systems for Implementing Maintenance Schedules of Offshore Power Systems", *IEEE Transactions on Smart Grid*. (provisionally accepted)

[2] F. Yang and C.S. Chang, "Multi-objective Evolutionary Optimization of Maintenance Schedules and Extents for Composite Power Systems", *IEEE Transactions on Power Systems*, v 24, n 4, Nov. 2009, p 1694-1702.

[3] F. Yang and C.S. Chang, "Optimisation of Maintenance Schedules and Extents for Composite Power Systems using Multi-objective Evolutionary Algorithm", *IET Generation, Transmission & Distribution,* v 3, n 10, Oct. 2009, p 930-940.

[4] F. Yang, C.M. Kwan and C.S. Chang, "Multi-objective Evolutionary Optimization of Substation Maintenance using Decision-varying Markov Model", *IEEE Transactions on Power Systems,* v 23, n 3, Aug 2008, p 1328-1335.

[5] C.S. Chang and F. Yang, "Evolutionary Multi-objective Optimization of Substation Maintenance using Markov Model", *Engineering Intelligent Systems for Electrical Engineering and Communications,* v 15, n 2, June 2007, p 75-81.

[6] C.M. Kwan, F. Yang, and C. S. Chang, "A Differential Evolution Variant of NSGA II for Real World Multiobjective Optimization", *Progress in Artificial*

Life, Lecture Notes in Artificial Intelligence, Springer-Verlag, Berlin, Germany, 2007.

Conference Papers:

[7] H. Bai, F. Yang, X. German, C.S. Chang#, S.K. Panda and W.W. Tan, “Stability Analysis of Adjustable-speed Induction-motor Drive using Genetic Algorithm”, *Advances in Power System Control, Operation and Management*, Hong Kong, China, 8-11 Nov., 2009.

[8] D. Wu, C.S. Chang#, F. Yang, and H. Bai, “Performance Improvement of V/f Induction-motor Control in the Low-frequency Range”, *Advances in Power System Control, Operation and Management*, Hong Kong, China, 8-11 Nov., 2009.

[9] Z.X. Wang, F. Yang, W.W. Tan and C.S. Chang, "Intelligent Maintenance Advisor for Marine Power System using Type-2 Fuzzy Logic for Handling Condition Updates and Operation Uncertainties", *5th International Conference on Engine and Condition Monitoring* (Invited paper), ONE°15 Marina Club, Singapore, 9-10 Oct., 2008.

[10] C.S. Chang, F. Yang, Z.X. WANG and W.W. Tan, "Intelligent Maintenance Advisor for Offshore Power System using Type-2 Fuzzy Logic with Learning Ability" (Presentation), *Universitas 21 Conference on Energy Technologies and Policy*, University of Birmingham, U.K., 8-10 Sep., 2008.

[11] F. Yang, and C.S. Chang, "Multi-objective Evolutionary Optimisation of Maintenance Time and Extents for Composite Power Systems using Reliability

Equivalents" (Poster), *Universitas 21 Conference on Energy Technologies and Policy*, University of Birmingham, U.K., 8-10 Sep., 2008.

[12] C.M. Kwan, F. Yang, and C. S. Chang, “A Differential Evolution Variant of NSGA II for Real World Multiobjective Optimization”, *Proceedings of the Third Australian Conference, ACAL 2007*, Gold Coast, Australia, 4-6 Dec. 2007.

[13] C.S. Chang and F. Yang, “Evolutionary Multi-objective Optimization of Substation Maintenance using Markov Model”, *14th International Conference on Intelligent System Applications to Power Systems,* Kaohsiung, Taiwan, 4-8 Nov., 2007.

[14] C.S. Chang and F. Yang, “Evolutionary Multi-objective optimization of Inspection Frequencies for Substation Condition-based Maintenance”, *11th Naval Platform Technology Seminar 2007*, Singapore, 16-17 May 2007.

LIST OF FIGURES

LIST OF TABLES

LIST OF SYMBOLS AND ABBREVIATIONS

TLOC	Total loss of continuity
PLOC	Partial loss of continuity
GA	Genetic algorithm
SA	Simulated annealing
MOEA	Multi-objective evolutionary algorithm
NSGA II	Elitist non-dominated sorting genetic algorithm
DE	Differential evolution
D_1	As-good-as-new state
$D_2,\ldots,D_N$	Deterioration level
M1	No maintenance
M2	Minor maintenance
M3	Major maintenance
P_{ik}	Probability of performing M_k in state i
P_{ikj}	Probability of transiting from state i to j due to Mk
$\lambda_{i,i+1}$	Transition rate from state i to i+1 (/year)
$\mu_{i,j}$	Restoration rate from state i to j (/year)
MTTR	Mean time to repair (year)
MTTF	Mean time to failure (year)
A_a	Availability of component a
$EC_{m,a}$	Expected maintenance cost of component a (US$)
$EC_{r,a}$	Expected repair cost of component a (US$)

$I_{i,a}$	Inspection frequency in state i for component a (/year)
$C_{ins,a}$	Inspection cost for component a (US$)
$C_{mk,a}$	Average maintenance cost for maintenance activity Mk (US$)
$p_{i,a}$	Probability of state i for component a
$C_{r,a}$	Average repair cost for component a (US$)
$CapC$	Capital cost (US$)
λ_a	Failure rate of component a (/year)
μ_a	Repair rate of component a (/year)
A_s	System availability
Du_p	Yearly loss of expectation (hour)
EENS	Expected energy not served (MWh/year)
EOC	Expected operating cost (US$/year)
L_p	Loss of load of load point p (MW)
m	Number of load points in one substation
$f_{m,k}$	Frequency of minor maintenance (/decision interval)
$f_{M,k}$	Frequency of major maintenance (/decision interval)
$p^t_{i,i+1}$	Transition probability from state i to i+1 in time interval t
$C_{o,a}$	Operating cost of component a (US$)
$C_{min,a}$	Cost of minor maintenance for component a (US$)
$C_{maj,a}$	Cost of major maintenance for component a (US$)
M	Number of component

A_p	Availability of load point p
RBTS	Roy Billinton Test System
IEEE RTS	IEEE Reliability Test System
$P_j(t)$	Probability in state j at time t
P_f	Failure probability
C_{sysO}	Overall operational cost (US$)
C_{sysF}	Expected failure cost (US$)
U_p	Average annual disconnection duration of load point p (hours/year)
$E_{total,i}$	Energy loss due to total loss of continuity in substation i (MWh/year)
$E_{partial,i}$	Energy loss due to partial loss of continuity in substation i (MWh/year)
T1	Transformer 1
CB1	Circuit breaker 1

CHAPTER 1 INTRODUCTION

Maintenance scheduling is essential for operating power systems both reliably and economically. The first chapter introduces the background of this research, including different maintenance types, the approaches to optimize and implement the maintenance schedules. A systematic and integrated approach is outlined to find the optimal maintenance schedule which obtains a tradeoff between the reliability benefits and costs of maintenance in power systems.

1.1. Overview of maintenance management

Maintenance plays an important role in keeping reliability levels in power systems, and at the same time, the maintenance cost is one of the main expenditure items for power utilities. The amount of money spent on maintenance can reach 15-70% of overall cost [1, 2]. The need to satisfy the reliability requirement while at the same time to minimize the costs has led to the development of cost-effective maintenance management for power systems. The main task of cost-effective maintenance management includes optimization and implementation of maintenance schedules.

The primary goal of maintenance is to avoid or mitigate the consequences of failure of the component. Maintenance can be firstly categorized into two types: corrective maintenance and preventive maintenance [3]. *Corrective maintenance* is conducted after the failure occurs to restore the component by repairing it. Corrective maintenance is the strategy which first appeared in the industry [4]. However, this type of maintenance often causes serious damage to related equipment and personnel. Therefore, high competition among utilities encourages more effective maintenance, known as preventive maintenance, to be applied. *Preventive maintenance* is conducted before the failure occurs, aiming to extend the life of component by maintaining the component in satisfactory condition. In accordance with statistical analysis of electric equipment, the preventive maintenance is scheduled periodically to avoid possible failures. However, the periodic preventive maintenance cannot satisfy the requirement of the electric power systems. In the 1970s, condition-based maintenance was proposed to maintain the correct equipment at proper time, and it has been greatly applied in recent years, especially in electric power industry. Therefore, two divisions of preventive maintenance are further developed based on the techniques: *time-based maintenance* and *condition-based maintenance*. Nowadays condition-based maintenance has largely replaced time-based maintenance because it is essential to avoid the negative effects of failure by detecting the condition of system for performing preventive maintenance. In the literatures, predictive maintenance often refers to the same maintenance strategy with condition-based maintenance [5]. In the condition-based maintenance, diagnostic inspection is often used to assess the extent of deterioration of individual components and therefore determine the need and extent for its subsequent maintenance [6]. According to the efforts and effects of the maintenance activities, the preventive maintenance can be divided into two categories: *minor maintenance* and *major maintenance*. Minor preventive maintenance was proposed to reduce the deterioration with limited effort and effects [7]. In contrast, major maintenance eliminates the accumulated deterioration [8] but with sharply increased maintenance cost.

Frequent inspections usually give rise to high chances of detecting deterioration but at the expense of significant increase in the inspection and subsequent maintenance costs [9]. Furthermore, less or excessive maintenance could lead to deterioration rather than improvement. As stated in [5], almost one third of all the maintenance costs is wasted due to unnecessary or improper maintenance policies. Therefore, cost-effective strategies should be worked out to strike a balance between these two extremes to optimize both the costs and benefits of maintenance. Additionally, most substations are equipped with various components which are connected in various configurations. The configuration- and cost-dependency of the maintenance strategies for each component make the optimization of maintenance polices more complicated. The problem of optimizing the maintenance has been widely approached in the literature [10-17].

It is inadequate to perform the maintenance activities which are scheduled in the beginning of long term maintenance horizon, because the operational conditions of the components could vary from time to time due to many operational variations. Consequently, the deterioration process of the components varies, and makes the maintenance policy no longer optimal. The operational variations include continuing ageing, set-point, weather and load factors, uncertainties of measurement and human-judgment, and so on. In particular, the offshore power systems are often remotely located and their access for data acquisition, inspection and maintenance may be extremely difficult, especially during adverse weather conditions. The information collected can hardly avoid uncertainties. Therefore, powerful tools are needed to handle the operational variations and uncertainties in the modeling of deterioration process and adjust the maintenance schedules according to the operational variations realistically [4, 12, 13, 18].

Faced with the increasing complexity of power systems over the past years, the optimization and implementation of preventive maintenance schedules are becoming complicated. This problem usually involves multiple objectives, various substation configurations, multiple constraints, and real-time condition monitoring. Currently, *artificial intelligence* techniques are incorporated to overcome such difficulties. This work focuses on the application of multi-objective evolutionary algorithms and fuzzy logic system for the optimization and implementation of maintenance schedules. The following sections first review some of the important works in related area, and then outline the main objectives and overall approach for this research.

1.2. Literature review

1.2.1. Maintenance models

In order to relate spending on maintenance to reliability benefits, abstract models rather than analogous description need to be created. Various maintenance models were reviewed [14] for different maintenance strategies of systems. In order to represent the stochastic deterioration of component, probabilistic models are usually adopted in the prediction of component reliability and the evaluation of maintenance policies. Also, these models can be used to evaluate the costs and benefits of maintenance strategies either directly (analytical method) or by numerical experiments (simulation method). A comparative study of these two fundamental methods is discussed later in this section and summarized in Table 1.1. A conclusion is presented at the end of this section, constituting the methods adopted in this work.

Table 1.1 Comparison of Analytical Method and Simulation Method

	Analytical method	Simulation method
Computation time required	Short	Long [17]
Results	Same model producing the same results	Random results highly depending on repeated times
	Probabilistic value of reliability indices	Probability distribution of reliability indices

1.2.1.1. Individual component

The name Markov model is derived from one of the assumptions which allows this model to be analyzed, namely the Markov property. It makes it very easy to represent the multiple deterioration levels of individual component with finite number of states. The changes of state are called transitions, which follow the corresponding transition matrix of Markov process [19]. Condition monitoring technology enables it to collect the data which carries the performance signs of component. The experts then interpret the data to understand the deterioration level of component, such as motors [20], circuit breakers [12], and transformers [18, 21, 22].

In addition to the deterioration states, the inspection and maintenance activities can also be represented by Markovian states, and the transition between states follows the matrix of Markov model, where the rates can be estimated based on historical data [8, 9, 15, 16, 23-25]. The reliability indices of individual component can be calculated following standard methods [19].

Markov chain model is very useful to establish a quantitative connection between reliability and costs of maintenance [7, 9, 15, 16, 24-26]. A Markov model of transformers [9] and circuit-breaker [25] relating inspection frequencies with reliability and cost was established. The multi-unit maintenance problem cannot be reduced to single-unit maintenance problem, except if all units are independent of one another. Therefore, impacts of topological interdependency of multiple components cannot be optimized by considering individual components alone, but by the substation as a whole. Markov model can also be used for a multi-unit system by representing every combination of failures in a system. However, one of the shortcomings of Markov model is that the number of states grows in an exponential manner as the problem size increases.

1.2.1.2. Overall system

The configuration, protection schemes, and operating procedures of a power system directly affect the reliability of the power supply to the load points. There are several recognized reliability methodologies for evaluating the reliability of overall power systems [27]. *Network reduction method* creates an equivalent system by gradually combining the components to be connected in series or parallel [19]. One reason for the popularity of network reduction technique is its simplicity and the similarity between the network modeling and the configuration of power system. However, the network reduction method cannot be applied to the system containing meshed network, and it is not able to identify the components critical to the reliability of the system due to over simplification of this method. The *Zone Branch Model* [28-31] is then proposed to represent the actual circuit in terms of protective zones and accounts for the open- and short-circuit failure modes of protective devices. In this methodology, a zone is defined as a part of a power system in which a failure at any location within this zone will cause the upstream protective device to isolate the faulted component. The *total loss of continuity* (TLOC), which arises from all failures or a combination of failures within a substation, can be evaluated using the Zone Branch Model. Unfortunately, the methods are not able to assess the failure and violation of transfer limit between substations, leading to a *partial loss of continuity* (PLOC).

Two methods, *Monte-carlo simulation method* and *minimum cut set method* are able to overcome the shortcomings of the methods above. Monte-Carlo-based methodologies have been proposed to simulate behaviors of multiple components for evaluating the chronological performance of system [17, 32, 33]. However, it is pointed out in [17] that it is impractical to run the Monte-carlo simulation with accurate statistics for each feasible maintenance strategy when there is a great number of potential alternatives. Minimum cut set method is believed to be particularly well suited to the reliability analysis of power systems[27, 34]. This method is systematic and hence easily implementable on a computer. By definition, a minimal cut set is a unique and necessary combination of component failures which cause system failure. From a reliability point of view, all the component failures in a minimum cut set can be viewed as connected in parallel, while all the minimum cut set associated with one event can be viewed as connected in series. Therefore, a system can be converted into a reliability block diagram based on its minimum cut sets and then be evaluated easily following the rules used for the simple configurations (series or parallel).

1.2.2. Optimization techniques of maintenance schedules

In power-system studies, maintenance scheduling often involves multiple objectives. Life-cycle cost and reliability are the two major objectives each with several attributes:

- Life-cycle cost—inspection and maintenance costs, failure cost;
- Reliability—interruption cost of load point, expected loss of energy due to TLOC and PLOC.

With the reliability models for individual component and overall system, the reliability benefits and costs of maintenance can be expressed in the form of quantitative performance criteria. However, they are incommensurable, and it is impossible to establish a strict hierarchical order of the goals. Therefore, it is necessary to determine acceptable tradeoffs between those objectives. Various traditional methods, such as integer programming [35, 36], dynamic programming [37, 38], and heuristic techniques [39, 40], have been reported in the literature pertaining to the optimization of maintenance scheduling problem. Unfortunately, these techniques require specific domain knowledge, and some solutions could be stuck in local optima. Furthermore, the computational time increases exponentially with system complexity.

Several approaches using evolutionary computation were proposed to eliminate the shortcomings with traditional methods [41]. Evolutionary algorithms (EAs) utilize the principle of natural selection, and are readily used for searching in high-dimension space [42, 43]. They are relatively independent of problem formulation, making them easily applicable to a wide-range of problems without modeling every constraint and relationship in mathematical equations, or designing the objective functions in certain required form. EAs are increasingly applied to optimal scheduling of preventive maintenance [44] for both generation and transmission. Meta-heuristic-based optimization techniques like GA, TS and SA are known for their ability of solving real world problems, and are shown to be able to produce near-optimal solutions within reasonable timing. A hybrid approach of GA and simulated annealing (SA) has been used to optimize maintenance schedules of generators [45, 46]. However, all these works were formulated as single-objective problem. For solving multi-objective problems, many approaches optimize only one objective, while treating the other objectives as constraints. Other approaches linearly convert all participating objectives into a single objective as a weighted sum. One such work applies a mix of tabu search, GA and SA for optimal maintenance scheduling of thermal units [47], linearly combining all participating objectives into a weighted sum as an equivalent single objective. The weighted-sum method has the advantage of flexibility by simply varying the weights. Unfortunately, the approach requires multiple runs for all combinations of weights, whose choices are often subjective.

Through several stages of development, multi-objective evolutionary algorithms (MOEAs) have overcome the major shortcoming of multiple running of optimization process N times in order to obtain N Pareto-optimal solutions. Pareto-based Multi-objective Evolutionary Algorithm was shown to be advantageous over the aggregation-based approach in maintenance scheduling of aircraft engines [48]. Pareto Fronts give equal treatment to all objectives, which reach optima where none of the objectives can be further improved without degrading the others. More details about the Pareto optimality are given in Chapter 2. Difficulties of traditional methods, such as non-continuous objective functions and large scale search space, can also be eased with this approach.

Typically, operators like mutation, crossover and selection improve the quality of solutions in consecutive generations. Many different variants of evolutionary algorithms are being reported to solve multi-objective problems. Among them, Multi-objective Genetic Algorithm based on [49, 50], Non-dominated Sorting Genetic Algorithm (NSGA) [51], and Elitist Non-dominated Sorting Genetic Algorithm (NSGA II) [52] have reported to attain better spread of solutions and convergence near the true Pareto front with favourable comparisons over other well-known MOEAs, like strength Pareto evolutionary algorithm 2 (SPEA 2) [53] and others [54].

1.2.3. Implementation of maintenance schedules

The overall reliability performance of a system depends on the effectiveness of implementing a preventive maintenance schedule. However, a desirable reliability level cannot be achieved due to factors outside the engineer’s control, such as adverse weather, varying load demand, available maintenance resources, and so on. Several studies have examined the topic of reliability assessment using historical data as a basis to calculate the expected reliability of distribution system [55-57]. This method has the drawback that the historical data may not be accurate due to changes of conditions or lack of upgrading of database [58]. In power-system applications, operational uncertainties and variations occur continually, which can degrade the reliability and cost-effective maintenance scheduling of power systems. Such degradations can be more pronounced for off-shore power systems. Hence more powerful tools are needed to take into account those uncertainties in the reliability evaluation of offshore power substations.

Fuzzy sets theory was proposed by Zadeh [59] to resemble human reasoning under uncertainties by using levels of possibility in a number of categories. The application of fuzzy logic systems is simple to design, and can be easily understood and implemented. Known as type-1 fuzzy logic, the methodology has been successfully used in many applications, especially in power systems [60-63]. It is the most promising theory for efficiently incorporating the uncertainties and unpredictable information associated with the reliability data. Fuzzy set theory has been used to analyze the impact of uncertainties on adequacy assessment of a composite power system, and its feasibility has been demonstrated in [64]. Fuzzy sets theory has also been applied to evaluate the reliability of substations [65] and distribution systems [62, 66]. Besides, it is an effective tool in transformer asset management, identifying its criticality rank, rate of ageing, and remnant life [18, 67]. Consistent estimate of reliability measures has been carried out using type-1 fuzzy logic to handle uncertainties related to the component state probabilities [58] and transition rates [68] in power systems.

The ability of Type-1 fuzzy logic to model uncertainties is restricted due to absence of fuzziness in type-1 membership functions. Zadeh further proposed the alternative type-2 fuzzy logic [69], demonstrating greater success than type-1 fuzzy sets in various fields to handle uncertainties [60, 69-72]. However, type-2 implementation for large-scale problems can be limited due to its heavy computational requirements.

Viewed as one of the type-2 fuzzy sets, the qualitative fuzzy sets theory is proposed in [73] by tolerating a “small amount” of perturbations on each degree of membership functions. In contrast, non-stationary fuzzy sets are proposed in [74] by introducing perturbations to the parameters defining each membership function such as location, width, noises and others, without changing the inference process of the type-1 fuzzy logic. This method greatly reduces the computational complexity compared to type-2 fuzzy logic for solving the same the problem. Such perturbations may also be introduced in a hierarchical fuzzy system, which employs a set of high- or supervisory-level fuzzy rules for adjusting the settings of variables or input scaling factors of low-level rules as in a conventional fuzzy controller for tracking set-point changes and load disturbance [75].

1.3. Research objectives

Although work has been reported for evaluating reliability and optimizing the maintenance schedules of industrial systems, little effective work has been found in the area of power systems on improvement of overall system reliability by evaluating and optimizing the maintenance schedules of each individual unit. Only the threshold of preventive maintenance has been determined for multiple components in a system

[17]. Software commonly used for industry, such as ETAP [76] and PSCAD [77], only assesses the system reliability/stability without consideration of maintenance. Furthermore, the maintenance activities of the power substations are usually performed over the whole maintenance horizon once they are scheduled, which ignores the dynamic impact of operational variations and uncertainties on the reliability.

This thesis therefore aims to develop an integrated approach to optimize the condition-based maintenance schedules and dynamically update the schedule according to the operational variations for power systems. This objective can be achieved by three steps: a) first establish the quantitative relationship among multiple conflicting objectives of maintenance scheduling, b) find the best tradeoff among the multiple objectives, and c) dynamically re-establish the optimal solutions after evaluating the impacts of actual operational conditions on system reliability. The overall structure of this research is illustrated in Fig. 1.1, consisting of two functional blocks: maintenance optimizer for accomplishing the first two tasks and intelligent maintenance advisor for the third task by coordinating with the optimizer.

The specific aims of this thesis are:

1) to develop a two-level reliability model which is able to assess the reliability benefits and costs of various maintenance activities on individual component as well as overall system. The model of component-specific level would be able to predict the stochastic deterioration process of individual component under various inspection frequencies and subsequent maintenance schedules

and extents. The model of system-specific level would allow assessing the collective effects arising from all connected components in substations and composite power systems considering various failure modes, constraints, and structural and failure dependence.

2) to propose a multi-objective optimization method which is able to find the optimal maintenance schedules for a trade off between the reliability and costs of maintenance. This maintenance optimizer would optimize (i) the inspection frequencies of substations, (ii) maintenance schedules and extents of substations, and (iii) maintenance schedules and extents of medium-size power systems based on respective reliability model. The computational complexity increased with the size of system would be handled efficiently.

3) to develop a hierarchical fuzzy logic to estimate the changes of reliability parameters of key components in offshore substations due to the planned and unplanned operational variations during operation. Its two-level structure would provide greater flexibility and relieve the computational burden in dealing with additional uncertainties.

4) to design an integrated adaptive condition-based scheme, enabling it to re-establish optimal maintenance schedules dynamically according to the actual operational variations and uncertainties occurring continually in the offshore substation connected to a medium-size power grid. The maintenance advisor residing in each offshore substation should be linked to the maintenance optimizer of its connected power grid so that it is able to send the updated

reliability parameters to the maintenance optimizer. The optimizer either adopts the present maintenance schedule or adjusts the schedule on a day-to-day basis according to actual operational conditions for meeting the desired reliability at lowest possible cost.

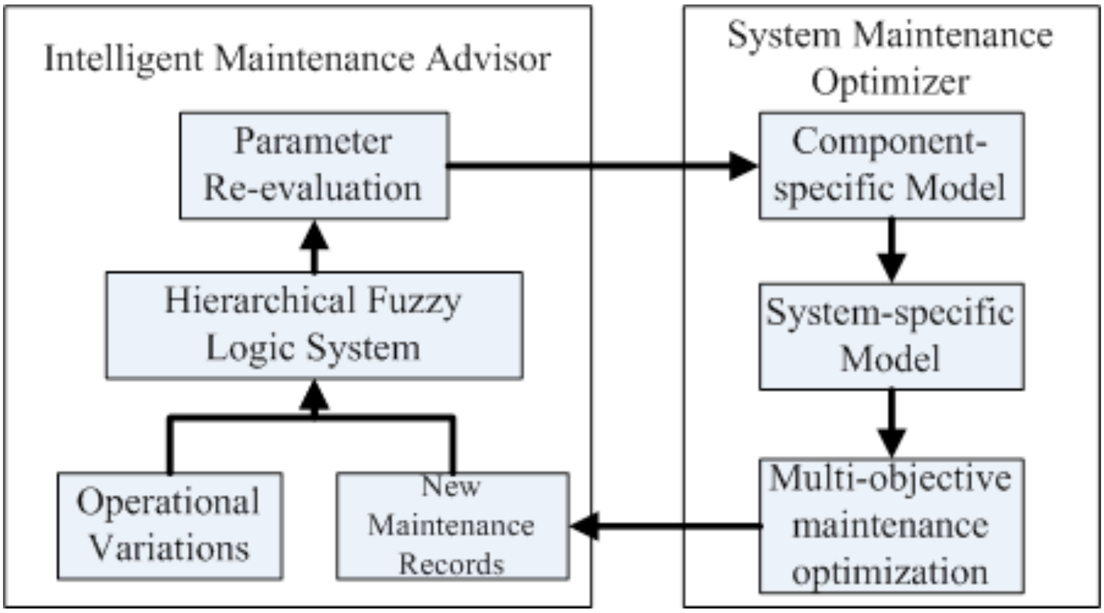

Fig. 1.1 Adaptive Maintenance Scheme for Optimization and Implementation of Maintenance Schedules

This proposed approach should contribute to a better optimization and implementation of preventive maintenance schedules for power systems.

This study is restricted to the development of probabilistic approach producing the average reliability gains and costs brought by the maintenance of electrical components over the investigated period. The chorological behaviors of the components are beyond the scope of this study. The investigation of other operating strategies for improving the reliability, such as load forecasting, load shedding, load transferring, or unit commitment, are interesting topics, but not the focus of this study either.

1.4. Thesis organization

The structure of this thesis follows the same order as the proposed approach being developed and furnished. The overall thesis can be broken into seven chapters, which are briefly described as below:

Chapter 1 introduces different maintenance strategies for asset management of industrial system, and identifies the necessity to optimize the condition-based maintenance of power systems. Previous work relevant to this thesis is reviewed. An overview of the proposed approach and the main objectives of this work are also presented.

Chapter 2 introduces the fundamentals pertaining to the adopted multi-objective evolutionary algorithms in this research work.

Chapter 3 presents a multi-objective approach to find a balance between the two objectives (reliability and operating cost) of substations by optimizing the inspection frequencies required for each component. This includes how to relate the impact of inspection frequencies with the deterioration process of individual component as well as the overall reliability of different basic substation configurations. The procedure to apply the Pareto-based multi-objective evolutionary algorithms with dynamic sharing distance method is descried in detail, and the set of Pareto-optimal inspection frequencies are obtained.

The assumption in Chapter 3 that all extents of maintenance activities will be performed probabilistically after each inspection will lead to excessive or insufficient maintenance policies. Therefore Chapter 4 optimizes the frequency of different maintenance extents (minor maintenance and major maintenance) of various substation configurations as an extension to the work in Chapter 3. Furthermore, models for more accurate prediction of system reliability are set up, which can analyze more complex substation configurations and incorporate various failure modes as well as protection and switching actions.

Chapter 5 further extends the approach for applying it to composite power systems. The previous approach evaluates only the total loss of continuity (TLOC), which arises from all failures or a combination of failures within a substation. Realizing that it is crucial in composite reliability analysis to include the power flow constraints, this approach is extended by including the failure and violation of transfer limit of all substation interconnections, which leads to a "partial loss of continuity" (PLOC). Another difficulty with the implementation of multi-objective evolutionary algorithms proposed in Chapters 3 & 4 is that the number of elements in each chromosome tends to increase in an exponential manner with the size of the system. Thus, a novel representation method of solutions is proposed and compared with previous method in Chapters 3 & 4. Optimization results of medium-size power systems are presented.

Chapter 6 addresses the issues involved in implementing maintenance schedules for offshore substations. This includes the planned and unplanned operational variations that affect the reliability, how to model them with great flexibility, and how to estimate the changes of reliability parameters accordingly with efficiency. Simulation results of the adaptive condition-based maintenance scheme on an offshore substation are presented.

Chapter 7 presents conclusions and recommendation for future research in the areas of optimization and implementation of maintenance schedules of power systems. Some limitations of the proposed approach are discussed.

Appendix A presents the background materials on Fuzzy Logic System. Appendices B, C, and D provide the data of studied substations, RBTS, and IEEE RTS.

CHAPTER 2 MULTI-OBJECTIVE OPTIMIZATION TECHNIQUES

Genetic algorithms (GAs) were developed by Holland in the early 1970s based on the principles of natural selection and genetics [78]. GAs use multiple solutions, known as population, and probabilistic rules to generate better solutions, which is more efficient in finding the optimal solutions [42]. In addition, GAs use information on the objective function itself rather than other information such as the function's gradients, which greatly simplifies the optimization problems in the mathematical aspect.

As reviewed in Section 1.2.2, since the early 1990's, GAs have been widely used in the problems of maintenance scheduling optimization. Optimization of maintenance scheduling is a combinatorial problem which often involves multiple contradictory objectives. Pareto-based multi-objective evolutionary algorithms are useful tools for the ability in trading off between multiple contradictory objectives. This chapter introduces the fundamentals pertaining to adopted multi-objective evolutionary algorithms in this research work.

Some material in this chapter has also appeared in [2-6, 10-14] of the candidate's publications.

2.1. Operations of genetic algorithms

GAs work with a population of candidate solutions, rather than a single solution. Each solution is characterized by a chromosome representing each individual. A population of individuals undergoes a sequence of transformation by means of genetic operators (selection, crossover, and mutation) to form a new population. Individuals less fit on the given problem are discarded, while more fit ones are copied and used to produce variants of themselves. As a result, the population will improve over time and produce optimal solutions. Typically, a GA consists of the following steps:

1) Initialization – An initial population is generated.
2) Evaluation of fitness value– The fitness value for each individual in the population is calculated according to its fitness function.
3) Selection – More highly fit individuals receive higher number of copies in the “mating” pool.
4) Crossover and mutation – They are applied in the “mating” pool to form a new population.
5) Repeat steps 2-4 until some conditions are met.

2.2. Pareto-optimal set

A multi-objective optimization problem can be stated as follows:

$$\begin{aligned}&\textit{Minimize}\ F(x) = (f_1(x), f_2(x), \cdots, f_M(x))^T \\ &\text{subject to } x \in \Omega\end{aligned} \tag{2.1}$$

where Ω is the decision variable space, and M is the number of objectives.

Since most objectives contradict with each other, there is no point in Ω that minimizes all the objectives simultaneously. One has to balance them. Therefore, unlike the single-objective optimization problems, multi-objective optimization problems output a group of non-dominated solutions known as Pareto-optimal set of solutions. The corresponding values in the objective space line themselves up in a Pareto front.

To illustrate the Pareto-optimality concept, let us consider N candidate solutions belonging to the set Ω, i.e. $X_1, X_2, X_3 \ldots X_N \in \Omega$. As can be seen in Fig. 2.1, X_2 is said to be dominated by (or inferior to) X_3 if $f_i(X_2)$ is partially more than $f_i(X_3)$, i.e. $f_i(X_2) \geq f_i(X_3)$ for $\forall i = 1, 2, 3, \ldots, M$ and for $\exists i = 1, 2, 3, \ldots, M$ with $f_i(X_2) > f_i(X_3)$. X_1 is said to be Pareto-optimal (or non-dominated), if there do not exist in the set $X \in \Omega$ such that X_i dominates X_1. In other word, any improvement in a Pareto optimal point in one objective must lead to deterioration in at least one other objective.

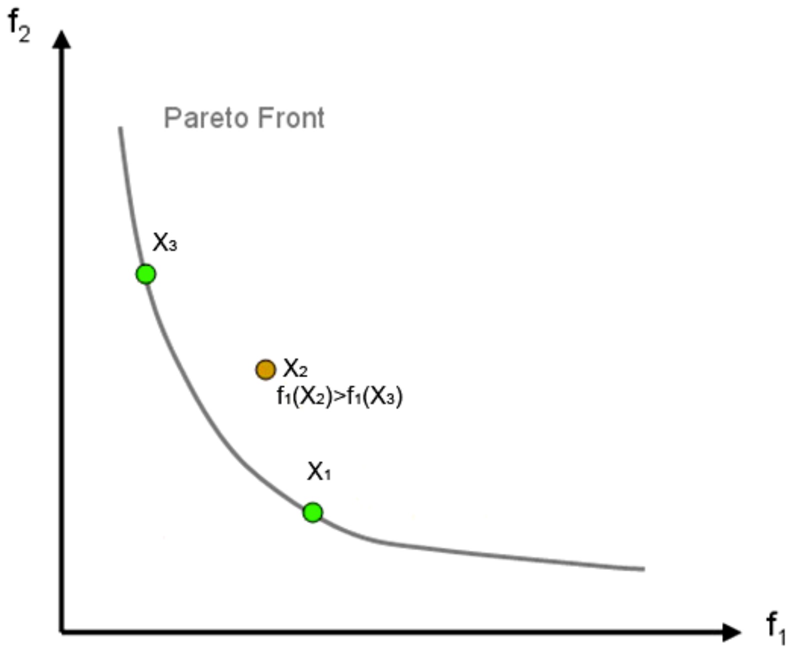

Fig. 2.1 Pareto Front

2.3. Selection of most compromised solution

It is subjective and imprecise to solely depend on the decision maker's judgment to select one solution from the set of Pareto-optimal solutions. On the other hand, the decision maker may not be interested in having a large number of Pareto optimal solutions to deal with due to the overflow of information. Therefore, a real-life multi-objective optimization problem prefers to get good representatives of the entire Pareto optimal set. It is necessary to introduce the membership function μ^k to evaluate the solutions in the Pareto-optimal set [79]. The best compromise solution is the one with the maximum μ^k . The steps for calculating μ^k are given as follows:

First, the ith objective function of a solution is presented by a membership function as μ_i :

$$\mu_i = \begin{cases} 1, & F_i \le F_i^{\min} \\ \dfrac{F_i^{\max} - F_i}{F_i^{\max} - F_i^{\min}}, & F_i^{\min} \le F_i \le_i^{\max} \\ 0, & F_i \ge F_i^{\max} \end{cases} \tag{2.2}$$

where F_i^{max} and F_i^{min}: the maximum and minimum values of the i^th objective function, respectively.

The normalized membership function for solution *k* is calculated by:

$$\mu^k = \frac{\sum_{i=1}^{M} \mu_i^k}{\sum_{j=1}^{N} \sum_{i=1}^{M} \mu_i^j} \tag{2.3}$$

where *N* is the number of non-dominated solutions.

2.4. Adopted multi-objective evolutionary algorithms

In this research work, MOEA with dynamic sharing distance, NSGA II and NSGA II-DE are used for finding the Pareto-optimal maintenance schedules of substations and power grid. As stated in Section 1.2.2, many different variants of evolutionary algorithms are reported to solve multi-objective problems [80]. A multi-objective evolutionary algorithm incorporating advanced features, like dynamic sharing distance, is reported to be effective in a benchmark optimization problem [49]. The main attraction of NSGA II is its fast non-dominated sorting algorithm that is more computationally efficient than most available non-dominated sorting techniques. A crowding distance assignment algorithm with a parameter-free niching operator for maintaining the diversity and spread of solutions adds to the attraction of this algorithm. NSGA II is currently one of the most successful MOEAs, which is reported to find better spread of solutions and convergence near the true Pareto front with favourable comparisons over other well-known MOEAs.

Within a few years, multi-objective DE-based techniques are reported in works like [81] and [82]. Notably, a similar attempt to replace the crossover and mutation rates by a rotationally invariant DE variant was reported in [83]. In this work, a variant of DE is proposed to replace the crossover and mutation operators of the original NSGA II algorithm, termed NSGAII-DE.

2.4.1. MOEA with dynamic sharing distance

2.4.1.1. Flow chart of MOEA

The main steps of MOEA are described as follows:

1) Set $g=0$ (the t^{th} iteration)
2) Randomly generate N solutions, variables of which are within the upper bound and lower bound. This is known as the parent population $P^{(g)}$.
3) Use crossover and mutation to generate an offspring population $Q^{(g)}$ of size N.
4) $R^{(g)} = P^{(g)} \cup Q^{(g)}$
5) Non-dominated sorting $R^{(g)}$
6) Until the next parent population $P^{(g+1)}$ is filled with N solutions from $R^{(g)}$ by perform *crowding distance estimation and comparison* F_i.
7) $g = g + 1$.

8) Loop back to (3) until terminating condition is achieved.

2.4.1.2. Non-dominated sorting scheme

In the absence of preference of objectives, ranking scheme based on the Pareto optimality is regarded as an appropriate approach to represent the strength of each individual [50]. In step (5), the non-dominated sorting scheme assigns the same smallest cost for all non-dominated individuals. The rank of an individual corresponds to the number of chromosomes in the current population by which it is dominated. Consider, for example, an individual x_i is dominated by n_i individuals in the current generations. Its current position in the population can be given as equation (2.4):

$$rank(x_i) = 1 + n_i \tag{2.4}$$

In order to find the solutions that belong to the first non-dominated front, each solution has to be compared with every other solution in that generation. After that, the solutions in the first non-dominated front will be discarded temporarily. The procedure above is repeated to find the solutions in the second and higher non-dominated front.

2.4.1.3. Dynamic computation of sharing distance

In order to obtain equally distributed solutions along the Pareto front, a sharing function is often used in evolutionary algorithms [42, 84, 85]. This method degrades an individual fitness upon the existence of other individuals in its neighborhood defined by the sharing distance σ_{share}. Unfortunately, σ_{share} needs to be estimated upon the usually unknown trade-off surface [84]. The performance of sharing function largely depends on the chosen σ_{share} value. Therefore, an approach of dynamic sharing distance computation is proposed [49]. It adaptively computes the sharing distance σ_{share} at generation g as half of the distance between each individual in the (M-1) hyper-volume in terms of the diameter $d^{(g)}$ and the population size θ by:

$$\sigma_{share}^{(g)} = \theta^{1/(1-M)} \times (d^{(g)}/2) \tag{2.5}$$

where $d^{(g)}$ is the diameter of (M-1) dimensional hyper-volume covered by the non-dominated solutions at generation t. It can be approximated by the average distance between the possible shortest and longest diameters $d_{\min}^{(g)}$ and $d_{\max}^{(g)}$ respectively, as shown in Fig. 2.2. F_a and F_b are the objective values of two individuals with maximum distance within each other. Then $d_{\max}^{(g)}$ can be approximated as $d_1^{(g)} + d_2^{(g)}$.

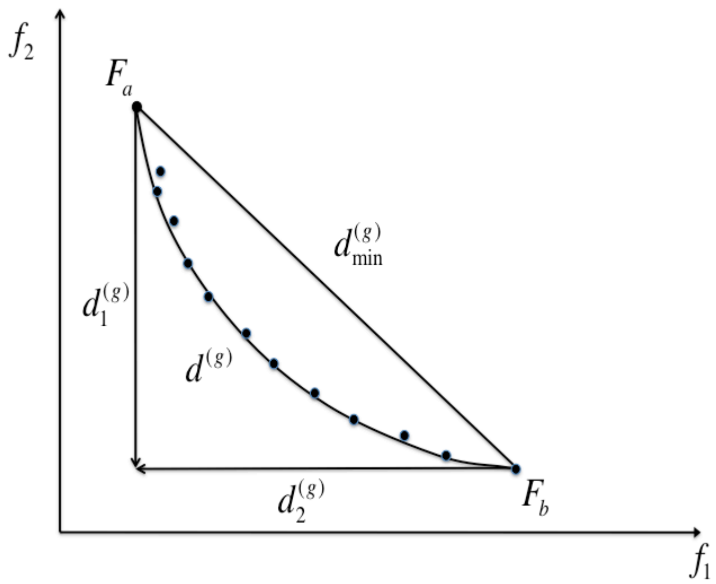

Fig. 2.2 The $d^{(g)}$ of a Trade-off Curve

Equation (2.5) provides a simple method to compute σ_{share} which is able to evenly distribute the population along the Pareto front without any a-priori knowledge of the trade-off curve. Furthermore, it is more effective than conventional sharing methods because σ_{share} is adaptively computed based on each generation instead of using a pre-assumed constant value.

2.4.2. Features of NSGA II

Compared with the flow chart of MOEA introduced above, NSGA II is mainly different in two steps, (5) and (6). The operations, fast non-dominated sorting and crowing distance estimation, to replace steps (5) and (6) will be further introduced in the following paragraphs.

2.4.2.1. Fast non-dominated sorting

A fast non-dominated approach is proposed for NSGA II, which reduces the computational complexity than the conventional non-dominated sorting algorithm [52]. In this approach, for each individual, besides the domination count n_i , another entity S_i, a set of solutions that x_i dominates, is calculated. All the individuals with $n_i = 0$ belong to the first non-dominated front. Then, for each individual with $n_i = 0$, each member x_j in the set S_i is visited and its domination count n_j is reduced by one. If $n_j - 1 = 0$, the solutions x_j belongs to the second non-dominated front. The procedure above will be repeated with each individual in the second non-dominated front, and the third non-dominated front can be identified. This process continues until all the fronts are identified.

2.4.2.2. Crowding distance estimation

In the NSGA II, a crowded distance estimation approach is used to replace the sharing function approach. After ranking all the individuals, crowding distance estimation is performed as follows:

1) Sort population according to each objective function value and normalize the objective function.

2) Assign an infinite distance value to the solutions with smallest and largest function values.

3) Calculate the crowding distance $i_{distance}$, which is defined as the distance of two individuals on either side of this individual along each of the objectives is calculated. As shown in Fig. 2.3, the crowding distance of the i^{th} solution in its front is the side length of the cuboid (dashed box).

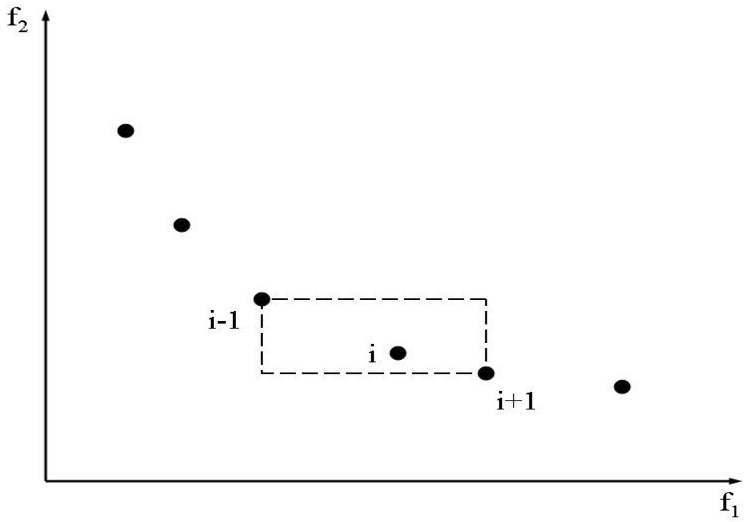

Fig. 2.3 Crowding-distance Calculation.
The points are solutions of the same non-dominated front

2.4.3. NSGA II-DE

The main idea of Differential Evolution (DE) is a scheme for generating the trial population member [86]. Basically, DE generates a new member by adding a weighted difference between two members to a third member. For a minimization problem, the newly generated member will replace the predetermined member in the next generation if the new one produces a lower objective value than the one with which it is compared.

The new population member $V_{i,G+1}$ is generated by:

$$V_{i,G+1} = \lambda X_{rBest,G} + F(X_{r2,G} - X_{r3,G}) \\ r2 \neq r3, \tag{2.6}$$

where $r2$ and $r3 \in [1, N]$ are randomly chosen solutions from the population of size N. In the single objective case, $X_{rBest,G}$ is merely the best solution for the G^{th} generation.

In the multi-objective case, however, the notion of 'best' is no longer a single optimum term, but can either be chosen from a set of non-dominated or Pareto-optimal solutions. The same operations of fast non-dominated sorting, crowding distance estimation and comparison as in NSGA II are conducted to identify the Pareto-optimal solutions. Including the term $X_{rBest,G}$ equation (2.6) in this work speeds up convergence by encouraging non-dominated solutions to be generated near the regions of $X_{rBest,G}$. The random nature of how $X_{rBest,G}$ is chosen and the diversity mechanism in the NSGA II ensures that solutions do not cluster around one region of the Pareto-front, which is undesirable.

The 'crossover' operation of DE generates a trial vector $U_{i,G+1}$ as presented in equation (2.7):

$$U_{j\,i,G+1} = \begin{cases} V_{ij,G+1}, \text{if } r(j) \le CR \text{ or } j = rn(i) \\ X_{j\,i,G}, \text{ if } r(j) > CR \text{ or } j \ne rn(i) \end{cases}, \tag{2.7}$$

where CR is the crossover rate. j denotes the j^{th} decision variable of the i^{th} candidate solution. $r(j)$ is a randomly chosen number in [0, 1]. Thus, if the randomly generated $r(j)$ of the j^{th} decision variable is smaller or equal to the crossover rate CR, $U_{ji,G+1}$ will take the value of the mutated vector $V_{ji,G+1}$, or else it will take the value of the original candidate solution $X_{ji,G}$. In addition, to prevent degeneration, the term $rn(i)$ is a randomly chosen decision variable j in the i^{th} candidate solution which will be chosen to be replaced by the mutant vector.

Unlike in the single objective problem, $U_{i,G+1}$ does not replace the current $X_{i,G}$ if it is better, but it is treated as a member of the child population candidate as provided in the NSGA II structure.

The above scheme has been modified and applied to two real world problems: (i.) a mass rapid transit scheduling problem and (ii.) the optimization of inspection frequencies for power substations in [6] of the candidate's publications. The case studies on optimization of maintenance extents for power substations are presented in Chapter 4.

2.5. Diversity preservation

The diversity of solutions obtained from MOEA with dynamic sharing distance, NSGA II, and NSGA II-DE is guaranteed by the selection process based on two attributes of every individual x_i in the population: 1) non-domination rank ($rank(x_i)$), and 2) shared cost or crowding distance $i_{distance}$. Between two solutions with different non-domination ranks, the one with lower rank is preferred. Otherwise, if both solutions have the same rank, the one with lower shared cost or located in a less crowded region is preferred.

2.6. Conclusion

This chapter presents the fundamental aspects of multi-objective evolutionary algorithms which are adopted in this work. The operations of standard genetic algorithms are introduced. Non-dominated sorting scheme, sharing distance calculation methods, Pareto-optimal set, and other fundamentals are presented.

Evolutionary algorithms application on case studies will be given in details in the following chapters.

CHAPTER 3 OPTIMIZATION OF INSPECTION FREQUENCIES FOR SUBSTATION

Improving the overall reliability and reducing the operating cost are the two most important but often conflicting objectives for substation. Condition-based substation maintenance provides a means of balancing these objectives. This chapter proposes a multi-objective approach to best compromise these two objectives for substations by optimizing the inspection frequencies required for each component. A Markov-chain model is developed to assess the impact of changing individual inspection frequencies on reliability and operating cost. A multi-component model is employed to evaluate the overall reliability of interconnected components. Pareto fronts are generated to optimize the trade-off between the two objectives for comparisons with other substation configurations. In this chapter, two typical different substation configurations are examined to demonstrate the effectiveness and potential of the proposed approach.

Some material in this chapter has also appeared in [14] of the candidate's publications.

3.1. Need for inspection optimization

Condition-based maintenance is gradually replacing time-based maintenance as a more effective approach to compromise the operating cost with reliability of substations. In recent years, many diagnostic techniques, such as transformer oil analysis and circuit breaker trip coil current signature, have been proposed to inspect conditions of the equipments and determine the need and extent for its subsequent maintenance [6]. Frequent inspections usually give rise to high chances of detecting deterioration but at the expense of high inspection and subsequent maintenance costs. Furthermore, a lack of proper maintenance or excessive maintenance after each inspection could result in failure rather than improvement. It is thus necessary to optimize the frequency of inspection as well as the extent of maintenance. In this chapter, only the inspection frequencies are optimized. Optimization of maintenance extents will be reported in the following Chapters 4, 5, and 6.

Fig. 3.1 demonstrates the proposed approach with three-block: component-specific level Markov model, system-specific reliability model, and a multi-objective evolutionary algorithm. A sound two-level reliability model addresses adequately the costs and benefits of inspection. On the device-specific level, only conditions of individual components are of interest. Therefore, the aim of this level is to obtain the reliability indices for each component, but the topological inter-dependence of components is not considered. The model in the system-specific level mainly focuses on the overall impact of individual components to the substation. Impacts due to changes of substation configuration and operation, as well as inspections on the overall reliability and cost are examined in an easy-to-use system reliability model. A brief description is given as follows:

- Using inspection frequencies as input, the Markov model will generate reliability indices for individual components,
- Using the system-configuration-related parameters and the load demand as inputs, the system reliability model will then generate the indices of the cost and availability at individual load points, and
- Outputs of the system reliability model are used to calculate the two objectives (expected energy not served & overall cost) to be evaluated by the optimization method, which will guide the search towards optimal inspection frequencies.

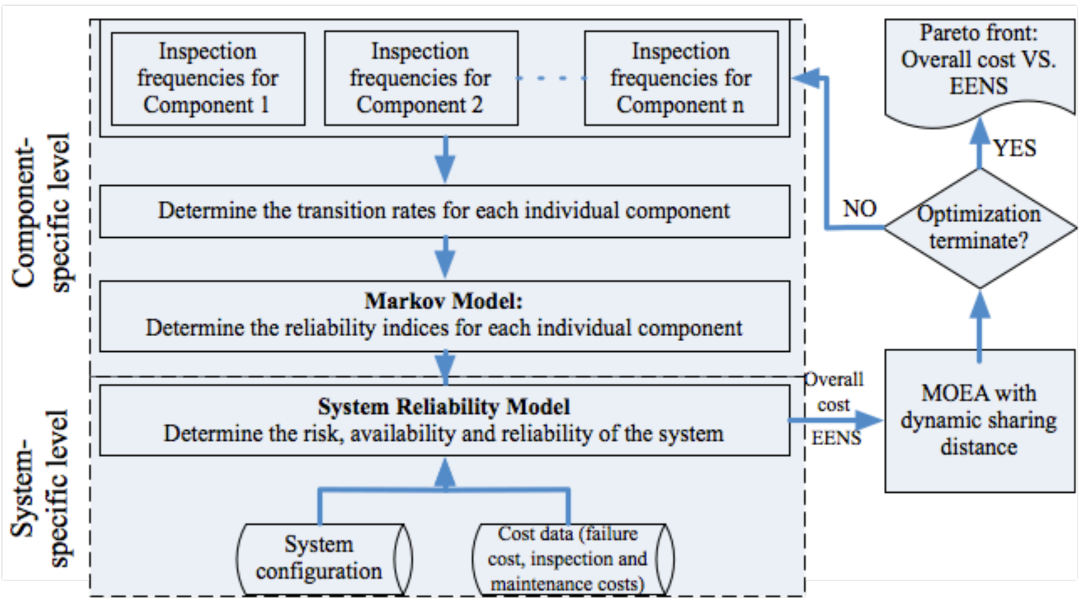

Fig. 3.1 Integrated Approach for Inspection Frequency Optimization

3.2. Modeling of inspection-dependent reliability of individual component

A Markov model is formulated to relate the deteriorations of each component with its inspection frequency. Each deterioration process of individual component is described in this work in a finite number of states. If such deterioration can be detected, preventive maintenance thus will be initiated to restore the respective condition back to a better state. Therefore, the inspection, which diagnoses the condition of the component, is important to trigger off such maintenance process.

The deterioration process of individual component is modeled by a multi-state Markov chain (Fig. 3.2), taking into consideration the effects of inspection and its subsequent probabilistic maintenance activities.

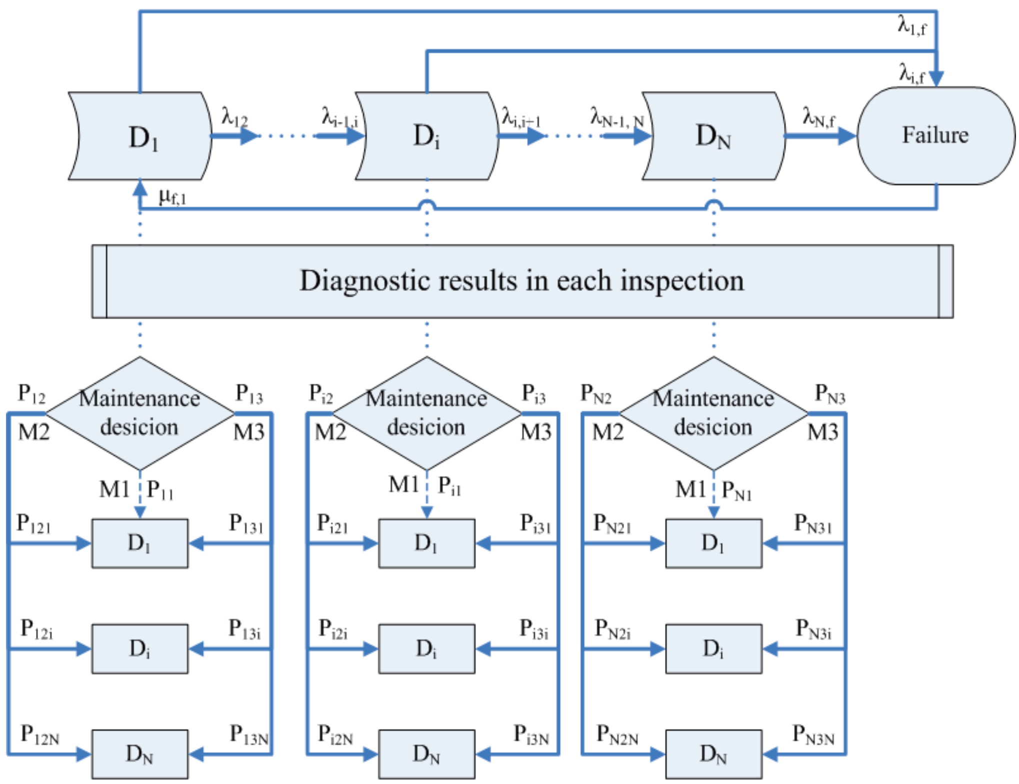

Fig. 3.2 Inspection-dependant Markov Model

A brief description of the states is given below:

- As-good-as-new state (D_1): In this state, the component operates well with no deterioration.
- Deterioration states (D_2, …, D_N): The deterioration level of these states from D_1 can be identified by maintenance crew through inspections.
- Maintenance (M1, M2, and M3): They represent the three extents of maintenance as determined by the inspection. M1 represents no maintenance action, and M2 and M3 are minor and major maintenance respectively.

Maintenance action Mk will be taken in state i with the probability P_{ik}. Consequently, this component transits from states i to j with the corresponding probability P_{ikj}. The probability P_{ik} is assigned corresponding to the component state. If the present state of a component is D_1, only M1 is chosen. On the other hand, if the component is in state D_2, three maintenance actions are available and are assigned with different probabilities. P_{22} for M2 will be higher than P_{23} for M3.

From the as-good-as-new state, the component progresses to a deteriorated state with the transition rate $\lambda_{i,i+1}$(occurrence/year), meaning that it takes $1/\lambda_{i,i+1}$ years in average to transit from state i to $i+1$. The duration in each deterioration state follows an exponential distribution with a constant rate $\lambda_{i,i+1}$. From the deteriorated state, this component can either continue to deteriorate with a transition rate $\lambda_{i+1,i+2}$, or go back to a better state with transition rate $\mu_{i,j}(i>j)$ because of an appropriate maintenance action. $\mu_{i,j}$ was influenced by the inspection frequency.

Specifically, $\mu_{i,j}$ will increase as inspection frequency increases, which means that the component can transit from a more deteriorated state to a better one within a shorter period. The restoration rate μ is assumed to be related with inspection and probabilistic maintenance by a known function (3.1). Based on historical operation data, parameter d in equation (3.1) is approximated to be equal to 2. Thus the restoration rate can be calculated by substituting 2 for d in equation (3.1) [87].

$$\mu_{i,j} = \frac{1 - \exp(-d \cdot I_i \times \sum_{k=1}^{3} P_{ik} P_{ikj})}{1 + \exp(-d \cdot I_i \times \sum_{k=1}^{3} P_{ik} P_{ikj})} \tag{3.1}$$

where I_i is the inspection frequency in state i.

For completeness, the model also incorporates random failures, where the system can transit directly from any present state to the failure state. However, inspection will not result in any warning before these failures occur, so this type of failure cannot be avoided by inspections. Transition rates $\lambda_{i,f}$ governing this type of failures can be estimated from historical data.

To investigate the impact of inspection frequency in every deterioration state, the quantitative relationship between inspection frequency and reliability is established. As usual, two of the most important reliability indices, mean time to repair (MTTR) and mean time to failure (MTTF), of individual component is used to indicate its reliability during the entire life-span [88] . The meaning of MTTF for repairable system are slightly different from that for non-repairable system. For a repairable system, MTTF can represent one of two things: (1) mean time to first failure (MTTFF), and (2) mean uptime (MUT) within a failure-repair cycle in a long run. Therefore, the term "MTTF" and "MTTFF" are interchangeable for repairable system. MTTF and MTTR of component n can be calculated by equations (3.2)-(3.5) [89]:

Truncated transitional matrix Q is constructed by deleting the 4th row and the 4th column of which are related to the absorbing states [90] from the transition matrix:

$$Q = \begin{bmatrix} 1-(\lambda_{12}+\lambda_{13}) & \lambda_{12} & \lambda_{13} \\ \mu_{21} & 1-(\mu_{21}+\lambda_{23}) & \lambda_{23} \\ \mu_{31} & \mu_{32} & 1-(\mu_{31}+\mu_{32}) \end{bmatrix} \quad (3.2)$$

$$N = [I - Q]^{-1} \quad (3.3)$$

Thus, the MTTF is the summation of the elements in the *1*st row of N, given the starting state i. MTTF and failure rate λ can be calculated as follows:

$$MTTF = \sum_{j=1}^{n} N_{1j} \quad (3.4)$$

$$\lambda = 1/MTTF \quad (3.5)$$

where n is the number of deteriorated states before failure, and N_{1j} the *jth* element in row *1* of matrix N.

MTTR can be calculated in the same way by treating the first state D_1 as the absorbing state when constructing the transitional matrix Q and N. The component availability (A_a) is given as the total operating time over the total time (equation (3.6)):

$$A_a = MTTF \,/\, (MTTF + MTTR) \tag{3.6}$$

The steady state probability (p_i) is the i^{th} element in vector P, which can be calculated by equation (3.7):

$$P = \begin{bmatrix} -(\lambda_{12}+\mu_{13}+\lambda_{1f}) & \mu_{21} & \mu_{31} & \mu_{f1} \\ \lambda_{12} & -(\mu_{21}+\lambda_{23}+\lambda_{2f}) & \mu_{32} & \mu_{f2} \\ \mu_{13} & \lambda_{23} & -(\mu_{31}+\mu_{32}+\mu_{3f}) & \mu_{f3} \\ 1 & 1 & 1 & 1 \end{bmatrix}^{-1} \begin{bmatrix} 0 \\ 0 \\ 0 \\ 1 \end{bmatrix} \tag{3.7}$$

For component a, the expected maintenance cost, $EC_{m\cdot a}$, and the expected repair cost, $EC_{r,a}$, are calculated by the equations (3.8) & (3.9) :

$$EC_{m,a} = \sum_{i=1}^{n} (I_{i,a} \times p_{i,a} \times C_{ins,a} + I_{i,a} \times p_{i,a} \times \sum_{k=1}^{3} p_{ik,a} \times C_{mk,a}) \tag{3.8}$$

where $I_{i,a}$ is the inspection frequency in state i for component a, $C_{ins,a}$ is the inspection cost for component a, $C_{mk,a}$ is the average maintenance cost for maintenance activity M_k. $p_{i,a}$ is the probability of state i for component a.

$$EC_{r,a} = C_{r,a} \times (1 - A_a) \tag{3.9}$$

where $C_{r,a}$ is the average failure cost for component a.

The more frequently the inspections are taken together with appropriate maintenance actions, the more reliable the system will be. But inevitably, it will lead to higher operating cost. The collective effects on substations with multiple components are somewhat more complicated. Therefore, optimization of inspection frequencies for substations must be extended from component level to system level. In such context, a system reliability model for a substation connected in series and parallel is used in addition to the Markov model.

3.3. Reliability assessment of substation configuration connected in series and parallel

The adopted system reliability model is developed for assessing the composite reliability of power generation and distribution based on the model proposed by the Petroleum and Chemical Industry Committee of the IEEE Industry Application Society [28-31] Calculations of reliability in this model are based on the *network reduction method*, which views substation configurations as being connected in series or parallel or a combination of both (Section 1.2.1). The procedure for evaluating the reliability of overall system in this model is shown in Fig. 3.3.

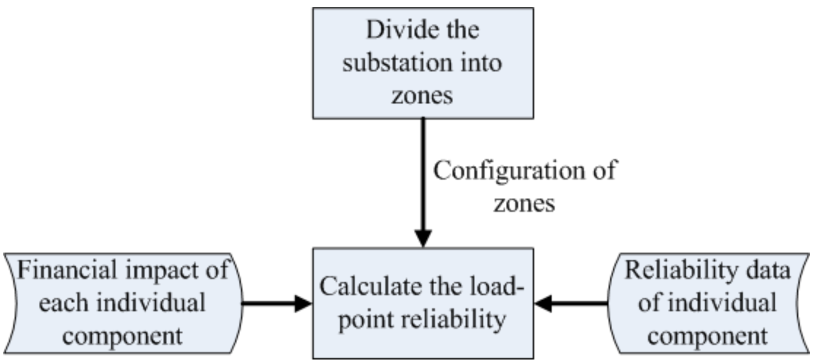

Fig. 3.3 Flow Chart for Evaluating System Reliability

As shown in Fig. 3.3, the substation is firstly divided into zones before evaluating the load-point reliability. In each zone, the failure at any point would bring about the same impact to the upstream protective device of this zone. Consequently, the protective devices will take action to isolate the system after a failure. Therefore, the failure rates of any location within this segment are always the same, and the upstream protective devices are used as the boundary between the zones [28].

Normally, we draw a circle around sections of the one-line diagram from the bottom (load side) of a protective device down to and including the bottom of the next downstream protective device. Fig. 3.4 [28] shows how zones are typically sketched onto the diagram of one substation.

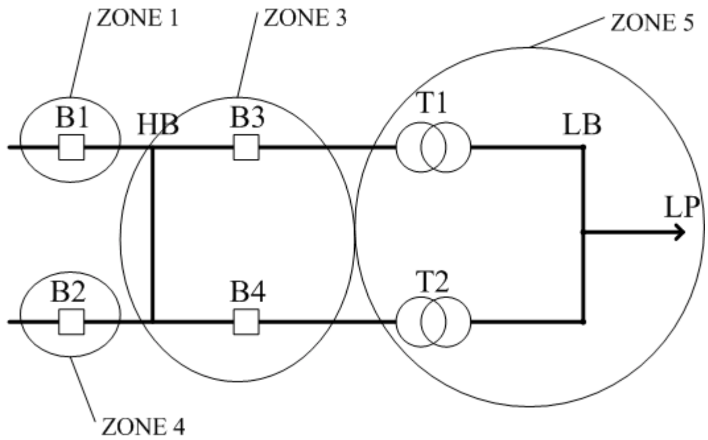

Fig. 3.4 Definition of Zones on One-line Diagram of Substation

The failure and repair rates of electrical component (λ_a and μ_a) which are reciprocals of the corresponding MTTF and MTTR are two of the most essential parameters for this model. As discussed earlier, using equations (3.4)-(3.6), the component reliability data are obtained. Once the zones are defined and the necessary parameters are available, the reliability of each zone as well as whole system is calculated relatively straightforward based on the network reduction method by equations (3.10) & (3.11) depending on the topological characteristics of each zone and whole system.

For the zone or system with components in series, the zone availability is obtained from equation (3.10).

$$A_s = \sum A_a \tag{3.10}$$

For the zone or system with redundant components, the system availability is given by equation (3.11).

$$A_s = 1 - \prod (1 - A_i) \tag{3.11}$$

Hence, the yearly loss of expectation at load point p can be calculated by equation (3.12):

$$Du_p = 8760 - 8760 \times A_p \tag{3.12}$$

3.4. Formulation of two conflicting objectives

The overall cost (containing the capital and operating costs) and the expected energy not served (EENS) are the two criteria to evaluate the performance of various configurations of substations under different inspection schemes. The operating cost is brought by inspection, maintenance, and repair actions. Normally, the best configuration is the one with minimum overall cost and maximum reliability. Therefore, we formulate the mathematic representations of the two objectives so that they can be optimized.

a) **Economic objective—overall cost.** The overall cost of a substation in this work consists of two parts, capital cost and expected operating cost (*EOC*).

The expected operating cost is the sum of expected inspection, maintenance, and repair costs of the components in this system, which is calculated by equation (3.13).

Therefore the expected overall cost (*EC*) in one substation can be easily calculated by equation (3.14):

$$EOC = \sum_{t=1}^{T} \sum_{a=1}^{M} (EC_{m,a} + EC_{r,a}) \qquad (3.13)$$

where *M* is the number of components in the system.

$$EC = EOC + CapC \times Rate \qquad (3.14)$$

where *CapC* is the capital cost, and *Rate* is the interest and depression rate.

2) Reliability objective—EENS. It measures the reliability worth associated with the cost of the customers due to the failure, which is expressed as:

$$EENS = \sum_{p=1}^{m} L_p \times Du_p \qquad (3.15)$$

where *m* is the number of load points in one substation, and L_p is the loss of load (MW) due to the failure at load point *p*.

Normally, the load demand usually varies with time at the same load point, and is not the same at different load points. In this work, the load demand is assumed to be constant over the maintenance period.

Basically, the increase of expected overall cost will improve the reliability in terms of decrease of EENS. To demonstrate the relationship between the two objectives explicitly, a substation is taken as an example (Fig. 3.5). The normalized values of

EENS and overall cost as functions of inspection frequency have been plotted in Fig. 3.6. The normalization of EENS can be done by equation (3.16), and the value of overall cost can be normalized in the same way.

$$Normalise(EENS) = \frac{EENS_{\max} - EENS}{EENS_{\max} - EENS_{\min}} \qquad (3.16)$$

$EENS_{max}$ and $EENS_{min}$ are the maximum and minimum values of EENS.

As seen in Fig. 3.6, as more inspections are carried out, the EENS will decrease, while the expected overall cost will increase. Since both of them are functions of the inspection frequency, they can be considered as two conflicting objectives. Thus, the multi-objective problem can be easily formulated as follows:

$$Minimize F(x) = (f_1(x), f_2(x)) \qquad (3.17)$$

where $f_1(x)$ is the economic objective—expected overall cost, $f_2(x)$ is the reliability objective—EENS, and x is the decision vector containing inspection frequencies.

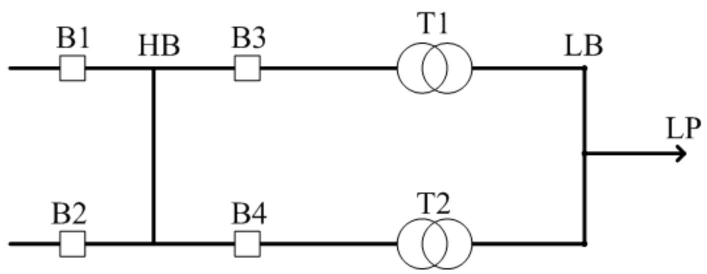

Fig. 3.5 Typical Substation Configuration

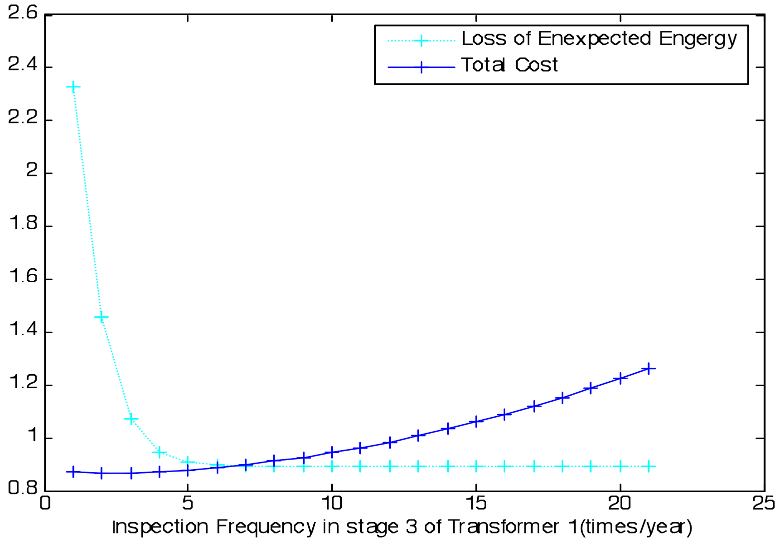

Fig. 3.6 EENS VS. Overall Cost with Varying Inspection Frequency (Normalized Value)

Fig. 3.6 is obtained only considering the inspection in the 3rd state of Transformer 1 (T1 in Fig. 3.5). In fact, if all the inspections are taken into account, it will definitely make the decision-making more complicated.

3.5. Implementation of MOEA with dynamic sharing distance

Unlike the conventional computation of sharing distance used in MOEAs, which requires *a-priori* knowledge of the usually unknown trade-off curve [91], an adaptive sharing algorithm based on current population is used. The procedure to apply MOEA with dynamic sharing distance for this problem is given in Fig. 3.7.

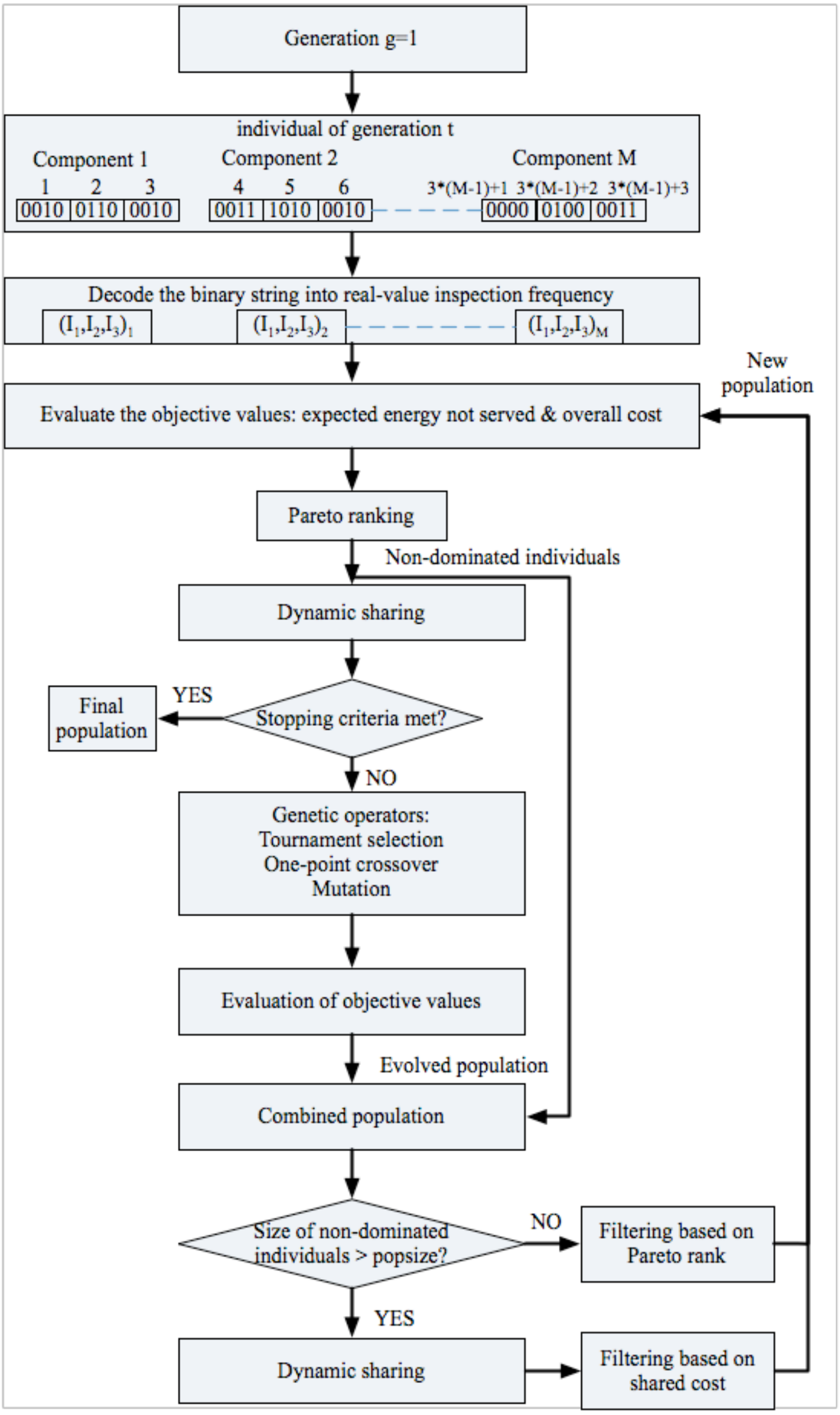

Fig. 3.7 Flowchart of Applying MOEA with Dynamic Sharing Distance

As shown in Fig. 3.7, an initial set of candidate solutions is generated randomly at the beginning. Each inspection frequency is represented by a binary string. The decoding then converts the binary alphabet into real-value inspection frequencies. High-fitness individuals, providing high reliability and low cost, stand a better chance of being selected as parents for the next generation. *Tournament selection* is employed in this work. Selection pressure is easily adjusted by changing the tournament size. If the tournament size is larger, weak individuals have a smaller chance to be selected. After selection, *1-point crossover* is used, and *mutation* is applied by preventing the chromosomes from becoming too similar to each other. These two random-based evolutionary operators evolve the populations towards optimality.

The results of MOEA toolbox developed by A/P Tan, K. C.[92] are used as a reference starting point to assess if other algorithms are able to produce a consistent and reliable Pareto-front across multiple runs. 'Trail and error' method is used to obtain the proper parameters of evolutionary algorithms. In the empirical studies in this thesis, the outcome of a run is not only viewed as a set of approximate non-dominated solutions, but more as the boundary which such solutions define in objective space. As long as that boundary provides decision maker a convenient means for comparing relative merits of substation configurations and for examining the effects of maintenance, the application of algorithms could be considered as being successfully applied. Those matrices to measure the divergence, convergence or other performance of algorithms are not within the scope of this work.

3.6. Case studies on typical substation configurations

3.6.1. Study parameters

Single-line diagrams of the two basic substation configurations analyzed here are shown in Fig. 3.8. Several assumptions are made before the simulation is conducted:

- Sub-transmission lines feeding the substations are completely reliable with availability of 100%.
- Only the transformers (T1 and T2) and circuit breakers (B1~B5) are modeled with the Markov-chain model and the system reliability model.

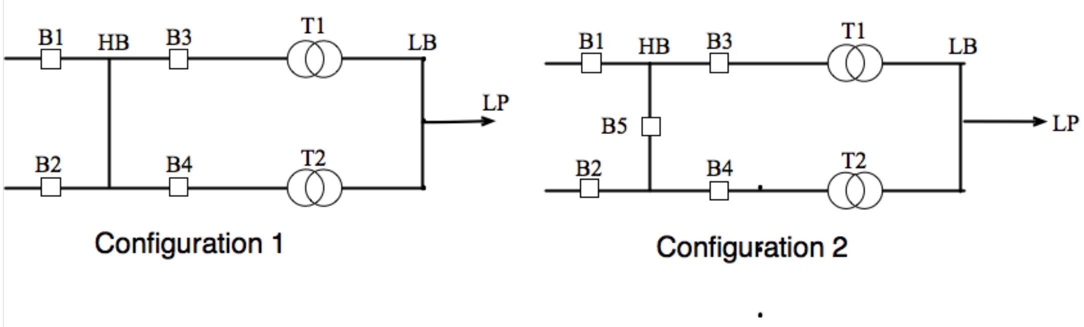

Fig. 3.8 Typical Substation Configurations

The number of breakers, transformers and other system equipment are used to calculate the capital cost based on typical data. The interest and depreciation rate is 12%. The main equipment used as well as their relative capital cost is listed in Table 3.1. Initial parameters used in the two reliability models are given in Tables 3.2 & 3.3, and the set of parameters for the optimization is given in Table 3.4.

Table 3.1 Equipment and Relative Cost for Substation Designs

Equipment Required	Cost, k$,	Number of components	
		Configuration 1	Configuration 2
Bus-50’	76.5	2	2
Main Breaker Section	33.8	2	2
MV Tie Breaker Section	42.0	0	1
MV Feeder Breaker Section	34.4	2	2
500mcm MV Cable-750’	41.3	2	2
Transformer	31.0	2	2

Table 3.2 Parameters of Transformers and Breakers for Markov-chain Model

Parameters / Components	λ_{12}	Λ_{23}	λ_{3f}	λ_{1f}	λ_{2f}	P_{11}	P_{12}
T1 ~ T2	1/5	1/3	1/2	1/30	1/15	0.80	0.15
B1 ~ B5	1/4	1/7	1/4	1/40	1/20	0.85	0.10
Parameters / Components	P_{13}	P_{21}	P_{22}	P_{23}	P_{31}	P_{32}	P_{33}
T1 ~ T2	0.05	0.10	0.80	0.10	0.05	0.15	0.80
B1 ~ B5	0.05	0.05	0.70	0.25	0.05	0.10	0.85
Parameters / Components	P_{111}	P_{112}	P_{113}	P_{121}	P_{122}	P_{123}	P_{131}
T1 ~ T2	1.00	0.00	0.00	0.99	0.01	0.00	0.97
B1 ~ B5	1.00	0.00	0.00	0.95	0.03	0.02	0.90
Parameters / Components	P_{132}	P_{133}	P_{211}	P_{212}	P_{213}	P_{221}	P_{222}
T1 ~ T2	0.02	0.01	0.00	1.00	0.00	0.25	0.65
B1 ~ B5	0.07	0.03	0.00	1.00	0.00	0.30	0.60
Parameters / Components	P_{223}	P_{231}	P_{232}	P_{233}	P_{311}	P_{312}	P_{313}
T1 ~ T2	0.10	0.50	0.45	0.05	0.00	0.00	1.00
B1 ~ B5	0.10	0.55	0.40	0.05	0.00	0.00	1.00
Parameters / Components	P_{321}	P_{322}	P_{323}	P_{331}	P_{332}	P_{333}	μ_f
T1 ~ T2	0.05	0.25	0.70	0.10	0.55	0.35	52
B1 ~ B8	0.05	0.35	0.60	0.10	0.65	0.25	122

Table 3.3 Cost-related Parameters ($\$\times10^3$)

Parameters / Components	B1~B4	B5	T1 ~ T2	LB	HB
CM_1 /inspection(k$)	0.1	0.1	0.2	---	---
CM_2 (k$)	0.5	0.5	1.0	---	---
CM_3 (k$)	2.0	2.0	4.0	---	---
Cr (k$)	5	5	8	10	20
MTTR(hours)	48	10	168	---	---

Table 3.4 Parameters for Optimization Method

	Configuration 1	Configuration 2
Population	100	110
Crossover rate	0.8	0.8
Mutation rate	0.01	0.01
Generation	50	70

3.6.2. Comparison of two substation configurations and discussions

The simulation is conducted on the two substations for assessing relative merits of the tie breaker in Configuration 2. As can be seen from the Pareto fronts in Fig. 3.9, EENS can be effectively reduced in Configurations 2 by the isolation of failure when a normally closed tie breaker was installed between two bus-bars, but inevitably the extra component would lead to more capital cost.

Fig. 3.9 also shows that Configuration 2 requires higher cost than Configuration 1. Therefore, Configuration 1 should be preferred if the budget is limited. Providing the same reliability, Configuration 2 costs more than Configuration 1 (points (2.1) to (2.2)). However, higher reliability can be guaranteed by Configurations 2 if given more cost (from points (2.2) to (2.3)).

An overall Pareto front is useful to guide a decision maker in selecting a substation configuration. This Pareto front should consist of the front of Configuration 2 from points (2.3) to (2.2), the front of Configuration 1 between points (1.2) and (1.1).

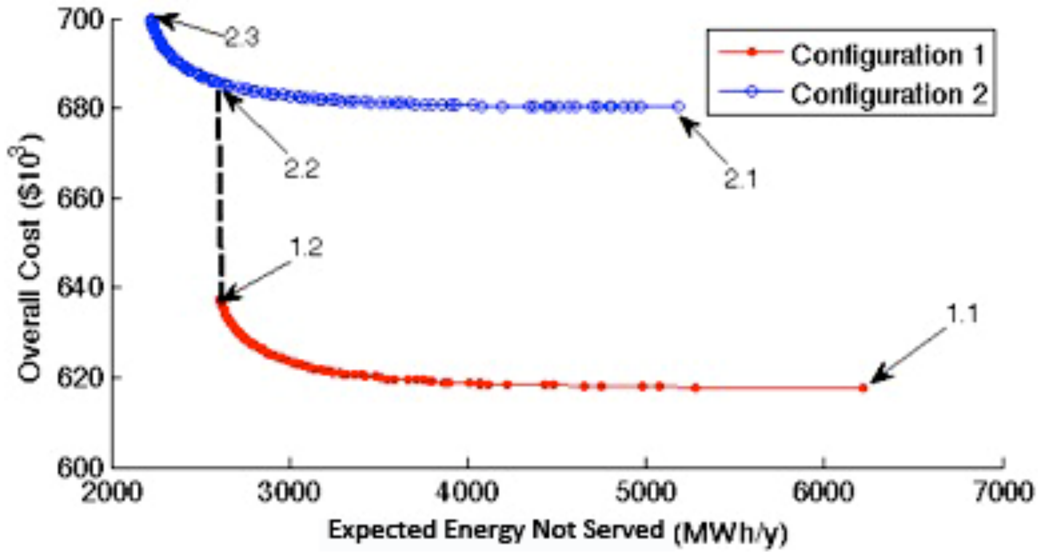

Fig. 3.9 Pareto Fronts of Overall Cost vs. EENS of Four Configurations.

3.7. Conclusion

The proposed methodology has been successfully applied to optimal inspection frequencies of a study substation, which is typically used for connecting a power source to load points. Both the objectives of overall cost and expected energy not served are optimized for the study configurations. Both objectives are seen sensitive to inspection frequencies. Pareto Fronts provide decision makers a convenient means for comparing relative merits of substation configurations leading to the optimal choice of inspection frequencies to fulfill different budgetary and reliability needs. Through case studies, the work has demonstrated the potential of the proposed approach for application to more complicated substations.

CHAPTER 4 OPTIMIZATION OF MAINTENANCE EXTENTS

In Chapter 3, a trade-off between the reliability and cost is found for the substations by optimizing the inspection frequency in each deterioration state of individual component. Besides, proper scheduling of preventive maintenance provides a more effective means to tradeoff between the two objectives. As an extension of the work in Chapter 3, this chapter optimizes the frequency of different maintenance extents (minor maintenance and major maintenance). A series of decision-varying Markov models relating the deterioration process with various maintenance actions are proposed to predict the reliability of individual component. Minimum Cut-sets Method is employed to evaluate the overall reliability of substation. A multi-objective evolutionary algorithm, NSGA II, is proposed to optimize the two objectives to provide Pareto-fronts or trade-off curves for a holistic view of the conflicting relationships between them.

Some material in this chapter has also appeared in [4-5,13] of the candidate's publications.

4.1. Need for optimizing maintenance extents

It is assumed in this research that each inspection is followed by no maintenance necessary, a minor or major maintenance. Minor preventive maintenance [7] aims to restore components to a healthier state with limited efforts and yield. On the other extreme, major maintenance restores components towards "as good as new" states but with sharply increased maintenance cost [8]. In Chapter 3, the effect of each inspection is a probabilistic combination of the effects after performing all the extents of maintenance actions (no maintenance, minor maintenance, and major maintenance). It assumes that all the extents of maintenance actions rather than one specific maintenance action are probabilistically performed. The probability of performing a maintenance action k when the component is in state i (P_{ik}), is previously assigned corresponding to the component state. More specifically, if the present state of a component is "as good as new"(state 1), the probability of performing no maintenance is 1 ($P_{11}=1, P_{12}=P_{13}=0$). On the other hand, if the component is in more deterioration state, like state 2, three maintenance actions are available and P_{22} for minor maintenance is assigned to be higher than P_{23} for major maintenance. However, this assumption is not practical, and therefore a cost-effective strategy should be worked out to strike a balance between the costs and benefits of different maintenance extents.

There is another reason which makes it inadequate to only optimize the inspection frequency discussed in Chapter 3. Take one optimal inspection frequency as an example. If this solution recommends inspection in the 2nd state every four month, the optimal reliability and cost can only be achieved when this component is still in state

2 four months later. Unfortunately, this is always not the case in reality because of the stochastic nature of the deterioration process. Therefore, it is expected that we can get higher reliability and lower cost if the next inspection/ maintenance action could be optimized dynamically according to the deterioration process after last inspection/maintenance.

In order to optimize the maintenance frequencies and extents according to component conditions, the models and techniques used in Chapter 3 have to be improved. The layout of model is shown in Fig. 4.1. Compared to Section 3.1, four improvements are made in this chapter:

- Variables to be optimized are the frequencies of maintenance activities to be taken on individual components during decision interval t ($f_{m,t}$, $f_{M,t}$). The entire scheduling horizon is first divided into T intervals and maintenance decision (no maintenance, minor maintenance or major maintenance) is made in each interval. The time length of each interval can be adjusted according to practical requirements or varying importance for each component.
- Multiple decision-dependent Markov models are used to evaluate the reliability of each component over the whole maintenance horizon in place of one Markov model in order to incorporate the impacts of different extents of maintenance. Each Markov model represents one decision interval.
- The minimum cut sets method has been used at the system-specific level for the assessment of the reliability of substations with more complex configurations and protective actions.

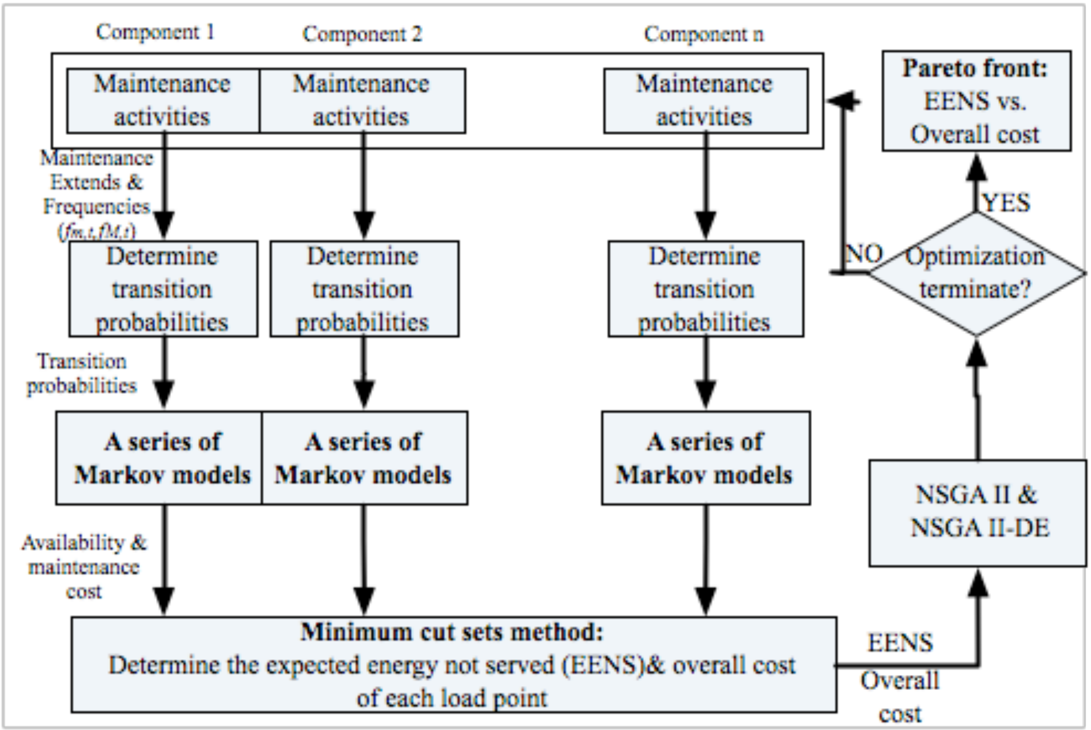

Fig. 4.1 Integrated Approach of Maintenance Optimization

4.2. Assessment of maintenance-dependent reliability of individual component

4.2.1. Homogeneous Markov model within one decision interval

The deterioration process and maintenance within one decision interval are modeled by a discrete time N-state Markov process [15] as in Fig. 4.2, where the definition of each state is the same as in Section 3.2. $f_{m,t}$ and $f_{M,t}$ represent the frequencies of minor and major maintenance activities during the decision interval t $(t \leq T)$. Markov chain [90] relates conditions of each component with different maintenance policies.

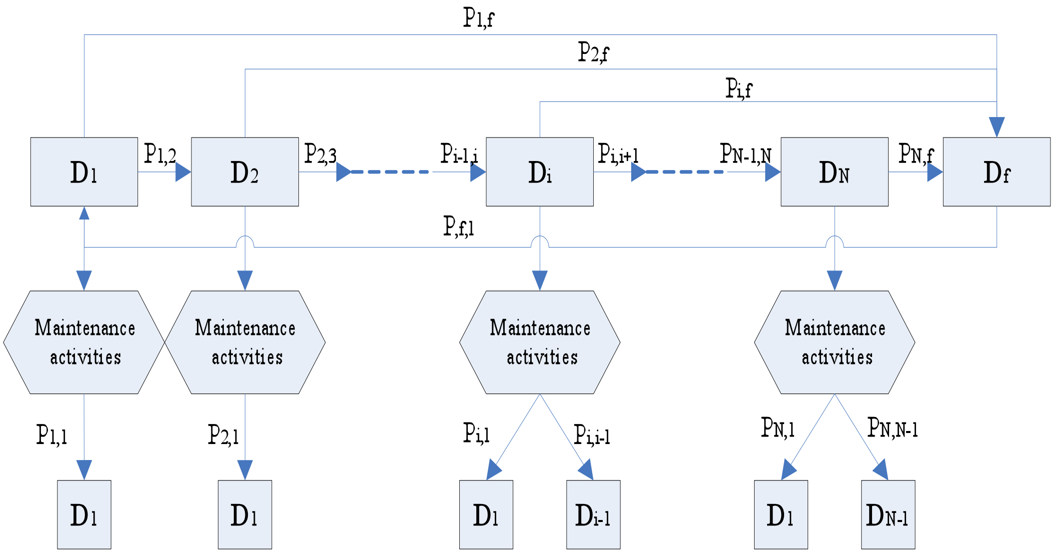

Fig. 4.2 Maintenance-dependent Markov Model

Transitions between states obey the transition matrix P of the Markov chain. Unlike the Markov model in Section 3.2, the element in matrix P is transition probabilities p_{ij}, which can be easily converted following the procedure given in equation (4.1).

$$p_{ij} = \lambda_{ij} \cdot \Delta t \tag{4.1}$$

where p_{ij} is the transition probability, and λ_{ij} is the transition rate from state i to j, Δt is the time interval.

As time progresses, the component undergoes a transition from state i $(i<N)$ to the next state $i+1(i+1\leq N)$ with a given probability $p_{i,i+1}$. From the deteriorated state $i+1$, this component can either continue to deteriorate with a transition probability $p_{i+1,i+2}(i+2\leq N)$, or be restored to a better state with probability $p_{i,j}$ $(i, j\leq N, i>j)$ by the appropriate maintenance. $p_{i,j}$ is updated according to the maintenance actions performed in the last interval. Generally, $p_{i,j}$ after a major maintenance increases more than after minor maintenance. Therefore, preventive maintenance is able to reduce or even eliminate accumulated deterioration by increasing the probability of transition to a better state. The method for updating $p_{i,j}$ will be presented in detail in Section 4.2.2. This model also incorporates the transition from any present state to a chance failure, the probability of which is governed by $p_{i,f}$.

4.2.2. Decision-dependent Markov models in different decision intervals

Homogeneous Markov chain is used within each decision interval. However, it will become more likely to make a transition from a deteriorated state to a better one when more frequent and more effective maintenance is performed. As a result, a new set of transition probabilities needs to be deduced as the model advances to the next interval.

The present and future transition matrices P_{t-1} and P_t are utilized in this model for decision intervals $t-1$ and t. The transition probability from a worse state to a better state is a function of maintenance activities. Here, the mathematical relationship between P^t and $(f_{m,t-1}, f_{M,t-1})$ can be estimated from existing maintenance and failure data. The rest of transition probabilities are related to each other by assuming that the ratio of the two present transition probabilities and the ratio of two future transition probabilities are equal [93]. It is a property of Markovian model that the future transition matrix largely depends on the present one. The assumption "the ratio of two future transition probabilities is equal to that of two present transition probabilities" is just one of feasible assumptions for this application. The parameters of Markov model are difficult to obtain, but the parameters can be easily elaborated further if given real-world long-term history data. In this work, this relationship can be elaborated by:

$$p_{i1,j1}^{t} / p_{i2,j2}^{t} = p_{i1,j1}^{t-1} / p_{i2,j2}^{t-1} \tag{4.2}$$

where $p_{i1,j1}^{t}$ and $p_{i2,j2}^{t}$ are the transition probabilities from states *i1* to *j1* and *i2* to *j2* respectively in interval *t*, and $p_{i1,j1}^{t-1}$ and $p_{i2,j2}^{t-1}$ are the transition probabilities from states *i1* to *j1* and *i2* to *j2* respectively in interval *t-1*.

Based on the updated probability, the transition probabilities in the future transition matrix are computed by equation (4.3) [94]:

$$P^{t}(f_{m,t-1}, f_{M,t-1}) = P^{t}(f_{m,t-1}, f_{M,t-1} \mid S_{t-1} = i) P(S_{t-1} = i) \tag{4.3}$$

where $P^{t}(f_{m,t-1}, f_{M,t-1} \mid S_{t-1} = i)$ is the conditional transition probability matrix, influenced by the maintenance actions taken in interval *t-1*, given the component is in the state *i*. $P(S_{t-1} = i)$ is the probability of being in the state *i* at the beginning of interval *t-1*.

Using this model, the deterioration level of the component in terms of state probabilities at the beginning of interval *t* can be inferred from past history, which involves all of the maintenance performed and previous deterioration process. Therefore, the probabilistic law of transitions can be influenced dynamically by making maintenance decisions. Fig. 4.3 illustrates a decision-varying Markov process. Each box contains a Markov model for one decision interval.

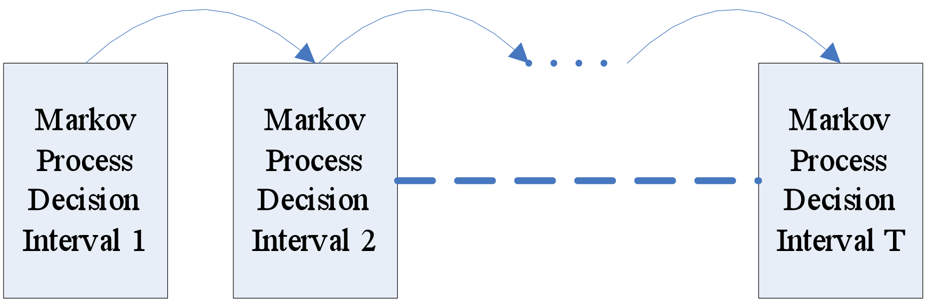

Fig. 4.3 Complete Maintenance Model

In decision interval *t*, availability is used to measure the reliability of a component. Availability is the sum of the probabilities of all working states. Therefore:

$$A_a = \sum_{i=1}^{N} P(S_t = i) \quad (4.4)$$

where $P(S_{t=i})$ is the probability of being in the state *i*.

For component *a*, the operational cost ($C_{o,a}$), including the inspection cost, maintenance cost, and expected failure cost, is calculated by:

$$C_{o,a} = T \times C_{ins,a} + \sum_{t=1}^{T} (C_{\min,a} \times T_{m,t} + C_{maj,a} \times T_{M,t} + C_{f,a} \times p_{f,t}) \quad (4.5)$$

where $C_{ins,a}$ is the cost of inspection of component *a*, $P_{f,t}$ is the probability of failure in interval *t*, $C_{f,a}$ is the cost of failure for component *a*, $C_{min,a}$ is the cost of minor maintenance for component *a*, and $C_{maj,a}$ is the cost of major maintenance for component *a*.

Reliability of component can generally be improved at expense of higher cost with more frequent maintenance. Reliability of each substation is related to its configuration in a unique way, which requires careful evaluation for all substation components in totality. In such context, a system reliability model using minimum cut set method is used in addition to the Markov chain model.

4.3. Reliability assessment of system with complex configurations and various failure modes

Similar to the optimization problem in Chapter 3, the optimization can only be achieved when the optimization of maintenance schedules is extended from component-specific to system-specific. There are several advantages to use minimum cut sets method. First, the technique is easily implemented on a digital computer. Second, the technique can handle “bridges” or meshed structure in a network that cannot be characterized by either a series connection or a parallel connection. Third, minimum cut sets can give insight on critical component. The failure modes considered include:

- first-order failure event,
- second-order passive failures, and
- primary protection failures (additional active failure of the first-order failure and additional active failure with a switching device being jammed).

Following the procedure shown in Fig. 4.4, all the minimum cut sets leading to the failure of individual load point can be identified.

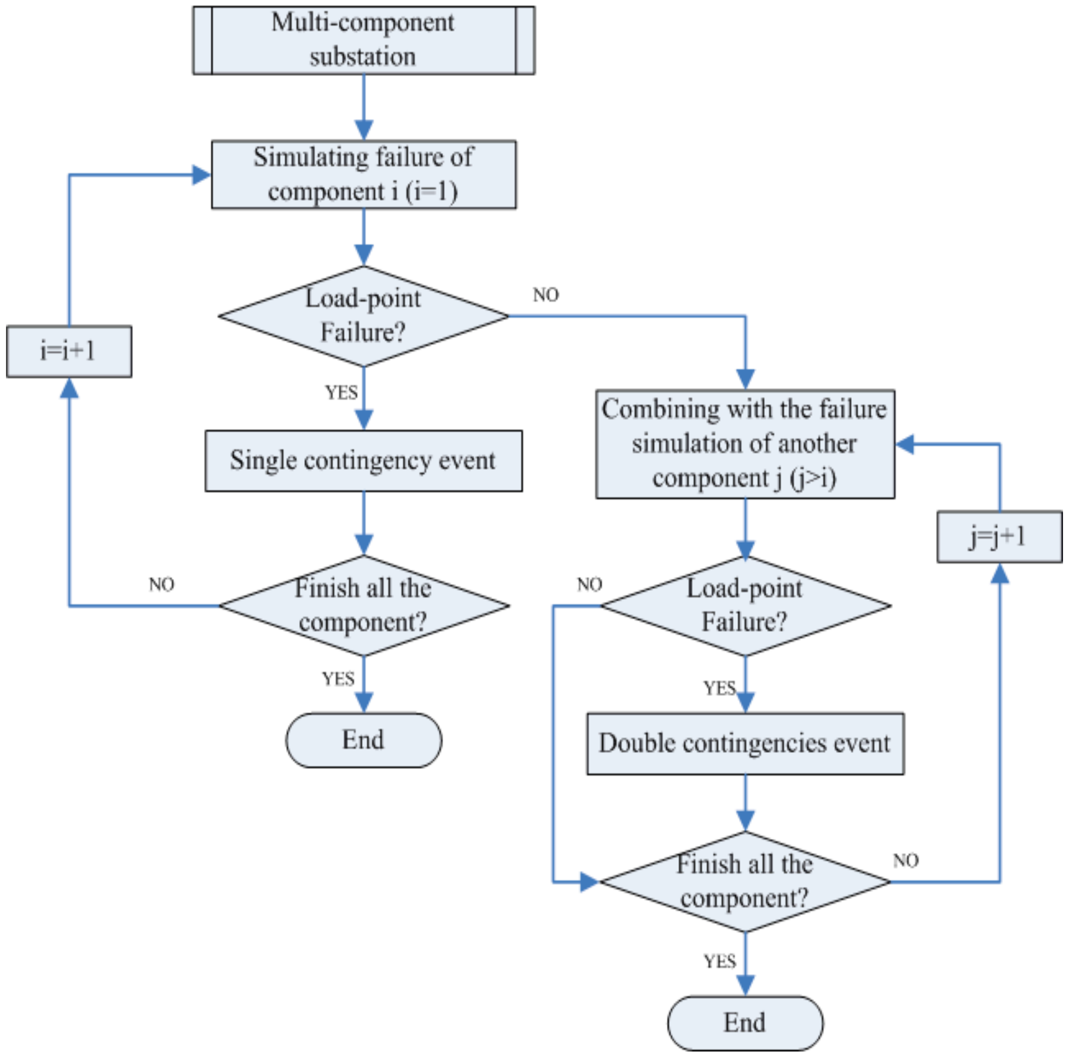

Fig. 4.4 Flowchart of Minimum Cut Sets Analysis for Substations

From a reliability point of view, the reliability of one system can be represented as a block diagram consisted of minimum cut sets leading to the failure of this system, which is shown in Fig. 4.5, where *Fmn* represents the failure *n* in minimum cut set *m,* and n_1, n_2, …, n_n are the number of failure events involved in minimum cut set *1, 2, …, n*. As can be seen in Fig. 4.5, all the failures within one minimum cut set can be viewed as being connected in parallel, and all the minimum cut sets are in series.

Therefore, the reliability of a system can be evaluated easily following the rules used for the simple configurations (series or parallel).

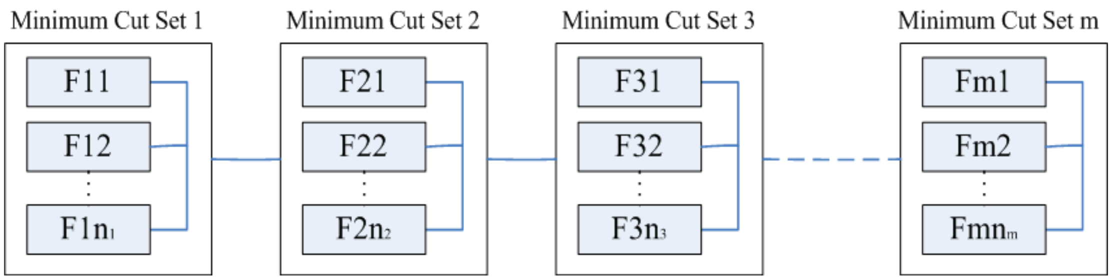

Fig. 4.5 Block Diagram of Minimum Cut Sets

The order of minimum cut set in this work is up to two, and higher contingencies are neglected due to their small probabilities. The availability for a cut set of two components can be calculated following the methods for the parallel outage as:

$$A_s = 1-(1-A_1)(1-A_2) \tag{4.6}$$

where A_1, A_2 are the availabilities of two components respectively.

The system indices can therefore be evaluated by applying the methods for series components:

$$A_{sys} = \sum_{s=1}^{n} A_s \tag{4.7}$$

where A_s is the availability of the s^{th} cut set.

4.4. Calculating two objective values of optimization

Unlike Section 3.4, different objectives are chosen here due to the changes of model of individual component and the method used for evaluating the system reliability. Overall cost including the capital and maintenance costs and expected energy not served (EENS) are calculated in the following paragraphs. Normally, the configuration with minimum overall cost and maximum reliability is the best one.

1) Economic objective—overall cost. The overall cost, C, of a substation consists of two parts—capital cost and operational cost, which can be calculated by:

$$C = \sum_{a=1}^{M} C_{o.a} + CapC \times Rate \tag{4.8}$$

where M is the number of component in this substation, $C_{o,a}$ is the operational cost of component a, $CapC$ is capital cost in one substation, and $Rate$ is the interest and depression rate.

2) Reliability objective—EENS. It is the expected energy not-served which evaluates the system reliability at all the load points:

$$EENS = \sum_{t=1}^{T} (\sum_{p=1}^{m} 8760 \times (1 - A_p) \times L_p)_t / T \tag{4.9}$$

where m is the number of load points in one substation, A_p is the availability at load point p, L_p is the loss of load (MW) due to failure at load point p in one decision interval, and T is the number of decision intervals.

Since the load demand at each load point is time-varying, the EENS in each decision interval (year) has to be calculated separately. In this work, load growth is reasonably considered to be 5% as suggested in [95]. EENS is the average expected energy un-served per year over the whole scheduling horizon.

In this work, both of the two objectives are functions of the maintenance frequencies ($f_{m,t}$, $f_{M,t}$). They can be handled as two non-commensurable and contradictory objectives. Therefore, the multi-objective problem can be easily formulated using equation (3.15) (pp. 45), where $f_1(x)$ represents the overall cost, and $f_2(x)$ is EENS, and x is the vector containing the maintenance frequencies over the scheduling horizon.

4.5. Application of NSGA II and NSGA II-DE

4.5.1. Representation of solutions

Due to the computational burden of binary representation, the proposed approach has been improved by using real-coded genetic algorithm [96]. In each interval t $(1 \leq t \leq T)$, two integers which are chosen from 0, 1, or 2 are used to represent the frequencies of minor and major maintenance for each component. In this way, the number of elements in the chromosome equals to 2 equals to $2 \times M \times T$ (where M is the number of component and T is the number of time intervals in years), which could be large in a complex system. An example of this representation method is given in Fig. 4.6.

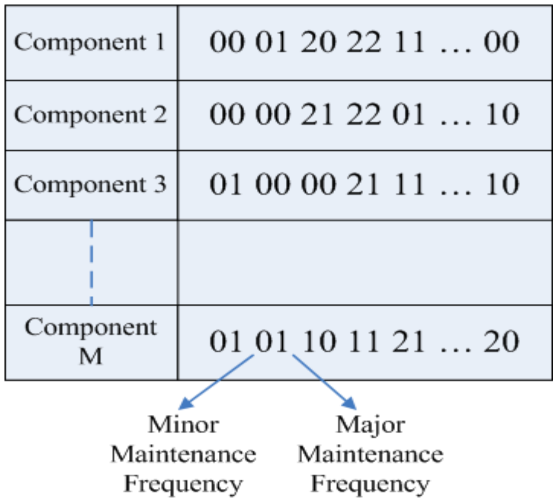

Fig. 4.6 Representation of Solution

4.5.2. Flowchart to apply NSGA II & NSGA II-DE

The approximation of Pareto-optimal solutions involves two objectives: (i) convergence over successive generations and (ii) diverse and even spread across the Pareto Front. NSGA II [52] has been improved over the earlier NSGA [51], by incorporating elitism for good convergence of solutions. In addition, NSGA II does not need any sharing of parameters for diversity assignment to be chosen as a priori. All these advantages guarantee NSGA II a powerful but simple tool to be implemented. NAGA II and NSGA II-DE as introduced in Section 2.4 are applied to solve this problem. In the simulation, the flow chart to apply NSGA II to this work is presented in Fig. 4.7.

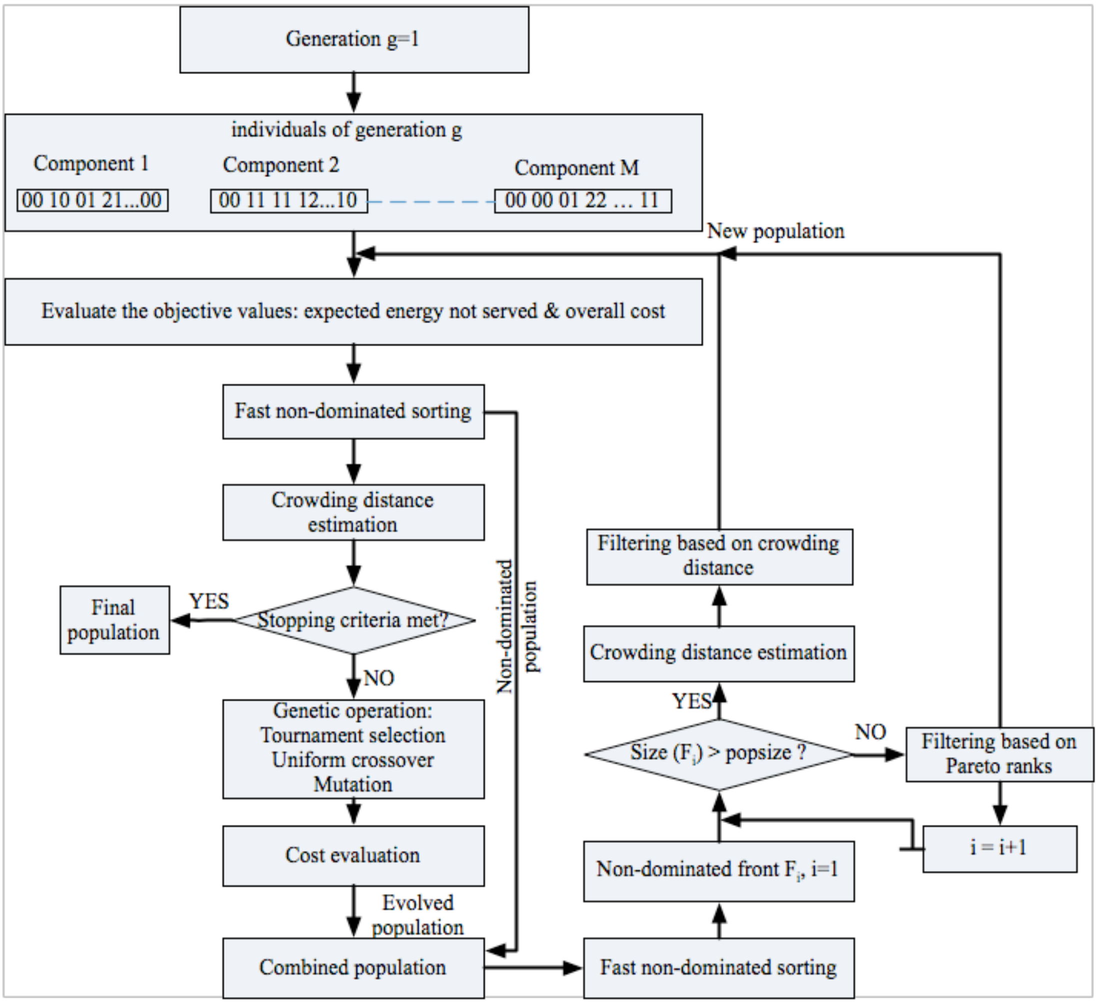

Fig. 4.7 Flowchart of Optimization Technique (NSGA II & NSGA II-DE)

The crossover and mutation operators in this integer-coded genetic algorithm are described as follows:

- *Uniform crossover*: the elements for offspring are randomly copied from the first parent or from the other parent.
- *Mutation*: new values of selected elements are chosen as 0, 1, and 2.

4.6. Case studies on four substation configurations

4.6.1. Configuration descriptions and parameters

The proposed approach is applied to four substation configurations as in Fig. 4.8 to assess potentials of the proposed approach for optimizing large maintenance problems with the following assumptions:

- availabilities of transmission lines feeding the substations are 100%, or can be set by other connected substations being considered,
- transformers (T1 and T2) and circuit breakers (B1~B6) are modeled each with a three-deteriorated-state Markov chain model and the system reliability model,
- average load demand during individual decision interval at each load point is constant, while it varies from one interval to another.

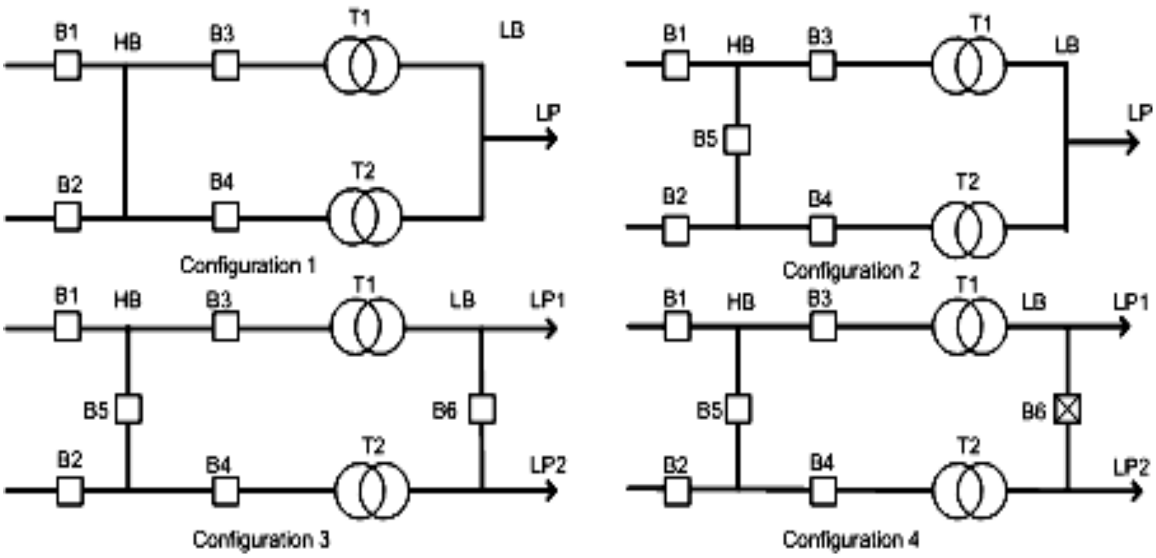

Fig. 4.8 Typical Substation Configurations

The capital cost of equipment is also the same as that in Table 3.1(pp. 51). Key parameters used in equations (4.8) and (4.9), *Rate = 12%, N = 3, and T = 24.* Other parameters are given in Table 4.1 and Table 4.2.

Table 4.1 Initial Parameters of Transformers and Circuit Breakers used in Markov Model

	T1~T2	B1~B4	B5~B6
p_{11}	27/40	44/64	45/64
p_{12}	¼	¼	5/32
p_{13}	2/40	3/64	3/32
p_{1f}	1/40	1/64	3/64
p_{22}	16/20	26/30	13/15
p_{23}	3/20	3/30	8/75
p_{2f}	1/20	1/30	2/75
p_{33}	6/7	9/10	21/25
p_{3f}	1/7	1/10	4/25
p_{f1}	1	1	1

Table 4.2 Cost-related Parameters

	B1~B4	B5 ~ B6	T1 ~ T2
Minor Maintenance ($\$\times10^3$)	0.50	0.50	0.35
Major Maintenance ($\$\times10^3$)	2.00	2.00	1.50

The capital cost is calculated based on the typical data about the bus configuration, and number of breakers, transformers and other system equipment.

The population size of NSGA II and NSGA II-DE is set at 200, and maximum iteration number is 600. Crossover and mutation probabilities for NSGA II are chosen as 0.9 and 0.05 respectively. Tournament size is set as 2.

4.6.2. Optimization results and suggestions for decision makers

(a) Comparison between configurations 1 & 2: NSGA II is implemented here. Configurations 1 and 2 are compared in Fig. 4.9, highlighting the impact of tie breaker B5. Should very low costs be preferred, the lower end of Pareto front 1 (from points (1.3) to (1.4)) should be chosen at the expense of very high EENS. In the intermediate range where the costs for configurations 1 and 2 are comparable, configuration 2 should be preferred to configuration 1 for providing higher reliability as seen between points (2.1) and (2.2). The higher end of Pareto front 1 should be least considered since it provides less reliability with higher cost than configuration 2. The benefit of B5 is apparent in Fig. 4.9.

(b) Comparison between configurations 3 & 4: Fig. 4.10 shows the relative impact from the operation of B6 between normally close (configuration 3) and normally open (configuration 4). B5 is installed in both configurations. In the lower ends of both configurations, the costs are comparable, but configuration 4 provides higher reliability (from points (4.1) to (4.2)). Between the points (3.1) and (3.2), configuration 3 costs more but does not provide higher reliability than configuration 4. Therefore, configuration 4 should be always preferred.

(c) Best overall Pareto front: Fig. 4.11 shows the overall "best" Pareto front considering the four configurations simultaneously. Configuration 2 is always the most reliable among all the four configurations. As a result, configuration 2 should be chosen as part of the overall best Pareto front. At the other hand, configuration 1 has the least overall cost (from points (1.2) to (1.3)). Summing up, the overall best Pareto front should cover points (2.1), (2.2), (1.2) & (1.3), as shown in Fig. 4.11. Should two load points instead of one load point be required, configuration 4 should be selected based on the analysis in part (b).

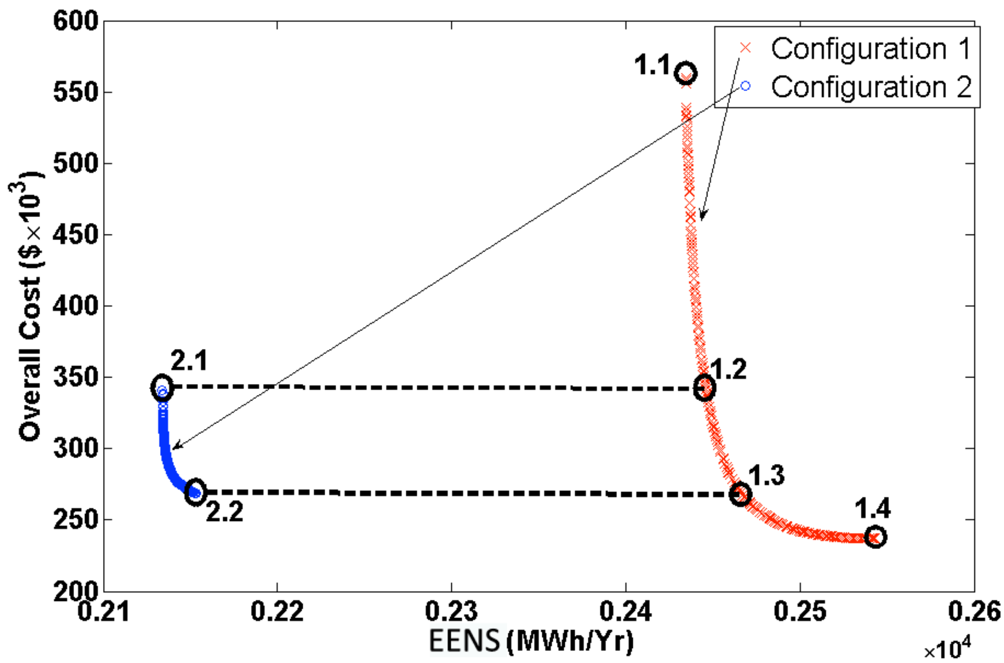

Fig. 4.9 Pareto Fronts of Configurations 1 and 2

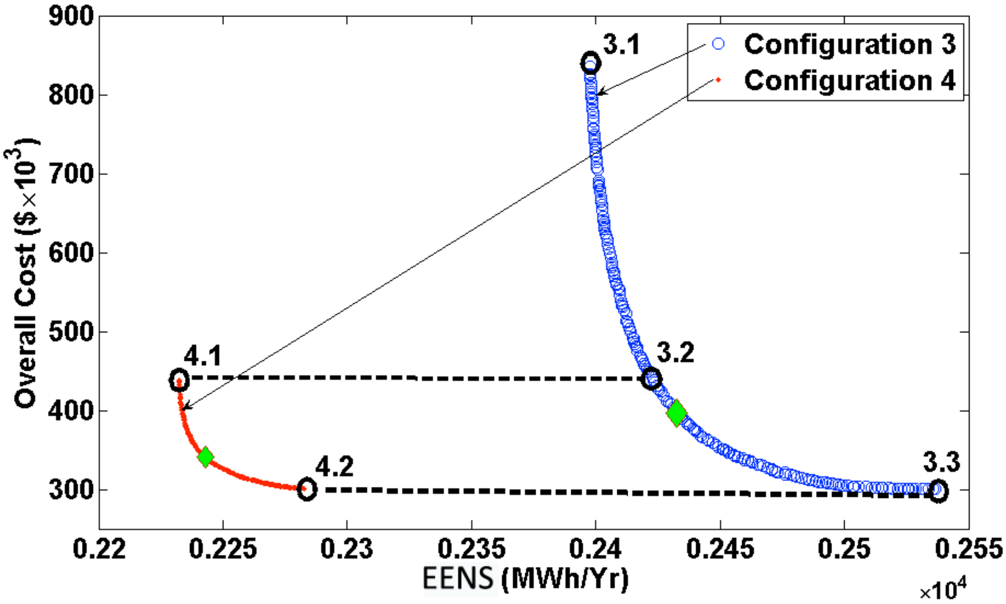

Fig. 4.10 Pareto Fronts of Configurations 3 and 4

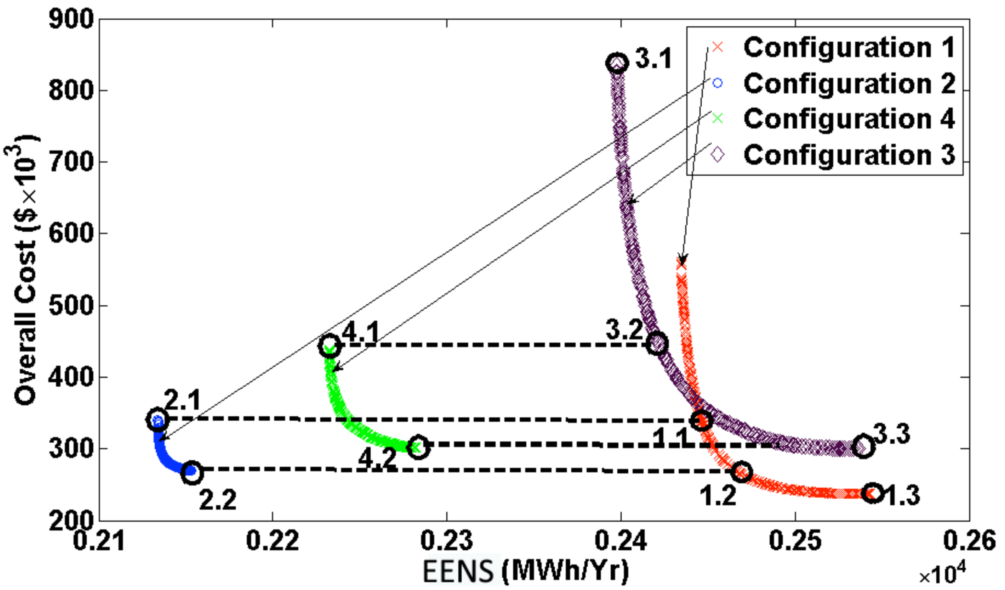

Fig. 4.11 Pareto Fronts of Configurations 1, 2, 3 and 4

(d) Overall impression on each configuration: On some occasions, the decision maker may like to have an overall impression on each configuration without closely examining the Pareto fronts. The procedure described in Section 2.3 provides a means of normalizing the two objectives for each point on the Pareto front using the membership function with equal priority given to each objective. This procedure is applied for all the four configurations with the best compromised solutions given in Table 4.3. The best compromised solutions on each Pareto front are highlighted in Fig. 4.9 & Fig. 4.10. Based on these, configuration 3 can be described as costly and unreliable. Configuration 1 is the cheapest and unreliable, and should be chosen for its low cost. Configuration 4 is inferior to configuration 2 in terms of both cost and reliability. The latter should thus be preferable for most occasions, as confirmed in Fig. 4.11. Other best compromised solutions would be chosen, should unequal priorities be given to the two objectives.

Table 4.3 Best Compromised Solution

	Cost ($\$\times10^3$))	EENS (MWh/Yr $\times10^3$)
Configuration 1	283.56	2.459
Configuration 2	287.27	2.138
Configuration 3	396.98	2.432
Configuration 4	340.41	2.243

(e) Impact of maintenance on load availability: Fig. 4.12 and Fig. 4.13 show the impact of maintenance on load-point availability for configurations 2 and 4. The availability variations of other configurations have similar trend. Rapid deterioration of availability occurs without any maintenance taken. According to the maintenance schedule, no maintenance has been performed for both configurations until the 8th interval for configuration 2 and 7th interval for configuration 4. Maintenance is seen to improve the availability progressively over the 24-year scheduling horizon.

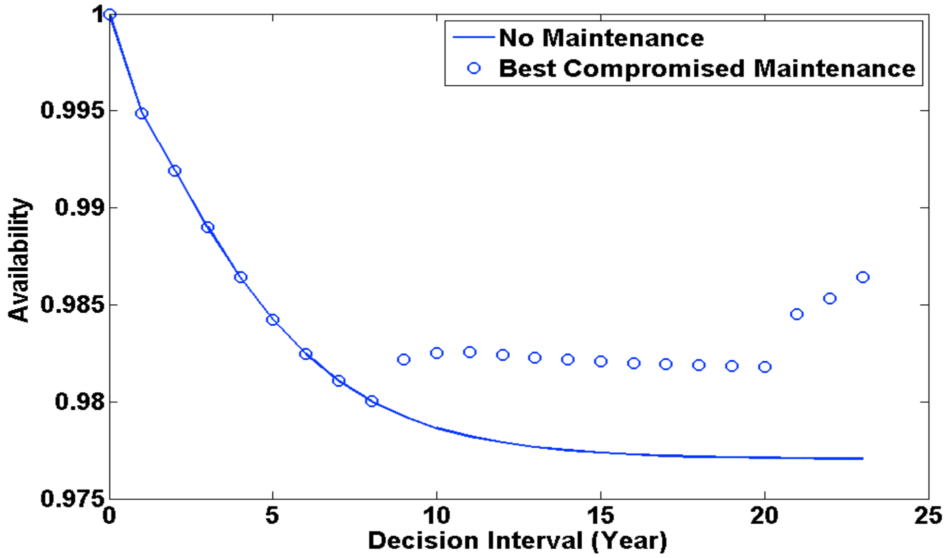

Fig. 4.12 Availability Variations under Maintenance Configuration 2

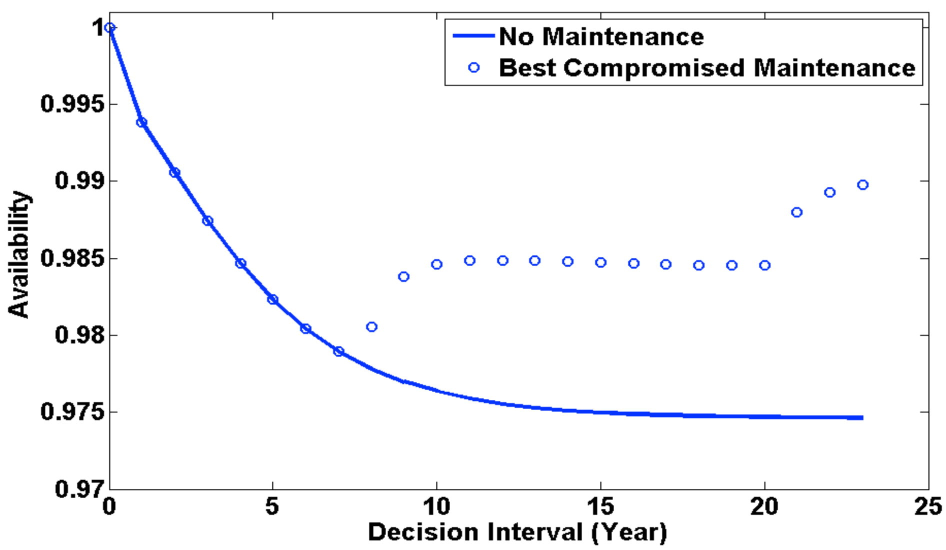

Fig. 4.13 Availability Variations under Maintenance Configuration 4

(f) Performance of NSGA II-DE: Ten different runs of NSGA II and NSGA II-DE are compared. On a computer with Intel Pentium 4, 3.00GHz CPU and 512 MB RAM, the average computational time over ten different runs are tabulated in Table 4.4. NSGA II-DE saves in average up to half of the computational time used by NSGA II. However, on all the four configurations studied, NSGA II generates Pareto fronts which are more widely spread than NSGA II-DE.

Table 4.4. Computational Time of Two Optimization Algorithms

	Computational time (s)			
	Case 1	Case 2	Case 3	Case 4
NSGA II	9219	26568	29652	28263
NSGA II-DE	5948	15223	18022	19027

4.7. Conclusion

A modular and integrated methodology is proposed to effectively schedule preventive maintenance on individual components in substation by optimizing the two objectives of overall cost and reliability of the substation as a whole. A series of Markov models is proposed to predict the availability of individual components based on the maintenance decision over the scheduling horizon. Minimum cut sets method is employed to identify the effects of various failure modes on the overall reliability of multi-components in complex configuration. Pareto fronts formulated using the two objectives provide a holistic view showing the relative advantages of one substation configuration over the others. Results presented on four different configurations demonstrate potentials and ease of application of the proposed approach for handling more complicated configurations.

CHAPTER 5 OPTIMIZATION OF MAINTENANCE SCHEDULES FOR COMPOSITE POWER SYSTEMS

Based on the successful optimization of maintenance schedules and extents for substations in Chapter 4, this chapter improves each of the three functional blocks in the proposed approach for handling larger systems. Instead of using a series of maintenance-dependent Markov chains described in Section 4.2 in the first block, a stochastic deterioration process of individual components is formulated as a time-and maintenance-dependent continuous-time Markov model. The second block extends the original minimum cut sets in Section 4.3, by identifying the loss of energy of a load point due to not only a loss of continuity within a substation, but also a loss of continuity and a violation of transfer limit between these substations. A novel representation of maintenance activities is introduced in this chapter specifying both the maintenance timings and extents, and is proven to outperform the previous representation, specifying the maintenance frequencies only. Optimization of the reliability, maintenance and failure costs is carried out on the Roy Billinton Test System (RBTS) and IEEE Reliability Test System (IEEE RTS) demonstrating the potential of this approach in handling complex systems, and substantiating its improvement over the previously work reported in Section 4.5.1.

Some material in this chapter has also appeared in [2,3] of the candidate's publications.

5.1. Improvement of overall approach for composite power system

Fig. 5.1 illustrates the present algorithmic structure, which is similar to that of previous approach as shown in Fig. 3.1 & Fig. 4.1. However, as can be seen in Fig. 5.1, all of the three blocks have been improved in this chapter to handle larger systems. Instead of using a series of decision-dependent Markov chains as in Section 4.2, a continuous-time Markov process is used to simulate stochastic deteriorations of individual components, the transition rates of which are updated not only based upon maintenance decision but also based upon time. In addition, fault tree analysis [97] replaces visual identification in previous work to generate minimum cut sets for investigating large-size problem. Besides, an improved evaluation of the loss of energy at a load point has been proposed. Our previous approach evaluates only the total loss of continuity (TLOC), which arises from all failures or a combination of failures within a substation. We extend this approach by including the failure and violation of transfer limit of all substation interconnections, which leads to a "partial loss of continuity" (PLOC). We are using the "reliability trip" to describe such events of PLOC. DC load flow is used to represent all potential overload and loss of angle stability on substation interconnection, and identify the minimum cut sets for assessing such events. More complex power systems, such as RBTS [95] and IEEE RTS [98] are studied instead of the four simple substation configurations in Fig. 4.8 (pp. 71).

In addition, this work extends the application of multi-objective optimization algorithm in Chapters 4, which employs Elitist Non-dominated Sorting Genetic

Algorithm (NSGA II), to optimize both preventive-maintenance timings and extents. This chapter describes the optimization of the extent of maintenance (for no, minor and major activities) in each time interval of each equipment's life span by employing a novel and more efficient method to represent solutions. Furthermore, the cost objective in Section 4.4 has been split to bring in a third and a second cost objectives. The present formulation has thus three objectives, namely: the operation cost, expected energy not served, and expected failure cost, which are minimized in a global search for the maintenance of individual components of the study system in every time interval.

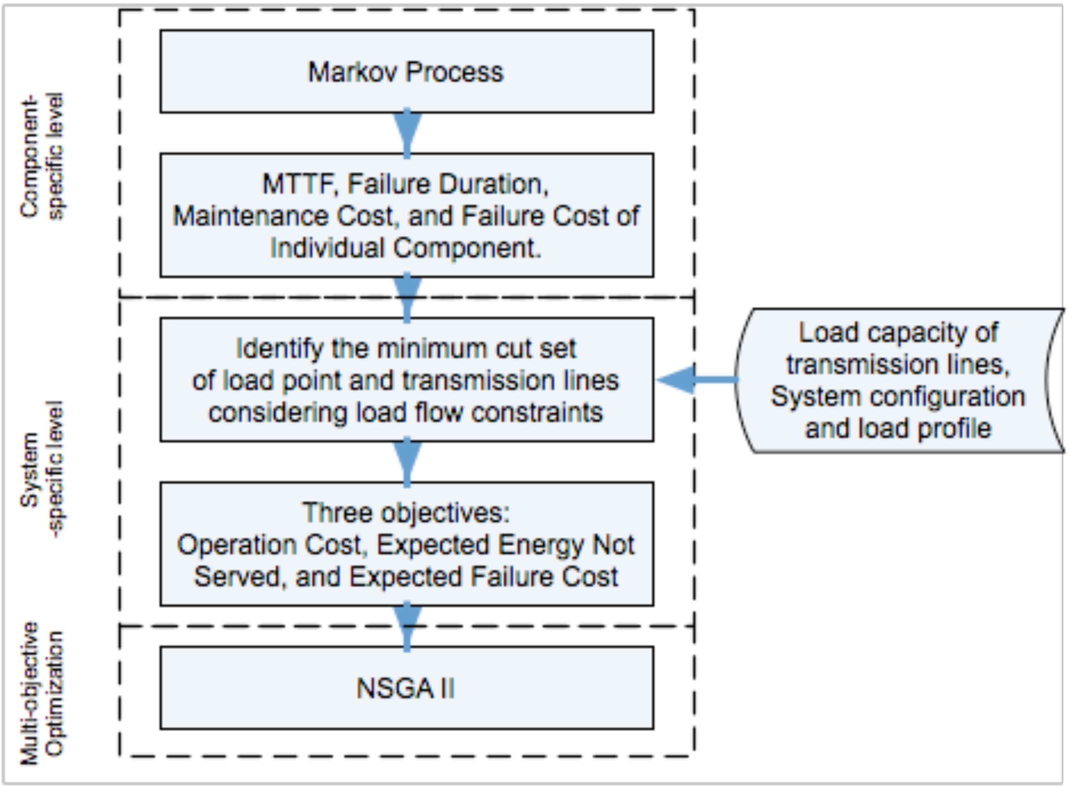

Fig. 5.1 Integrated Approach for Maintenance Optimization

5.2. Improvement of two-level reliability model

5.2.1. Time- and maintenance-dependent Markov process on component level

The deterioration rate of a component usually depends on time, with the rate varying over the life cycle of the system. A continuous-time Markov model can be easily viewed as a Markov process with time-dependent transition rates. Therefore, the improved Markov model is able to incorporate the varying rather than constant transition rates between different deterioration states.

If Q is defined as the transition matrix for this continuous-time Markov process, the elements $\lambda_{ij}(t)$ of Q indicate the rate of transition from states i to j at time t for $i \neq j$. If $i = j$, $\lambda_{ij}(t) = -\sum_{i \neq j} \lambda_{ij}(t)$.

The state at time t is denoted as $D(t)$, the probability that the process is in the state j at time t is denoted as

$$p_j(t) = \Pr\{X(t) = j\} \tag{5.1}$$

where $p_j(t)$ is the element of vector $P(t)$. Given Q, the time-dependent state probability $P(t)$ can be calculated as:

$$\frac{dP(t)}{dt} = P(t)Q \tag{5.2}$$

In the long run towards steady-state conditions, all time derivatives disappear; equation (5.3) is used to calculate the failure probability:

$$\begin{aligned} 0 &= PQ \\ \sum_{j \in D} p_j &= 1 \end{aligned} \tag{5.3}$$

The undergoing deterioration of each component during maintenance is modeled here in 4 states as in Fig. 5.2, and the definitions of D_i, $i=1, \ldots, N$ and the rules of transition among multiple states are the same as that in Chapters 3 & 4. The procedure to measure the reliability and economic cost of individual components is demonstrated in Fig. 5.3. The mean time to active failure ($MTTF_a$), mean time to passive failure ($MTTF_p$), failure duration (r), and failure probability (p_f) are calculated using the standard methods given in [19, 88].

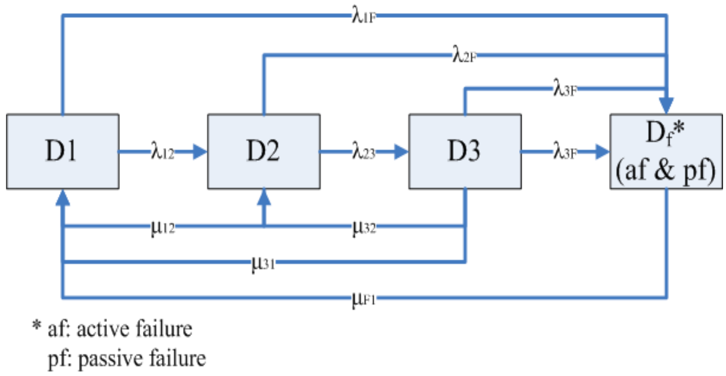

Fig. 5.2 Time- and Maintenance-dependent Markov Model

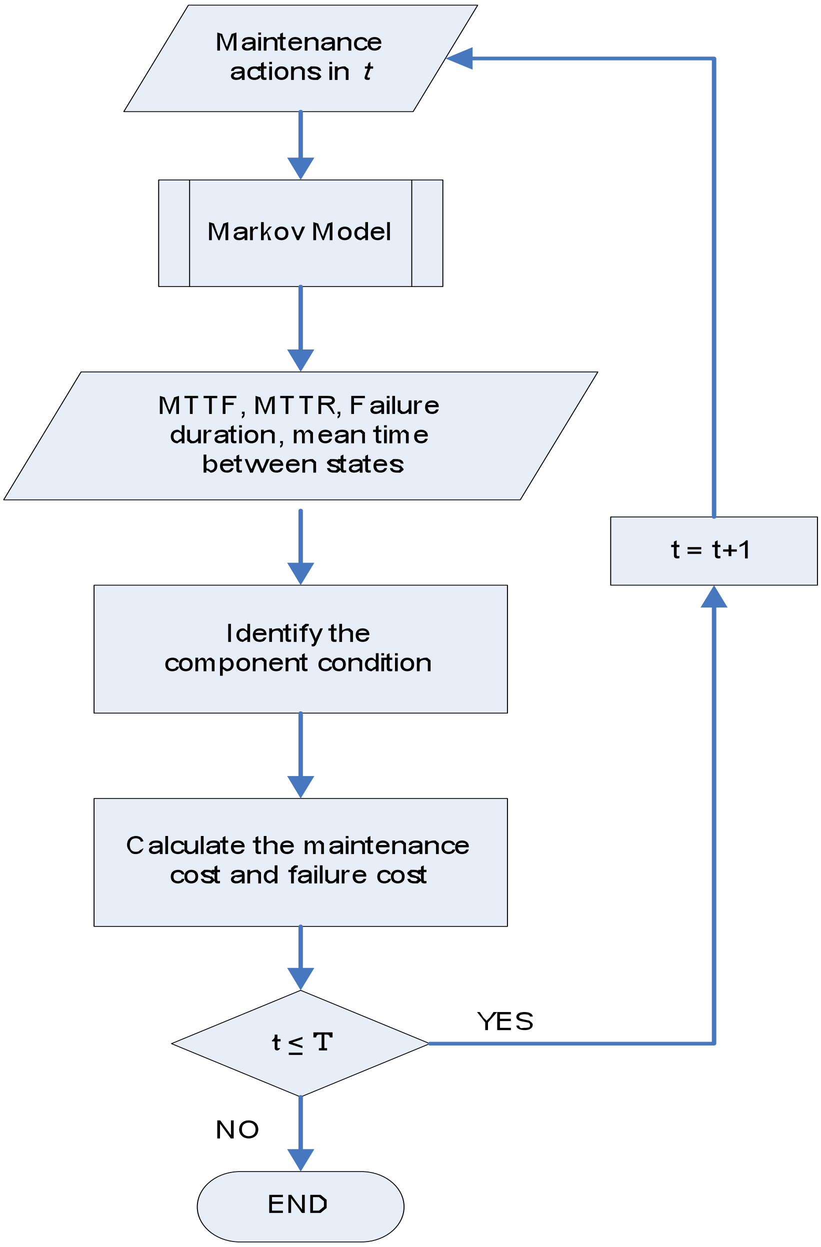

Fig. 5.3 Flow Diagram of Markov model

The component operation cost for component *a* ($C_{o,a}$), including the inspection cost and maintenance cost, is calculated by:

$$C_{o,a} = T \times C_{ins} + \sum_{D=1}^{3} (C_{\min,D} \times T_{\min,D} + C_{maj,D} \times T_{maj,D})$$
$$T_{\min,D} = \sum_{t=1}^{T} (T_{\min}^{t} \times p_D(t)) \tag{5.4}$$
$$T_{maj,D} = \sum_{t=1}^{T} (T_{maj}^{t} \times p_D(t))$$

where C_{ins} is the inspection cost of component a, $T_{min,D}$ and $T_{maj,D}$ are the times of minor and major maintenance in state D, and $C_{min,D}$ and $C_{maj,D}$ are the average costs of minor and major maintenance for component a in state D.

Expected failure cost of component a, $C_{f,a}$, is calculated by:

$$C_{f,a} = C_{avef,a} \times \sum_{t=1}^{T} p_f(t) \tag{5.5}$$

where $p_f(t)$ is the failure probability in interval; and $C_{avef,a}$ is the average cost of failure for component a.

When the system size grows, it is necessary to use a more effective system reliability model for assessing the collective effect of maintenance on overall system.

5.2.2. Fault tree analysis on system level

Fault-tree analysis is one principal method for the reliability evaluation of complex system, which includes three main steps—definition of the top event, construction and evaluation of fault tree. A fault tree is so structured that the sequence of events leading to the undesired event are linked under the top event and related to the undesired event by logic gates (OR and AND). These undesired events are further developed until they reach the basic causes, known as “basic events”.

After the identification of the fault tree for the load-point failure, minimum cut sets method is used to perform the quantitative evaluation of fault tree. By definition, a minimum cut set is the smallest set of basic events which can lead to the top event [99].

Reliability analysis has been carried out in the RBTS and IEEE RTS. The failure of each load point is defined as the top event, and individual or combined failure modes of components, which can cause top events, are those lower level events. Besides providing the visibility of overall system, fault-tree analysis also allows focus on one particular part of system at a time. For example, in RBTS, A1, A2 and A3 in Fig. 5.5 are relatively independent in view of functions they serve. The influences on reliabilities due to other sub-systems are only brought about by transmission lines connecting them. Therefore, it is convenient for the decision maker to assess individual subsystem without analyzing the bulk power system.

The order of minimum cut sets considered here is limited to four. The higher orders are neglected because of their small probabilities of occurrence. For the four-order events, the failure rate and failure duration can be evaluated with the methods of parallel outage given in equation (5.6). The evaluation of events of lower-order can be deduced following the same rule.

$$\lambda_{cs} = \lambda_A \lambda_B \lambda_C \lambda_D (r_A r_B r_C + r_B r_C r_D + r_A r_B r_D + r_A r_C r_D)$$
$$U_{cs} = \lambda_A \lambda_B \lambda_C \lambda_D r_A r_B r_C r_D$$
$$\mu_{cs} = U_{cs} / \lambda_{cs} \tag{5.6}$$

where λ_{cs} and μ_{cs} are the failure rate and duration of one cut set, respectively, λ_A, λ_B, λ_C, and λ_D are the failure rates of events A, B, C, and D, r_A, r_B, r_C, and r_D are the duration of events A, B, C, and D, and U_{cs} is the annual duration of one cut set.

As discussed earlier, the duration of a load point failure is obtained by applying the methods for series components equation (5.7)

$$U_{top} = \sum_{cs=1}^{n} U_{cs}$$
$$U_p = U_{top} \tag{5.7}$$

where U_{top} is the annual duration of top event in one interval, U_p is the annual failure duration of load point p, and n is the number of minimum cut sets leading to the top event.

5.3. Optimization of maintenance schedules with three objectives

5.3.1. Adding in the third objective

Power systems are expected to operate as economically as possible (low cost), while providing good reliability (low EENS). Besides the expected energy not served and operation cost, the failure cost due to the repair of failed components are also included as an extension to the work in Chapters 3 & 4. Therefore, the problem is formulated as a three-objective search, aiming at searching for a set of maintenance schedules which are comparatively 'equally good' for multiple objectives (minimization of operational cost, failure cost, and EENS).

The reliability objective is EENS, which is the approximated average expected energy not-served caused by the deterioration failure and chance failure. Including all the load points, EENS is calculated by equation (5.8):

$$EENS = (\sum_{t=1}^{T}\sum_{p=1}^{m}(U_p \times L_p))/T \tag{5.8}$$

where m is the number of load points in one substation, L_p is the loss of load at load point p in one decision interval t, and T is the number of decision interval.

Economic objective includes the overall operational cost, C_{sysO}, and expected failure cost, C_{sysF} , of a substation, which is calculated by:

$$C_{sysO} = \sum_{a=1}^{M} C_{o,a}$$

$$C_{sysF} = \sum_{a=1}^{M} C_{f,a} \tag{5.9}$$

where M is the number of component in the system, $C_{o,a}$ and $C_{f,a}$ are the operation cost and failure cost of component a respectively.

In this study, all three contradictory objectives are functions of maintenance actions. Therefore, the multi-objective problem is easily formulated as follows:

$$MinimizeF(x) = Minimize\{f_1(x), f_2(x), f_3(x)\} \tag{5.10}$$

where $f_1(x), f_2(x)$, and $f_3(x)$ are overall operational cost, EENS, and expected failure cost of overall system; x is the variable containing the potential maintenance schedules and extents over the scheduling horizon.

5.3.2. Implementation of NSGA II with new representation of maintenance schedules

There are three maintenance extents, no maintenance, minor and major maintenance, which are represented by integers 0, 1, and 2. The left-to-right order list of T integers indicates the maintenance actions in T intervals for each component. An example for a solution is shown in Fig. 5.4. The number of elements in the chromosome is equal to the number of components (M) times the number of time intervals (T Yrs), or $M \times T$ (=51×30=1530) in the RBTS and ((89+86)×20=3500) in the IEEE RTS. In this way, the new method has only half the number of the elements in one chromosome compared with our previous method in Section 4.5.1, which uses the frequencies of two maintenance actions (minor and major) in every interval for each individual component.

As mentioned before, the approximation of Pareto-optimal solutions involves two objectives: one is the convergence over successive generations, and the other is the spread (diverse or even) across the Pareto Front. In this work, the diversity of solutions is further guaranteed by incorporating domain-knowledge in the initialization. The initial generation has three specially added solutions, which are obtained by minimizing the three objectives individually. The three solutions could be maintained with high probability by elitism employed in NSGA II. Therefore, a set of solutions covering the whole approximated Pareto front can be obtained at the end of optimization.

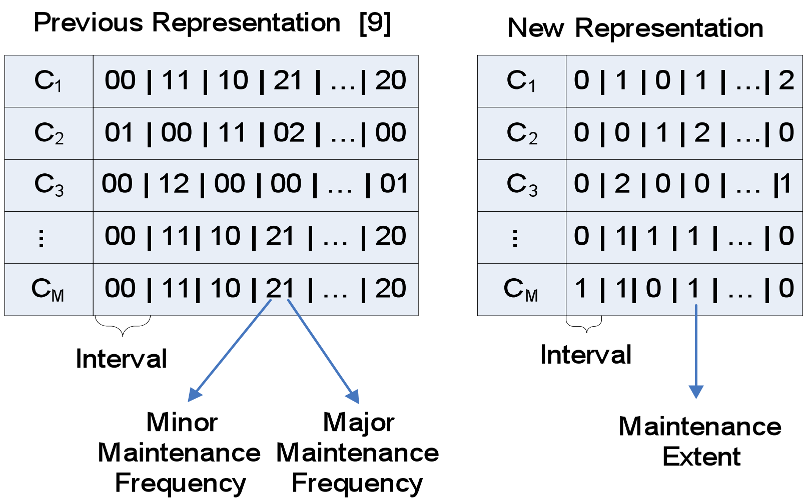

Fig. 5.4 Representation of Solution

5.4. Case study 1: RBTS

5.4.1. Description of RBTS and advantage of new representation of solutions

The system studied here is the RBTS as shown in Fig. 5.5. The initial transition rates in Markov models of breakers and transformers are tuned according to the reliability parameters given in [95]. In equation (5.8), *T* is set at *30*, and in equation (5.9), *M* is set at 51. The population size is set at 50, and the iteration number is 150. The crossover and mutation probabilities are chosen as 0.8 and 0.05 respectively. As stated in Section 5.3, the new representation method greatly saves the storage space than the previously proposed method in Chapter 4. Furthermore, the average computation time required by new representation is 2.115×10^3s, while by previous method is 2.564×10^3s. The initial model parameters regarding the average costs of inspection, maintenance, and failure are reported in Appendix C. This set of data is chosen according to reviewers' recommendation of [100].

Before we assess the potential of proposed approach for solving the maintenance optimization problem, we make the following assumptions:

- availability of transmission lines feeding the substation are 100%,
- the loss of continuity between substations is not included in this case study,
- only transformers and circuit breakers are modelled with the three-deteriorated-state Markov and the system reliability model, and
- the average load demand during individual decision interval at each load point is constant, which can be varied from one interval to another for other case studies.

The assumptions above may not be true in practical systems. However, our proposed approach has been extended to incorporate the unavailability of transmission line as well as the violation of transfer limits between substations. More results on this issue will be reported in Section 5.5.

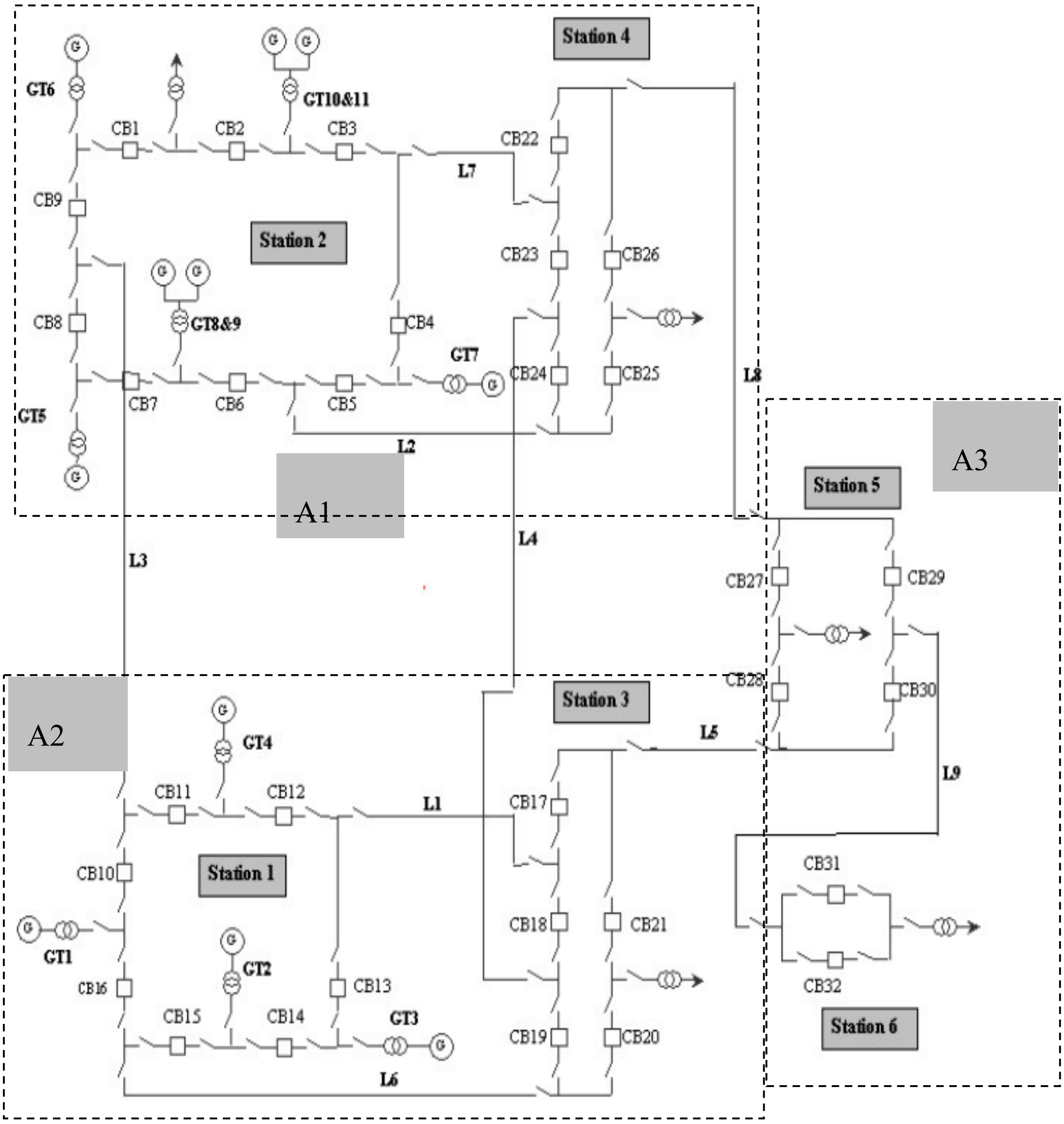

Fig. 5.5 Single Line Diagram of the RBTS

5.4.2. Pareto-optimal solutions of RBTS

NSGA II has successfully solved this multi-objective problem. A holistic view of optimal solutions is given with Pareto fronts of entire system in Fig. 5.6. It can also be seen in Fig. 5.6 that the solutions occupying two extremes of each Pareto front are consistent with those obtained by optimising each individual objective. That means that elitism of NSGA II has effectively maintained the extreme solutions, which are initialized at the beginning so that more diverse choices can be provided for decision makers.

The most compromised solution is provided to decision maker by normalizing the three objectives for each solution with equal priority (Section 2.3). The most compromised solution is marked on the Pareto fronts in Fig. 5.6 (a)&(b).

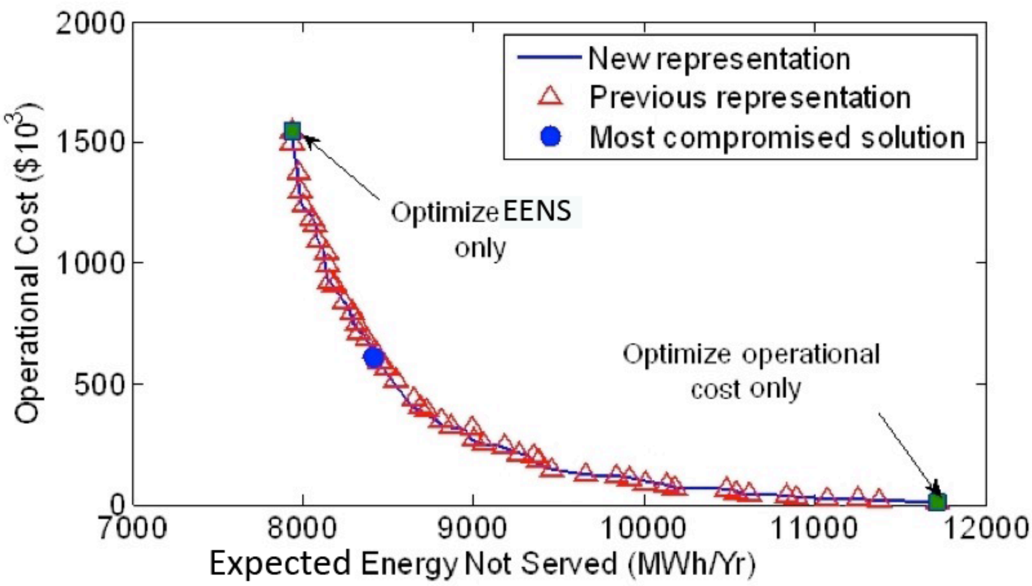

(a)

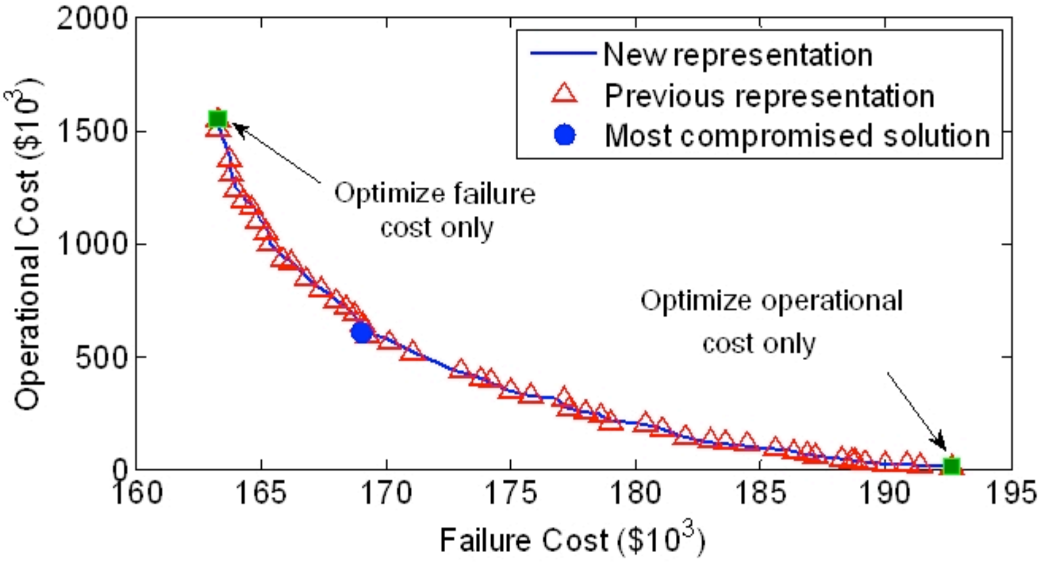

(b)

Fig. 5.6 Pareto Front of Entire System: (a) Operational Cost VS. EENS, and (b) Operational Cost VS. Failure Cost

Table 5.1 shows the cost-effectiveness of the most compromised maintenance. As can be seen in Table 5.1, the most compromised solution will result in an additional operational cost of $\$609.97\times10^3$ over a thirty-year maintenance horizon, which will lead to a decrease of the *EENS* by 0.33×10^4MWh/Yr (28.2% of *EENS* under no maintenance) and a decrease of expected failure cost by $\$23.56\times10^3$ (12.2% of that under no maintenance). The large percentage decreases in *EENS* and expected failure cost mean that they have led to a very significant improvement in overall reliability.

Table 5.1 Cost-effectiveness of Most Compromised Maintenance

	Overall Operational Cost ($\$\times10^3$)	Expected Energy Not Served ($MWh/Yr\times10^4$)	Failure Cost ($\$\times10^3$)
No maintenance/ inspection	0	1.17	192.61
Most Compromised maintenance	609.97	0.84	169.05

5.4.3. Comparison of different maintenance strategies on chosen components

The concept of a life curve is used to illustrate the effects of the aging and different maintenance actions on chosen equipment. Fig. 5.7 shows the life curves of two chosen equipment under four maintenance strategies. As can be seen in Fig. 5.7, if a more effective maintenance action is taken, the equipment can operate longer and at a particular time, its condition will be better.

With no maintenance, we assume the life curve is a smooth line, and the percentage of condition deterioration during one stage is proportional to the time duration of that stage. A percentage of 100 is used to represent the condition of a new component, while a percentage of 0 is a failed component. With maintenance, the deterioration towards the same percentage takes longer time. Therefore, the life curve is no longer smooth. Accordingly, the borderlines lie between different deterioration stages D_1, D_2, and D_3, in terms of the percentage equipment condition can be decided. In Fig. 5.7, the borderlines are marked on the vertical axis, and four points on each curve are included to highlight the starting and ending of each deterioration stage.

It is impossible to investigate all maintenance schedules and extents during the whole maintenance period. For demonstrational purpose, we select three maintenance strategies (no maintenance, minor maintenance and major maintenance) and one most compromised maintenance solution for each type of equipment. The effects of different maintenance strategies can be seen in Fig. 5.7. It should be noted that the effect of most compromised solution on reliability is dependent on the setting of parameters in the model. In this case study, the improvement of reliability obtained by taking the most compromised maintenance is lower than that by taking minor maintenance. However, changes of some parameter may produce different results.

Take the most compromised maintenance strategy for one breaker CB12 (Fig. 5.7 (a)) as an example, maintenance schedules will only cost $\$25.2\times10^3$ over the thirty-year planning horizon. It, however, will lead to an increase of average life of the breaker by 13.9% (from 77.8 years to 88.7 years) compared to the expected life without any maintenance. The minor maintenance over 30 intervals will cost $\$37\times10^3$, and will extend the life of the breaker further from 88.7 years to 95.0 years. It also can be seen in Fig. 5.7(a) that the major maintenance will extend the breaker's life to the utmost extent of 114.1 years, but the cost will sharply increase to $\$138\times10^3$. Such results show that the most compromised solution provides the most cost-effective maintenance strategy by extending the breaker's life at a relatively low cost. Similar results are also seen in Fig. 5.7(b) for the transformer.

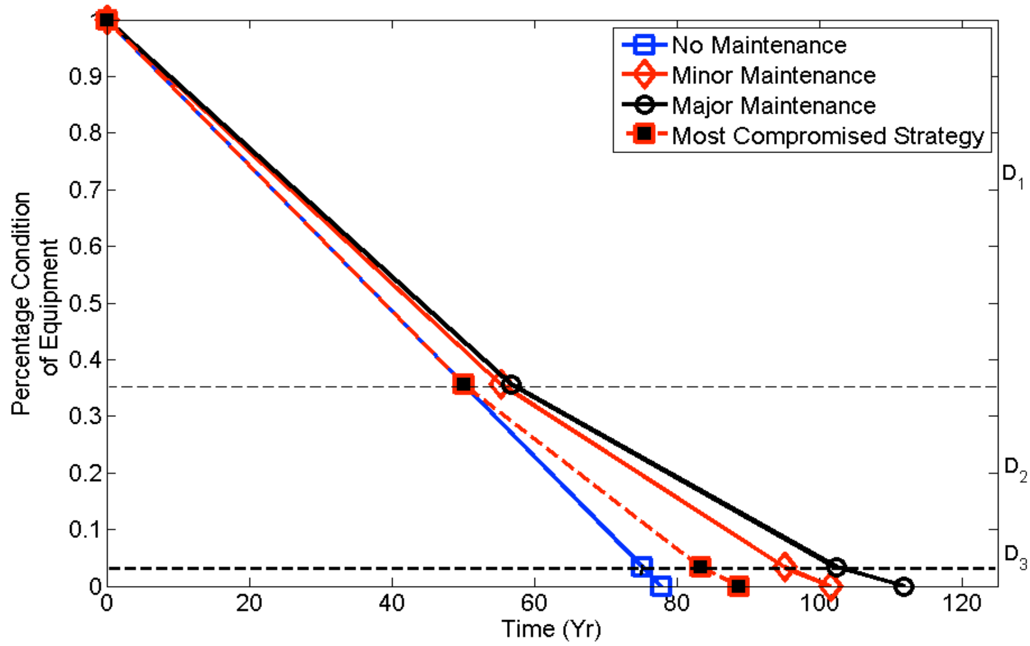

(a)

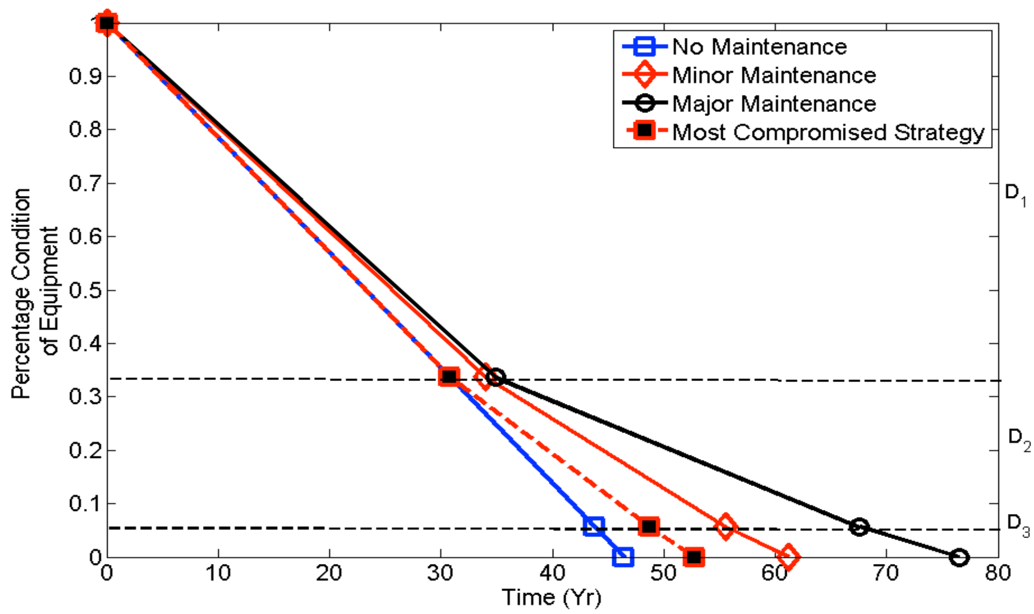

(b)

Fig. 5.7 Life Curves under Three Maintenance Strategies (a) circuit breaker, (b) transformer

5.5. Evaluation of loss of continuity between substations

In case study 1, the "total loss of continuity" (TLOC) of load point within each substation has been identified. However, it is crucial in composite reliability analysis to include the power flow constraints and unavailability of transmission lines. Therefore, the loss of continuity due to the violation of flow constraints and failures of transmission lines between substations is included in the following work.

The approach of evaluating TLOC is extended by including the failure and violation of transfer limit of all substation interconnections, which leads to a "partial loss of continuity" (PLOC). The "reliability trip" is used to describe such events of PLOC. DC load flow is used to represent all potential overload and loss of angle stability on substation interconnection, and to identify the minimum cut sets for assessing such events.

The minimum cut sets method is used to cooperate with DC load flow analysis in the reliability evaluation of IEEE RTS (Fig. 5.8). The order of minimum cut sets considered in this work is limited to two. Higher orders are neglected because of their small probabilities of occurrence. Unlike case study 1, minimum cut sets in this work are grouped according to the type of energy loss they caused. As a result, the reliability of one substation can be represented as a block diagram consisting of minimum cut sets leading to TLOC and "reliability trip" which are connected in series. F_n ($n = 1, 2, \ldots$) in Fig. 5.9 represents the failure event.

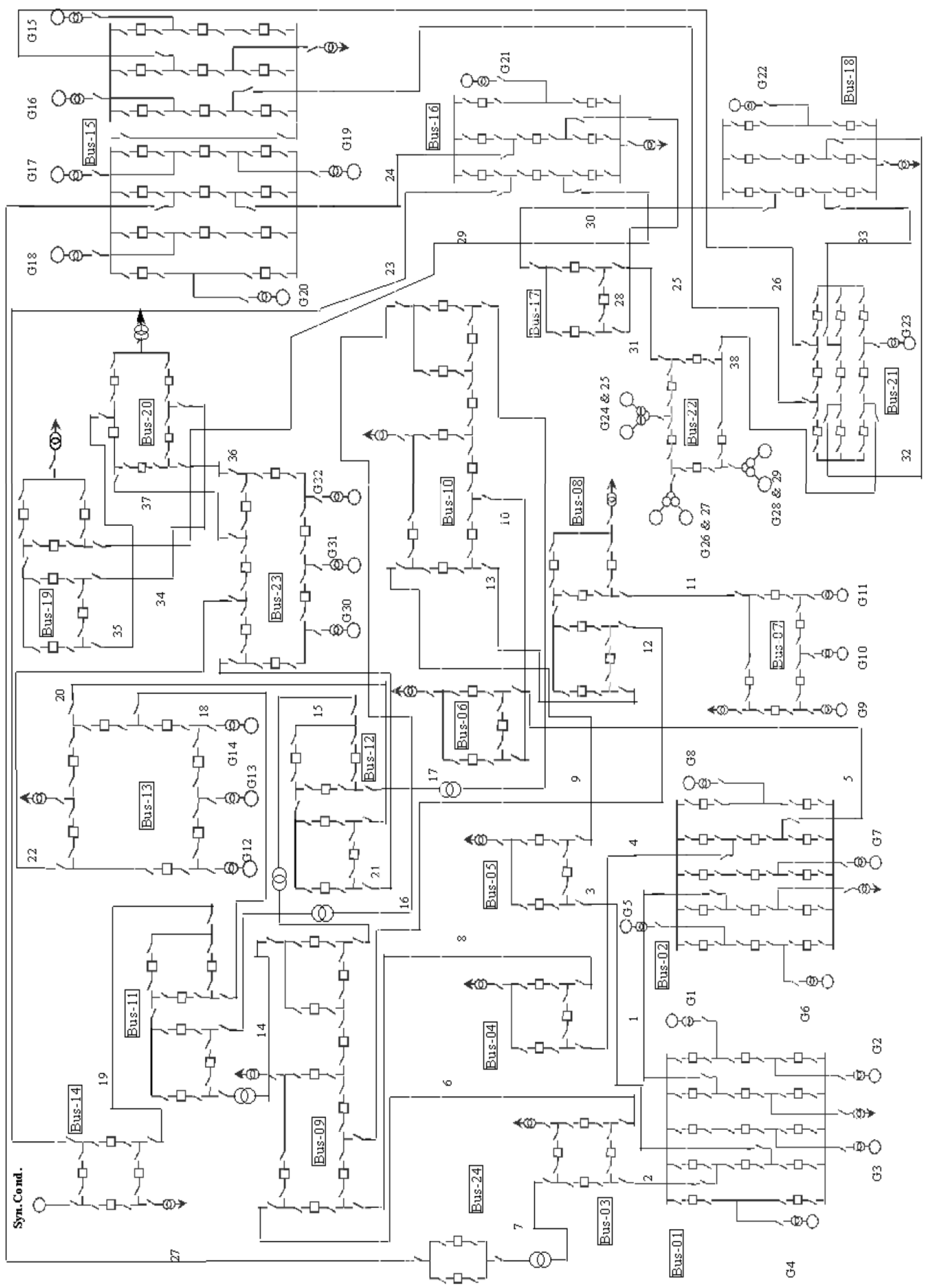

Fig. 5.8 Single Line Diagram of the IEEE RTS with Substations

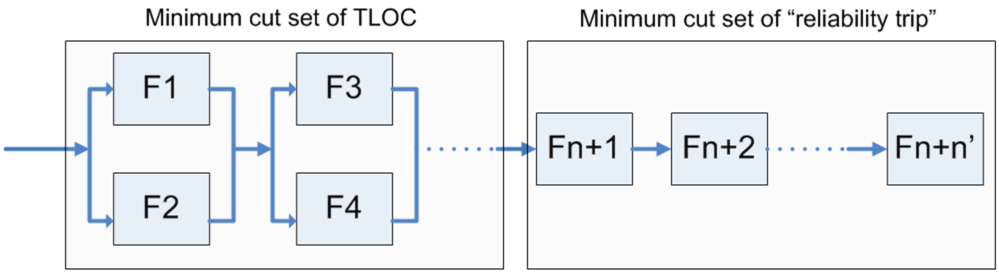

Fig. 5.9 Reliability Block Diagram of One Load Point

The aim of TLOC analysis is to identify the minimum cut sets that lead to total disconnections of either load point or transmission lines within each substation. Various failure modes are taken into account, including bus bar failure, breaker failure (active and passive), and malfunction of breakers in different protection zones. The reliability indices of minimum cut sets causing the disconnection of the same load point or transmission line are combined using the equations for system in series:

$$U_p = \sum_{cs=1}^{n} U_{cs} \tag{5.11}$$

$$U_{i,j} = \sum_{cs'=1}^{n'} U'_{cs'} \tag{5.12}$$

where U_p is the average annual disconnection duration of load point p, $U_{i,j}$ is the average annual disconnection duration of line j caused by the component failures within a substation i. U_{cs} is the average annual duration of one cut set cs for load point, $U'_{cs'}$ is the average annual duration of one cut set cs' for transmission line, and n and n' are the number of minimum cut sets for the load point and transmission lines respectively.

The energy loss brought by “total loss of continuity” ($E_{total,i}$) in substation i is caused by disconnection of load point, which can be calculated by equation (5.13):

$$E_{total,i} = \sum_{LP \in i} U_p \bullet Load_p \tag{5.13}$$

where $Load_p$ is the load demand of load point p.

Furthermore, "reliability trip" caused by the violation of transfer limits between substations may also lead to the loss of energy, which is evaluated by the following procedure:

(i). Identify the transmission line whose outage will lead to the overloading on other lines, and then form the minimum cut sets for the overloading events with those identified transmission lines. One of the network sensitivity factors [101], line outage distribution factor, is used in this approach. $d_{l,k}$ denotes the line outage distribution factor when monitoring line l after an outage on line k. This line outage distribution factor can be calculated beforehand and stored such that each row and column corresponds to one line in the network. For example, $d_{l,k}$ can be obtained by finding line l along the rows and then finding line k along that row in appropriate column. This factor has the following meaning:

$$d_{l,k} = \frac{\Delta f_l}{f_k^0} \tag{5.14}$$

where Δf_l is the change in MW flow on line l, and f_k^0 is the original flow on line k before it was outaged.

Once $d_{l,k}$ is found, the flow on line l with line k out is determined:

$$f_l = f_l^0 + d_{l,k} f_k^0 \tag{5.15}$$

where f_l^0 , f_k^0 are the pre-outage flows on lines l and k, respectively, and f_l is the flow on line l with line k out.

If $-f_l^{\max} < f_l < f_l^{\max}$, then line k belongs the minimum cut sets of the overloading events. This approach is illustrated in Fig. 5.10.

All the $d_{l,k}$ of every transmission line is computed and saved in a matrix as a lookup table. For each interval, the minimum cut sets leading to the violation of transfer limit can be easily identified with significant savings in term of computational time.

(ii). Modify the reliability parameters of transmission lines belonging to the minimum cut sets in order to include the effects of maintenance and reliability of substation component into the evaluation of “reliability trip” duration [102]. By doing this, the outage duration of transmission line is the sum of its original outage duration and the duration of disconnection caused by the component failures within the substation being connected [102]. With two ends of line k connecting substations $i1$ and $i2$, the new outage duration of link k, $U_{new,k}$, is calculated by equation (5.16). The duration of overloading or “reliability trip” of line l caused by the outage of line k, $U_{l,k}$, is thus obtained by equation (5.17).

$$U_{new,k} = U_{org,k} + U_{i1,k} + U_{i2,k} \tag{5.16}$$

$$U_{l,k} = U_{new,k} \tag{5.17}$$

where $U_{org,k}$ is original annual failure duration of line k, $U_{i1,k}$ and $U_{i2,k}$ are annual disconnection durations of line k due to the failures of components within substation $i1$ and substation $i2$, respectively.

(iii). Evaluate the expected energy not served caused by "reliability trip" in substation i with equation (5.18) as:

$$E_{partial,i} = \sum_{l \in i} \sum_{k \in MCS_l} U_{l,k} \bullet OL_{l,k} \tag{5.18}$$

where $OL_{l,k}$ is the overloading amount on line l due to failure of line k, and MCS_l is the minimum cut set for line l.

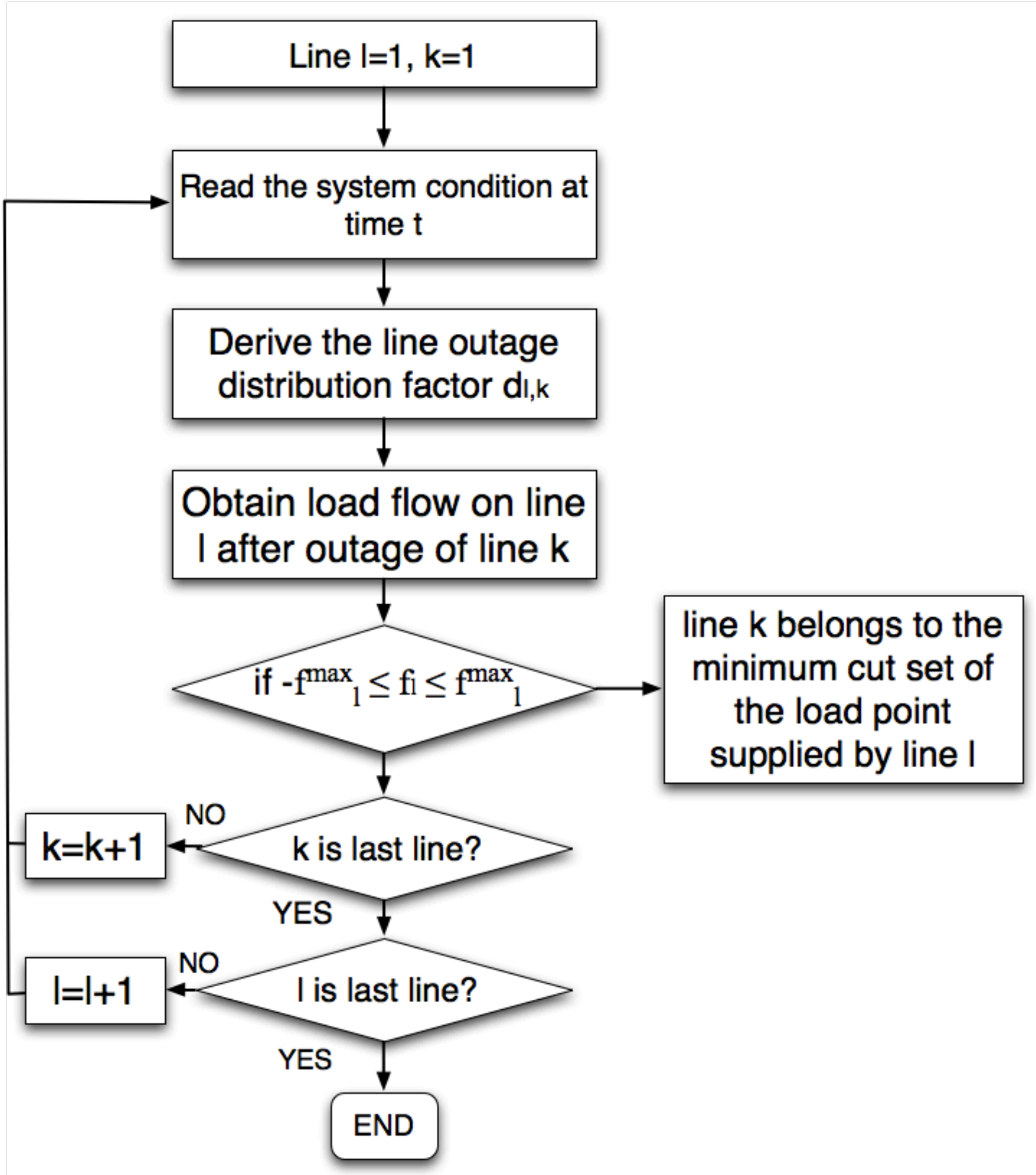

Fig. 5.10 Procedure to Identify the Minimum Cut Sets of "reliability trip"

Based on the previous analysis, the expected energy not served (EENS) of all the substations in a system is obtained by equation (5.19):

$$EENS = \sum_{i \in sys} (E_{total,i} + E_{partial,i}) \tag{5.19}$$

5.6. Case study 2: IEEE RTS

5.6.1. Description of IEEE RTS

Reliability analysis has been carried out on IEEE RTS as shown in Fig. 5.8. The transition rates among different states of each individual component are tuned according to the original reliability parameters as given in [98]. Other parameters used in this paper, such as load bus data, generation data, and transmission line data can be found in [102], and also given in Appendix D.

IEEE RTS is analyzed here to assess the potential of proposed approach for solving the optimization of maintenance problem. The following assumptions are made:

- circuit breakers and bus bars are the components to be maintained, and other components only participate the simulation without any maintenance,
- the transmission lines are not always available, and their reliability parameters are provided [102],
- the generation units are assumed to be 100% available,

The simulation computation is made on this system with 24 buses, 29 generating units, 38 transmission lines between substations and 168 circuit breakers. As proved in case study 1, the new representation has two advantages over the one in Section 4.5.1. First, it saves the storage space for variables. Among all the components, 89 circuit breakers and 70 bus bars are to be maintained in a twenty-year period. The new representation produces the chromosome of (89+70)×20=3180 elements, which is 3180 elements less than the previous method. Second, it reduces the computation time. In the application of NSGA II, the population size is 60, the iteration number is 80, and the crossover and mutation probabilities are set at 0.8 and 0.05 respectively. The program was run on a Pentium 4 computer with 3.00GHz CPU and 512 M RAM. The average computation time for ten optimization runs with new presentation is 2.488×10^3s. In contrast, the optimization takes a longer time of 3.026×10^3s using the representation method in Section 4.5.1.

5.6.2. Pareto-optimal solutions for IEEE RTS

NSGA II has been implemented as the optimization technique to this problem. Pareto fronts of entire system are shown in Fig. 5.11&Fig. 5.12, giving a holistic view of optimal solutions. It is quite clear that the problem has been efficiently solved by this technique.

As can be seen in Fig. 5.11&Fig. 5.12, the solutions occupying the two extremes of each Pareto front in the figures are consistent with those obtained from optimizing each individual objective. That means elitism of NSGA II has effectively maintained the extreme solutions so that more diverse choices can be provided for decision makers. The most compromised solutions on each Pareto front are highlighted in Fig. 5.11&Fig. 5.12 in order to give the decision maker an overall impression of the system reliability.

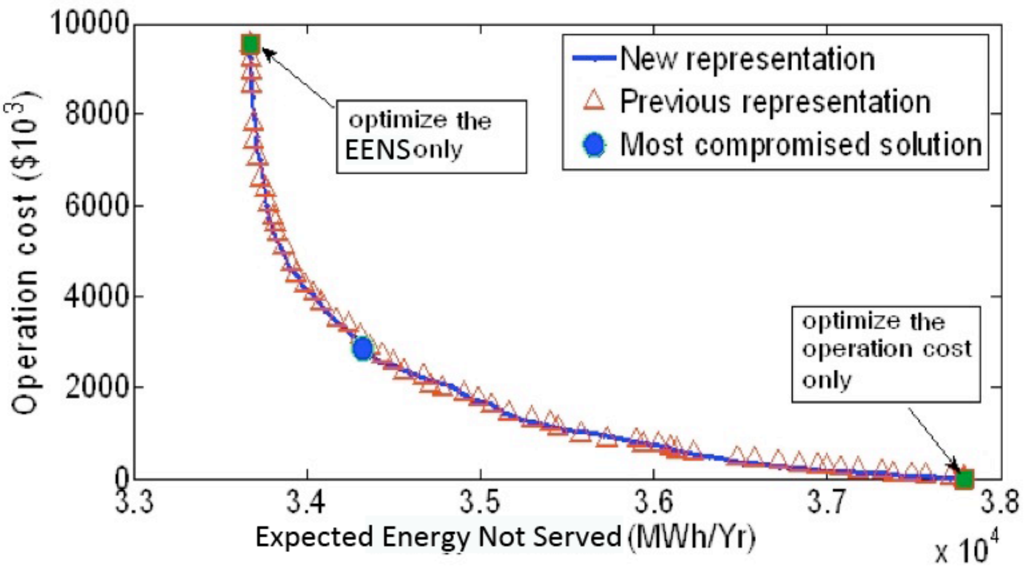

Fig. 5.11 Pareto Front of Entire System: Operation Costs VS. Expected Energy Not Served

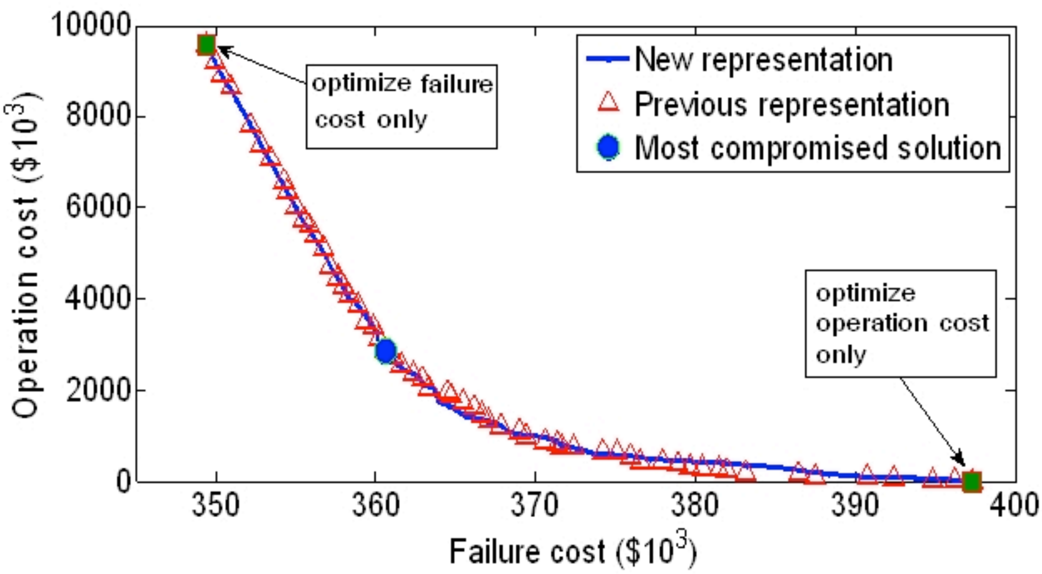

Fig. 5.12 Pareto Front of Entire System: Operation Cost VS. Failure Cost

Take the most compromised maintenance strategy as an example, this optimized maintenance actions will result in a decrease of the EENS by 3473.7MWh/Yr (9.2%

of EENS under no maintenance) and a decrease of expected failure cost by 36.7×10^3 \$/Yr (9.2% of that under no maintenance). It shows that a very significant improvement has been achieved by this solution. On the other hand, if comparing with the major maintenance, the most compromised solution will save $\$6.7\times10^6$ maintenance cost (70.2% of major maintenance cost), while only causing an increase of EENS by 647.8MWh/Yr (1.9% of EENS under major maintenance) and an increase of expected failure cost $\$1.1\times10^4$ (3.2% of that under major maintenance). The small decreases in reliability with an appreciable percentage of saving in cost indicate that this solution is more cost-effective.

Violation of inter-substation transfer limit on transmission line is a significant cause of energy loss. Fig. 5.13 shows the impact of “reliability trip” in terms of expected energy not served. As can be seen in Fig. 5.13, the Pareto front considering only TLOC lies on the left hand side of the diagram, meaning less loss of energy than the other one which includes “reliability trip”. For example, with the solution located at the lowest extreme of Pareto front (no maintenance) and no limits on power flow, the energy loss is 33793 MWh/Yr, which is 3997.7 MWh/Yr less than the one having power flow constraints. Therefore, ignoring the expected energy not served caused by overloaded lines will yield an overoptimistic result in the evaluation of system reliability.

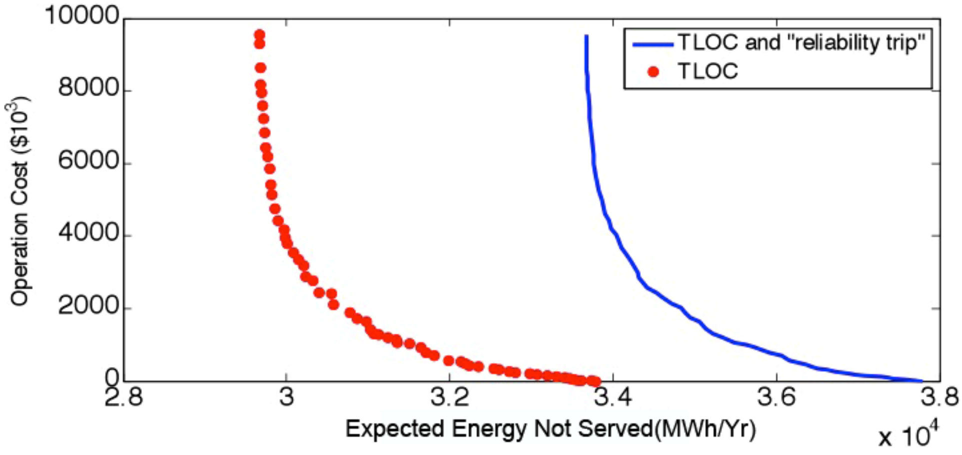

Fig. 5.13 Evaluation of the Expected Energy Not Served Before and After Including "Reliability Trip"

5.6.3. Improvement of different maintenance strategies on circuit breakers and bus bars

Generally speaking, if a more effective maintenance actions are taken, the equipment can operate longer, and at a particular time, its condition will be better. Such effects of different maintenance actions on the circuit breaker and bus bar are illustrated in Fig. 5.14 with life curves.

The concept of life curve has been introduced in Section 5.4.3, and the way to generate a life curve has been described in case study 1: RBTS. In this case study, two extreme maintenance strategies, namely no & major maintenance, and one most compromised maintenance solution are selected for demonstration purpose. The minor maintenance strategy is not shown here as in case study 1, because the relative merits of the most compromised maintenance with comparison to minor maintenance is sensitive to the setting of parameters of maintenance cost. Major maintenance aims to restore components to "as good as new" with sharply increased costs [8]. Effects of both extreme and the most compromised maintenance strategies are shown in Fig. 5.14.

Take the most compromised maintenance strategy for one circuit breaker in Bus-01 as an example, maintenance will cost $\$1.61\times10^5$ over the twenty-year planning horizon; it however will lead to the increase of average life of the breaker by 13.5% (from 114.3 years to 129.7 years).

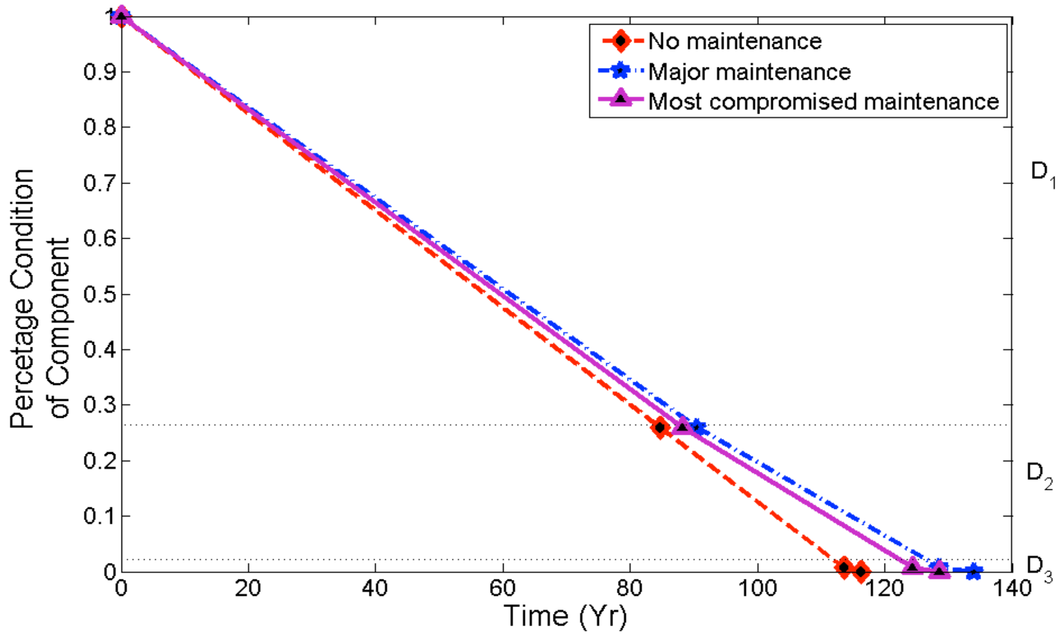

(a)

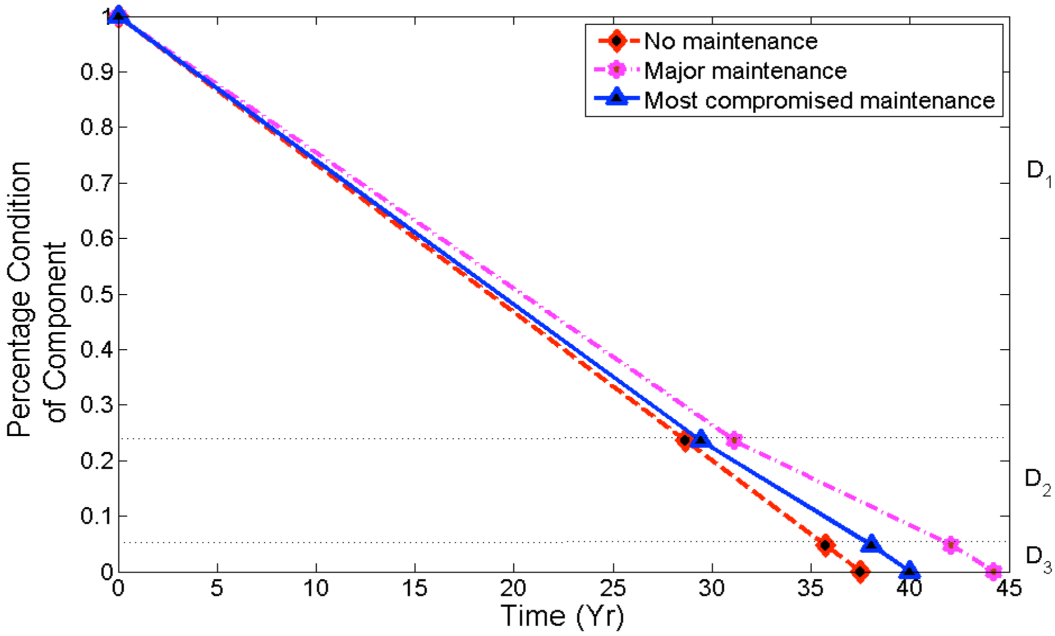

(b)
Fig. 5.14 Life Curves under Different Maintenance Strategies of:
(a) circuit breaker, and (b) bus bar

5.7. Conclusion

An integrated methodology is proposed to effectively schedule preventive maintenance for key components in a composite power system by optimizing the three objectives of reliability, maintenance and failure costs. A new time- and maintenance-dependent Markov process has been constructed for describing the impact of gradual deterioration and various maintenance strategies on the reliability of individual components over the maintenance horizon. The energy loss of each load point due to both the total loss of continuity within a substation and the loss of continuity and a violation of transfer limit between substations is evaluated using DC load flow and minimum cut set method. The three objectives have been evaluated by the models above and Pareto fronts are formulated to provide a holistic view showing the outcomes of these optimal maintenance strategies. An improvement of the representation of maintenance strategies is presented. Simulation results on the RBTS and IEEE RTS as well as the individual components demonstrate the potentials and ease of application of the proposed approach for handling complex configurations.

CHAPTER 6 IMPLEMENTATION OF MAINTENANCE FOR OFFSHORE SUBSTATIONS

Offshore systems are often remotely located and their access for data acquisition, inspection, and maintenance may be extremely difficult. The information collected during operation can rarely avoid uncertainties. Unlike traditional maintenance optimization methodologies that only consider the equipment's lifetime distribution [103-107], a systematic approach including an adaptive maintenance advisor and a system maintenance optimizer are proposed here for effectively handling the planned and unplanned operational variations for continuous condition-based maintenance. First, the maintenance advisor receives and implements the maintenance plans for its key components from the system maintenance optimizer, which optimizes the maintenance schedules with multi-objective evolutionary algorithm by considering only design/ average operational conditions. During operation, equipment in all the substations will experience continual ageing, control shifts, changing weather and load factors, and uncertain measurements. Residing on each substation, the maintenance advisor receives initial maintenance plans for all its equipments; and estimates using hierarchical fuzzy logic their reliability changes caused by all these operational variations. It will also report to the maintenance optimizer any excessive reliability deterioration in each substation. The maintenance optimizer will then re-optimize the maintenance activities in order to meet the overall reliability. An offshore substation connected to a medium-sized onshore grid will be studied here to demonstrate the ability of this proposed approach for handling operational variations occurring during implementation with manageable computational complexity.

Some material in this chapter has also appeared in [1] of the candidate's publications.

6.1. Introduction

In an offshore substation, operational uncertainties and variations occur continually, which can pronouncedly degrade the reliability and cost-effective maintenance scheduling of power systems. Unfortunately, it is often difficult to obtain exact reliability indices using conventional reliability analysis especially when conditions vary.

Fuzzy sets theory was proposed by Zadeh [59] to resemble human reasoning under uncertainties by using approximate information [34] to generate proper decision. Some attempt using type-1 fuzzy logic has also been carried out to handle uncertainties related to component reliability [58] in power-system maintenance problems. Fuzzy Markov model was employed to describe transition rates [68]. Zadeh further proposed the alternative type-2 fuzzy logic [69] in order to handle the uncertainties in type-1 membership functions. In power-system applications, planned and unplanned operational variations occur continually, which can degrade the quality of maintenance scheduling of power systems. Such degradations can even be more pronounced for offshore power systems. The unplanned operational variations occurring in offshore substations are represented in [108] by an independent set of fuzzy memberships for ensuring the quality of maintenance scheduling. In this work, a hierarchical fuzzy system with a variable structure, which engages low-level fuzzy memberships that represent planned operational variations occurring in each offshore substation; as well as supervisory- or high-level fuzzy memberships that map the unplanned operational variations as perturbations in parameters defining each respective membership function of the low-level system. As shown in Fig. 1.1, a maintenance advisor using the hierarchical fuzzy logic in each off-shore substation is linked to its connected power grid, for alternatively implementing and optimizing the maintenance schedules of the off-shore substation. This chapter will describe how these two tasks are efficiently carried out by careful management of computational complexity and design of fuzzy rule base.

Chapter 5 presents an optimizer using Pareto-based multi-objective evolutionary-algorithm is developed for synthesizing the maintenance schedules of a medium-sized power system**,** which provides the best tradeoff between its reliability and costs of maintenance. During implementation, the equipment reliability data will change according to the actual operational conditions. The initial optimal solutions will become sub-optimal, either under- or over-maintained. To re-establish the optimal solutions, the equipment reliability data will have to be re-estimated according to the new operational conditions and the maintenance schedules will have to be re-optimized according to the re-estimated reliability data.

Fig. 1.1 illustrates our proposed approach for re-establishing the Pareto-optimal maintenance solutions according to the actual operational variations during implementation. Residing on each substation, the maintenance advisor receives and implements the initial or updated maintenance plan for all its equipments from the system maintenance optimizer. In this process, the maintenance advisor will keep track of operational variations arising from ageing, weather, load factors, measurement and human-judgment uncertainties detected from key equipments.

Using a hierarchical fuzzy logic, the maintenance advisor estimates the change of reliability parameters due to the operational variations and uncertainties of its components and sends the changes back to the system maintenance optimizer. The maintenance optimizer assesses the load-point reliability and any drastic deterioration within the substation, which may lead to the dynamic re-optimization of the substation's maintenance activities during operation for balancing the reliability benefits and the cost of maintenance.

6.2. Updating reliability parameters for each component

Reliability indices, such as mean time to failure (MTTF) and failure probability (p_f), will not remain constant due to operational variations [108]. Changes of above reliability indices $\Delta\Lambda(t) = [\Delta\Lambda_{MTTF}(t)\ \ \Delta\Lambda_f(t)]$, which include MTTF ($\Delta\Lambda_{MTTF}(t)$) and p_f ($\Delta\Lambda_{p_f}(t)$), are calculated for each component using the following fuzzy logic system:

$$\Delta\Lambda(t) = f_H(C(t)) \qquad (6.1)$$

where C(t) represents the set of operational variations of each component, and f_H represents the mapping function of the proposed fuzzy logic system from input to output.

Having calculated $\Delta\Lambda(t)$, the actual reliability indices of components are updated according to operational variations by:

$$\begin{aligned} MTTF(t) &= MTTF(t-1) + \Delta\Lambda_{MTTF}(t) \\ p_f(t) &= p_f(t-1) + \Delta\Lambda_{p_f}(t) \end{aligned} \tag{6.2}$$

where MTTF and p_f are the original reliability indices obtained from the Markov model, and MTTF' and p_f' are the updated indices following the standard steps [90].

A hierarchical fuzzy logic system is proposed here for handling planned and unplanned operational variations of key components in each substation. Each operational variation as in *C(t)* is connected with the others by fuzzy linguistic rules, which are derived from both the expert knowledge and mathematical strategies [60, 69]. Once the rules are established, the fuzzy logic system is used as a mapping function f_H from the input *C(t)* to the output *ΔΛ(t)*.

6.3. Overall scheme of hierarchical fuzzy logic system

The proposed fuzzy logic system has a computationally efficient two-level structure for each component (see Section 6.5.2 for case studies). Inputs in the low level collect the amount of all planned operational variations occurring in each component. Fuzzy rules at this level then update the collective impacts of all planned operational variations on reliability indices on each respective component. The supervisory level deals with all the unplanned operational variations on each component in a similar manner. Several parallel fuzzy logic units in the supervisory level are engaged with each using one unplanned operational variation as the input for evaluating its respective impact on the component's reliability. The low level also connected all planned and unplanned operational variations on each component for evaluating their overall impacts $\Delta\Lambda(t)$ on its reliability indices.

Mathematically, all planned and unplanned operational variations are considered in parallel as follows:

$$\Delta\Lambda(t) = f_{1L}(X_{1L}, f_{2L}^{(1)}(X_{2L}^{(1)}),..., f_{2L}^{(i)}(X_{2L}^{(i)}),..., f_{2L}^{(n)}(X_{2L}^{(n)}) \qquad (6.3)$$

where X_{1L} represents the input of planned operational variations to the low-level fuzzy logic system, and $X_{2L}^{(i)}$ represents the input of unplanned operational variation to the i^{th} supervisory-level fuzzy logic unit. f_{1L} and $f_{2L}^{(i)}$ are the mapping functions from inputs X_{1L} & $X_{2L}^{(i)}$ to the output of the low-level fuzzy logic system and the i^{th} supervisory-level fuzzy logic unit respectively. n is the number of parallel fuzzy logic units in the supervisory level, which is equal to the number of unplanned operational variations considered for each component.

Taking for example the transformer in our study offshore substation, X_{1L} is an input vector representing variations of age, load, and operating temperature. Two supervisory-level fuzzy logic units are used in parallel, within which $X_{2L}^{(1)}$ and $X_{2L}^{(2)}$ represent respectively variations of insulation degradation level [109] and ambient temperature of the transformer. As shown in Fig. 6.1, $f_{2L}^{(1)}(X_{2L}^{(1)})$ and $f_{2L}^{(2)}(X_{2L}^{(2)})$ give the corresponding impacts on reliability indices, which are considered together with the planned operational variations X_{1L} (age and operating temperature) in the low level for calculating the overall impacts $\Delta\Lambda(t)$. For the circuit breaker, X_{1L} denotes the age variation from the design age in the low level. Only one supervisory-level fuzzy logic unit with $X_{2L}^{(1)}$ as the input is used for the circuit breaker for representing its defects level [12], which brings together the impact on the reliability indices with variation of age in the low level.

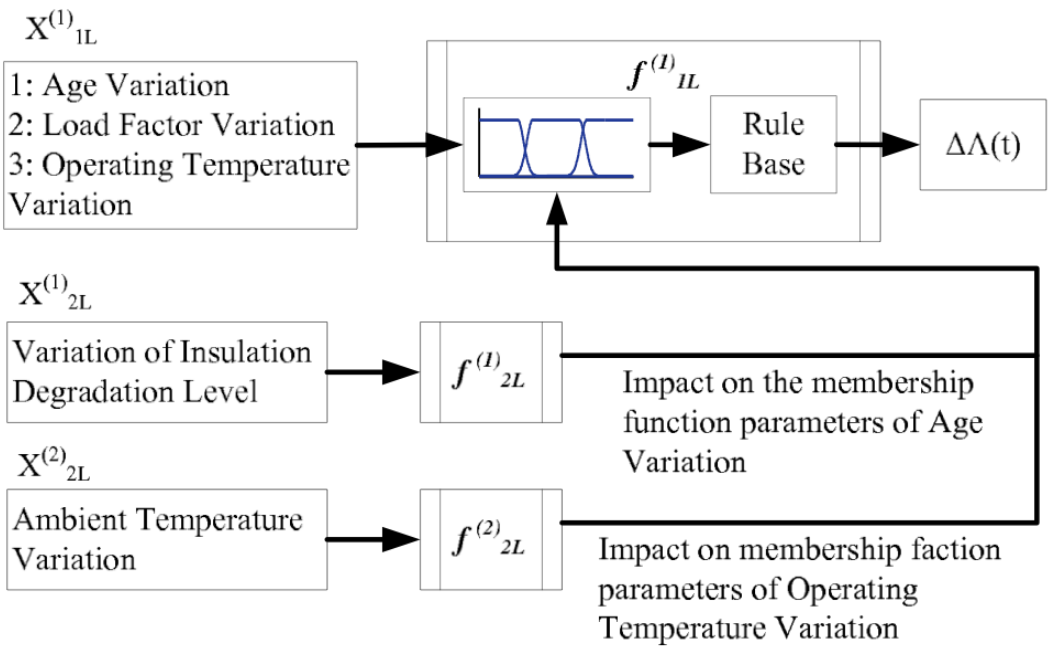

Fig. 6.1 Structure of Hierarchical Fuzzy Logic System for Each Transformer

6.4. Fuzzy representation of planned and unplanned operational variations and fuzzy inference process

The change of MTTF, $\Delta\Lambda_{MTTF}(t)$, is used here as the output to assess the impacts of operational variations on component reliability. The change in p_f, $\Delta\Lambda_{p_f}(t)$, can be treated as the output of a low-level fuzzy logic system obtained in a similar fuzzy inference process. The universe of discourse of each input and its output is quantized in overlapping fuzzy sets as represented by their corresponding low- or supervisory-level fuzzy membership functions:

(i) Low-level Fuzzy Membership Functions: Ageing, load and operating temperature increases, will worsen reliability. Figs. 6.2 (a)-(c) show these operational variations represented in various linguistic levels. Five output linguistic levels [MW, SW, UC, SB, MB] in Fig. 6.2(d) represent the change of MTTF of each transformer as in “Much Worse”, “Slightly Worse”, “UnChanged”, “Slightly Better”, and “Much Better”. Similar to Fig. 6.2(a), Fig. 6.4(a) shows the representation of age variations of circuit breaker. In Fig. 6.4(b), three low-level fuzzy logic variables [MW, UC, MB] are used to represent the change of MTTF for each circuit breaker. Each planned operational variation and the change of MTTF, are connected by the “IF-THEN” rules in the low-level fuzzy logic system. For example, in Figs. 6.2 (a)-(d), if inputs are [(a)(the age variation is “older”) and (b)(the load factor variation is “heavier”), and (c)(the operating temperature variation is “higher”)], then the output is [(d)(the change of MTTF for this transformer will be “MW”)].

(ii) Supervisory-level Fuzzy Membership Functions: The set of unplanned operational variations represented in this work are for each transformer its insulation degradation and ambient temperature variation, and each circuit breaker its defects such as those occurring in trip coils. Degradation in transformer insulation can be detected with Dissolved Gas Analysis [109] with transformer-oil samples. The universe of discourse of insulation degradation is quantized into [better, same, worse] as in Fig. 6.4(a); whereas variations of ambient temperature are quantized into [lower, same, higher] as shown in Fig. 6.4(b). The trip-coil defects in circuit breakers can be detected by current signature [12], which are quantized in [better, same, worse] as in Fig. 6.5(a).

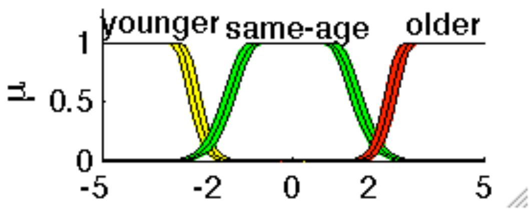

(a) Input: Age Variation (Yr)

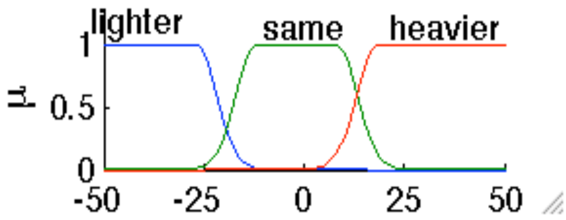

(b) Input: Load Factor Variation (%)

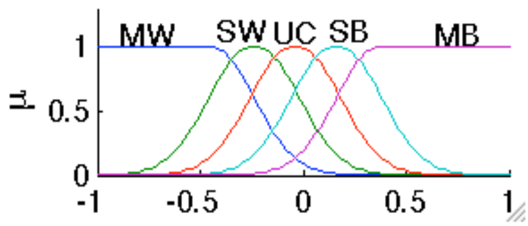

(d) Output due to Figs. 6.2 (a)-(c) & Figs. 6.4 (c)-(d)

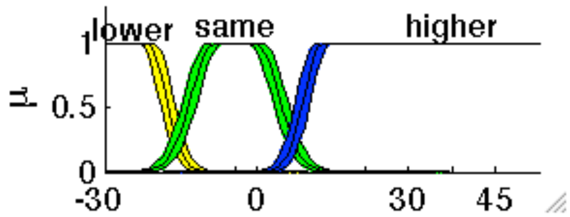

(c) Input: Operating Temperature Variation (°C)

Fig. 6.2 Low-level Membership Functions for Each Transformer

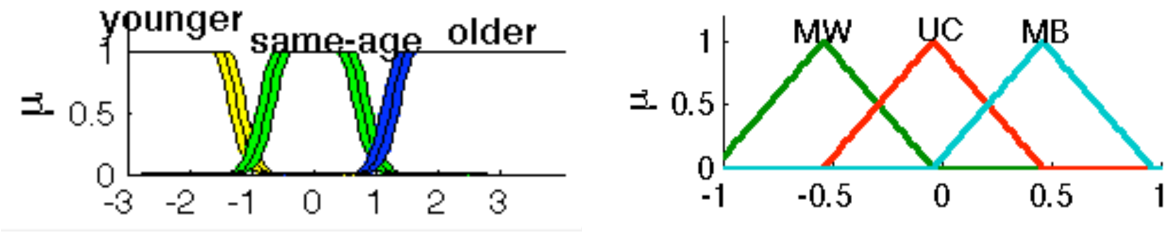

(a) Input: Age Variation (Yr) (b) Output due to Fig. 6.3 (a) & Fig. 6.5 (b)

Fig. 6.3 Low-level Membership Functions for Each Circuit Breaker

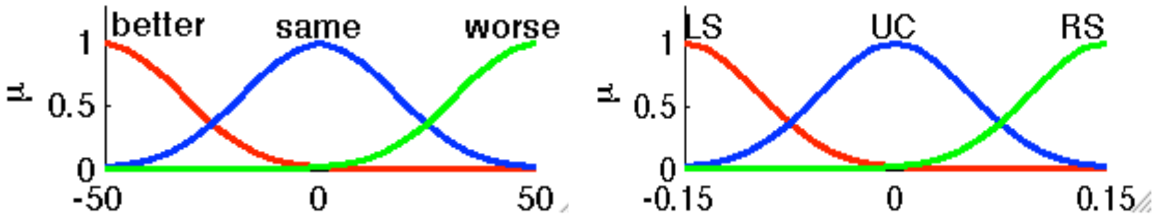

(a) Input: Variation of Insulation Degradation Level (%)

(c) Impacts on Functions in Fig. 6.2 (a) due to Variations in Fig. 6.4 (a)

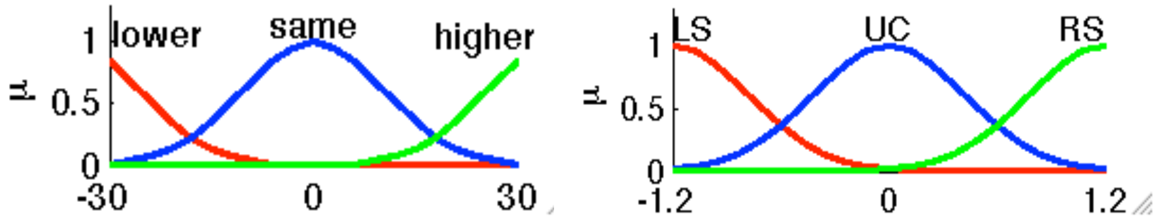

(b) Input: Ambient Temperature Variation (°C)

(d) Impacts on Functions in Fig. 6.2 (c) due to Variations in Fig. 6.4 (b)

Fig. 6.4 Supervisory-level Membership Functions for Each Transformer

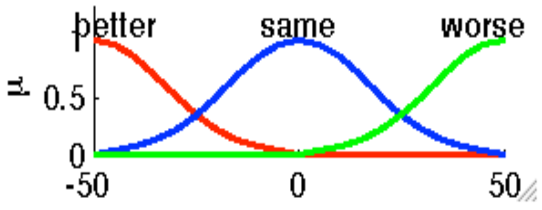

(a) Input: Variation of Trip-coil Defects Level (%)

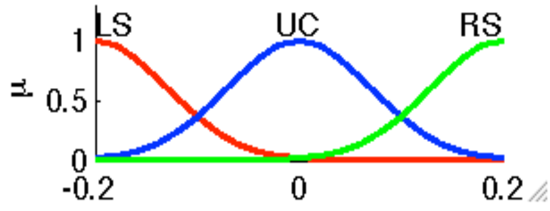

(b) Impacts on Functions in Fig. 6.3 (a) due to Variations in Fig. 6.5 (a)

Fig. 6.5 Supervisory-level Membership Functions for Each Circuit Breakers

(iii) Connecting Low- and Supervisory-level Fuzzy Membership Functions: Each unplanned operational variation brings about impact on reliability indices by influencing respective planned operational variation in the low level, as illustrated in Fig. 6.1. Taking for example Figs. 6.4 (a) and 6.2(a) as well as Figs. 6.4(d) and 6.2(c), the degradation of transformer insulation will speed up transformer ageing; whereas the change of ambient temperature will have an impact on each transformer's operating temperature. The influence on respective low-level input can be achieved by shifting its corresponding membership function along the universe of discourse. The resultant shifting is quantized into [LS, UC, RS] to represent "Left Shift", "UnChanged", and "Right Shift", as in Figs. 6.4(c)&(d) and Fig. 6.5(b). Each unplanned operational variation and the consequent shifting are connected by the "IF-THEN" rules in each supervisory-level fuzzy logic unit. For example, in Figs. 6.4 (a) &(c), if the input is [(a)(the variation of insulation degradation level is "worse")], then the output is [(c)(the shifting of membership function for the age variation (represented in Fig. 6.2(a)) will be "LS"]. The resultant shifting the low-level membership functions is represented by the shaded area in Figs. 6.2(a) & (c) and Fig. 6.3(a).

6.5. Results and discussions

6.5.1. Description of offshore substation used in case studies

Fig. 6.6 shows the ring substation of Bus 07 of IEEE-RTS [98], whose load-point reliabilities are affected by the reliabilities of transformers T1-T5 and circuit breakers CB1-CB5. Reliabilities of generators G1-G3 are assumed constant. As Bus 07 is assumed to be an offshore substation, the transformer and circuit breaker reliability are affected by planned as well as unplanned operational variations. The study period is set for 20 years.

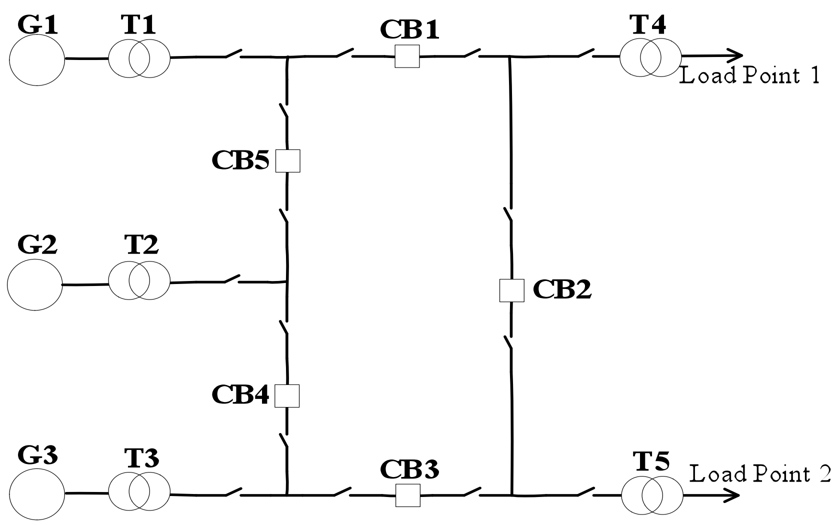

Fig. 6.6 One Line Diagram of Bus 07 in IEEE-RTS

The two load points in Fig. 6.6 are assigned different priorities with load point 2 having a higher priority because it transfers most of the output from generators G1—G3 to the connected grid. Load point 1 has a lower priority because it provides a smaller part of the output from generators G1—G3 to local consumers. The population size for NSGA II is set at 80, the number of generations is 90, and the crossover and mutation rates are set at 0.8 and 0.05 respectively. The maintenance cost data is listed in [100].

6.5.2. Specification of the base case and the three scenario-study cases

Three scenario-study cases are specified as below for showing the application of our proposed approach for re-establishing the optimal maintenance schedules during implementation and meeting ***new*** operational variations. For comparison, a base-case study is also carried out.

Specification of Base Case with maintenance plans previously optimized using assumed average operational conditions (Table 6.1). We assume a linear ageing process and the same age for all components from the beginning of the maintenance period. Other planned operational conditions (load and operating temperature) are assumed constant throughout the maintenance period. No unplanned operational conditions are considered. In other word, the unplanned operational variations are assumed to be zero.

Specification of the Three Scenario-study Cases:

During implementation, all components will experience different ageing and/ or different operational variations. To demonstrate this, three scenario study cases are listed below:

Scenario 1: worse-than-anticipated ageing & deteriorations where each transformer and each circuit breaker in Fig. 6.6 are suffering from worse ageing than the base case from the beginning of the study period. These elements will also experience a new set of insulation degradation and trip-coil defects as shown in Fig. 6.7. Consequently, the base-case maintenance activities will not be able to meet the required reliability leading to higher energy-not-served and failure cost. Therefore, maintenance activities will need to be re-optimized according to the excessive ageing and deteriorations for providing higher reliability.

Scenario 2: lower-than-anticipated transformer loading where reliability indices of the respective transformers have to be re-estimated according to the new loads (Fig. 6.8), which will necessitate re-optimization and scale-down of maintenance activities.

Scenario 3: worse-than-anticipated working environment and ambient temperature where transformer reliabilities are deteriorating excessively as in Fig. 6.9, which will necessitate re-optimization and scale-up of maintenance activities. This is similar but not exactly the same as Scenario 1, where our methodology will deal with them differently.

The remaining section will show how the proposed hierarchical fuzzy logic system is effective for re-establishing the optimal maintenance schedules for the four above study cases. We assume the same operational conditions for all the components of each same type in each scenario.

Table 6.1 Average Operational Conditions for Base Case Optimization

Condition \ Component	Transformer	Circuit breaker
Age (Yr)	Increase from 1 (beginning of study period) to 20 (end of study period)	Increase from 1(beginning of study period) to 20 (end of study period)
Load factor (%)	50	--
Average operating temperature (°C)	30	--

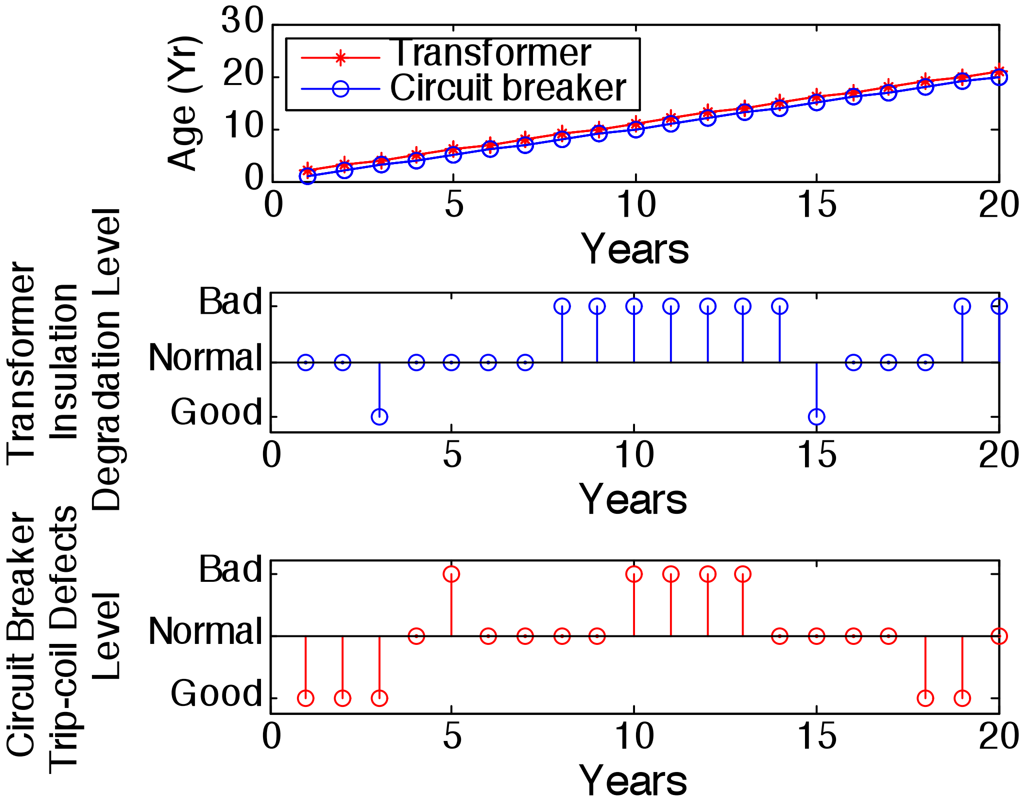

Fig. 6.7 Worse-than-anticipated Ageing & Deterioration

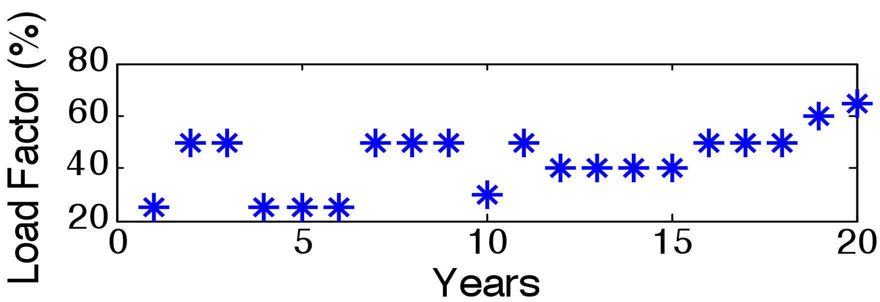

Fig. 6.8 Better-than-anticipated Transformer Load Factor

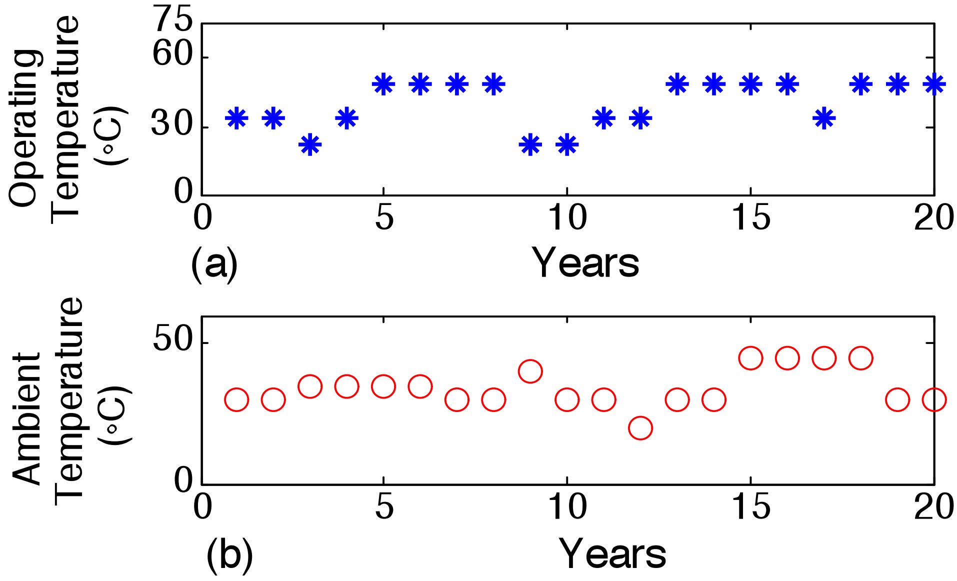

Fig. 6.9 Worst-than-anticipated Working Environment & Ambient Temperature

6.5.3. Study results -- impacts of operational variations and on optimal maintenance schedules

<u>**Scenario 1 Results: worse-than-anticipated ageing & deteriorations**</u> Age variations of each transformer and circuit breaker are represented by the low-level membership function as in Figs. 6.2(a)&6.3(a). Variations of insulation degradation level of each transformer and the trip-coil defects level of each circuit breaker are assessed as shown in Fig. 6.7 and each represented by the supervisory-level membership functions in Figs. 6.4(a)&6.5(a).

Figs. 6.10 (a) & (b) show the variation of MTTF of the transformer (T1) and circuit breaker (CB1) by implementing the base-case maintenance plan. Comparing with the base case, it is seen that due to excessive ageing and deteriorations, the MTTF's of each transformer and circuit breaker are lower than those under Scenario 1. The

overall expected energy not served (EENS) in Scenario 1 is also more than the base case as shown in Fig. 6.11.

The Pareto front in Fig. 6.12 shows that the proposed fuzzy expert system helps to re-establish optimal maintenance schedules and maintain the schedules *"Opt1"* on the pareto-optimal front. As shown in Fig. 6.12, one solution on the Pareto-optimal front for the base case, *Opt-base*, is chosen as the best solution with EENS of 1.204×10^4MWh/y, failure cost of $\$2.231\times10^5$, and operational cost of $\$4.890\times10^5$. However, *Opt-base* will no longer be optimal for Scenario 1 due to new operating conditions. Implementing *Opt-base* to Scenario 1 will result in higher EENS of 1.247×10^4 MWh/y and higher failure cost of $\$2.314\times10^5$, as denoted by *Sub1* in Fig. 6.12 (a)&(b). Therefore, a new Pareto-optimal front is obtained by re-optimizing the maintenance schedules. A new optimal schedule *Opt1* is obtained as a result of the collaborative effort of the maintenance optimizer and the maintenance advisor (Fig. 1.1), providing a higher reliability than *Sub1* with the same operational cost. The maintenance gains and costs of *Sub1* and *Opt1* are listed in Table 6.2.

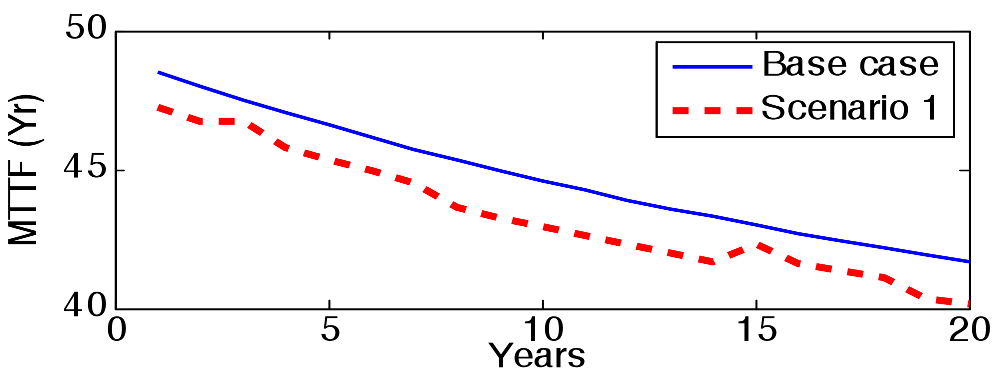

(a) Transformer

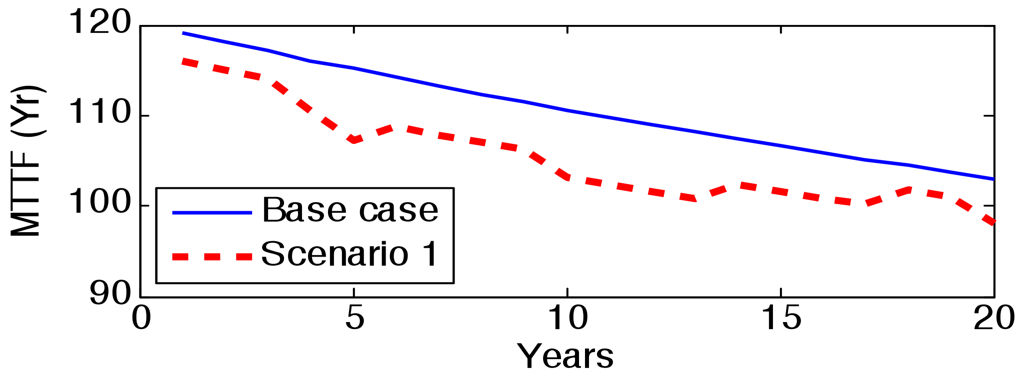

(b) Circuit Breaker
Fig. 6.10 Variations of MTTF after Implementing Base-case Maintenance Plan

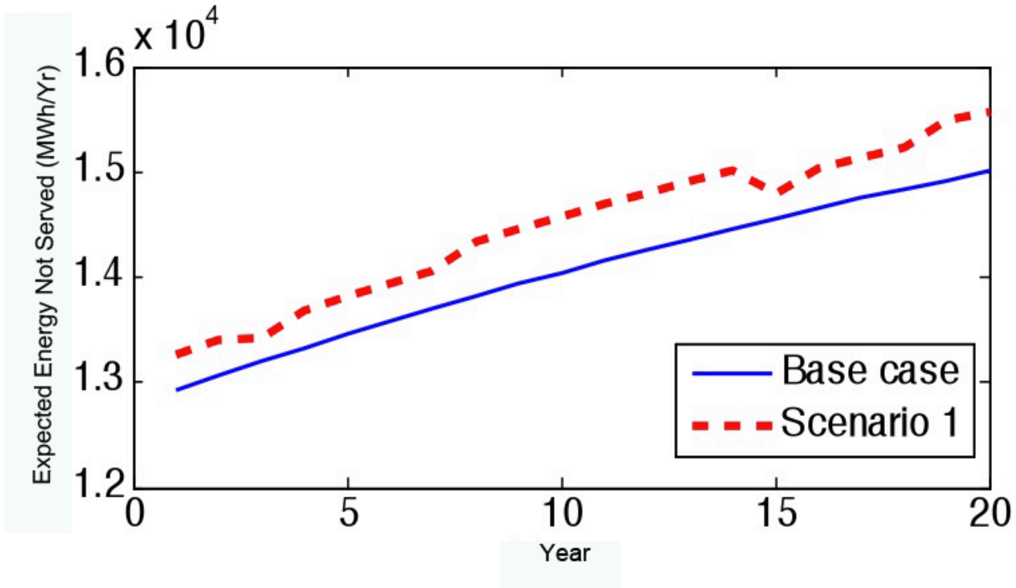

Fig. 6.11 Variation of Expected Energy Not Served after Implementing Base-case Maintenance Plan

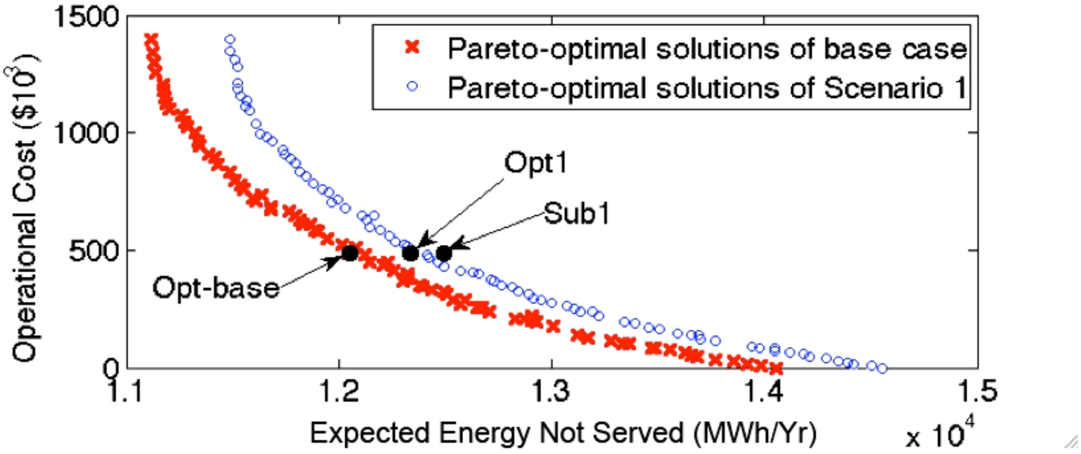

(a) Operational Cost VS. Expected Energy Not Served

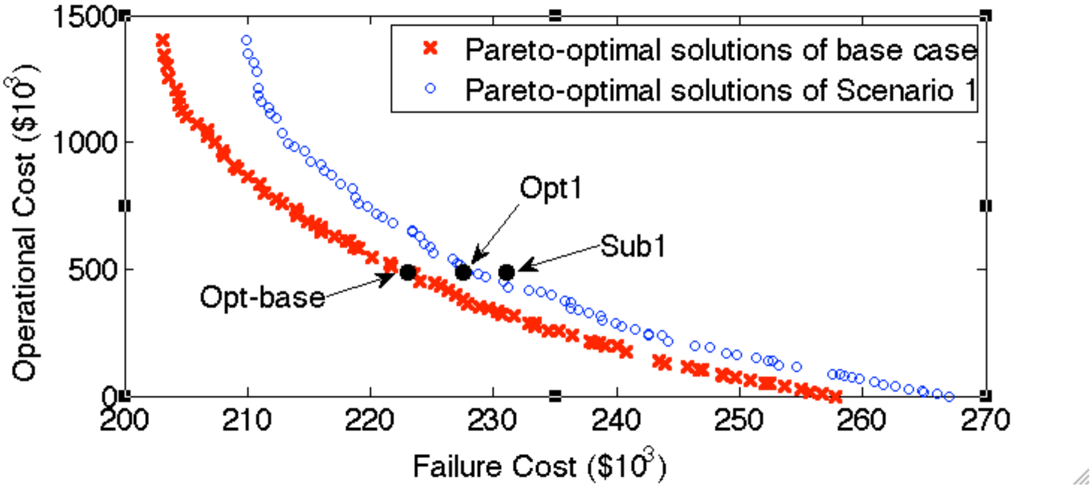

(b) Operational Cost VS. Failure Cost

Fig. 6.12 Pareto fronts of Base-case and Scenario 1 Studies

<u>Scenario 2 Results: lower-than-anticipated transformer loading</u> The load factor variation of each transformer is represented by the low-level membership functions in Fig. 6.2(b). In this scenario, maintenance activities will become excessive if the base-case schedules are implemented directly. Sub2 and Opt2 in Table 6.2 show the reliability gains and costs of directly implementing Opt-base to this scenario and re-optimizing the schedules, respectively. Comparing Sub2 with Opt2, it is seen that Opt2 provides lower EENS and failure cost than Sub2 with the same operational cost. The result here demonstrates the necessity of re-establishing optimal schedules for this scenario.

Scenario 3 Results: worse-than-anticipated temperature The operating temperature and ambient temperature of each transformer are each represented by the low- and supervisory-level membership functions in Figs. 6.2(c)&6.4(b). Our proposed hierarchical fuzzy logic indicates correctly that higher-than-anticipated operating temperature and ambient temperature degrade reliability. As a result, it is necessary to re-establish maintenance schedules. *Sub3* in Table 6.2 shows the reliability and costs from directly implementing *Opt-base* to this scenario, and *Opt3* is one re-established solution. It is obvious that *Sub3* is not optimal because it causes worse reliability with the same operational cost than *Opt3*.

Table 6.2 Reliability Gains & Maintenance Costs

Study scenarios	Maintenance schedules	Operational cost ($\$\times10^5$)	Expected Energy not served (EENS) ($MWh/y\times10^4$)	Failure cost ($\$\times10^5$)
Base case	Opt-base	4.890	1.204	2.231
Different Scenarios of Planned and Unplanned Operational Variations				
Scenario 1	Sub1	4.890	1.247	2.314
	Opt1	4.890	1.234	2.279
Scenario 2	Sub2	4.890	1.196	2.229
	Opt2	4.890	1.180	2.201
Scenario 3	Sub3	4.890	1.261	2.346
	Opt3	4.890	1.250	2.324

6.5.4. Computational simplicity of our proposed hierarchical fuzzy system

The proposed low-level fuzzy logic system for the transformer contains 3^3 rules with the 3 planned operational variations as inputs, each of which is quantized into 3 linguistic variables. In addition, the proposed supervisory-level fuzzy logic takes 2 unplanned operational variations as inputs, each of which is quantized into 3 linguistic variables. Altogether, our hierarchical fuzzy system for the transformer contains $33(=3^3+3\times2)$ rules. On the other hand, the standard type-1 fuzzy logic will need $243(=3^{(3+2)})$ rules to contain the same number of planned and unplanned operational variations. Therefore, the proposed hierarchical fuzzy is superior to the standard type-1 fuzzy logic in terms computational simplicity and rule-base size.

6.6. Conclusion

This chapter proposes a modular and flexible architecture for updating the change of load-point reliability resulting from operational variations during implementation of a system-optimized maintenance plan. The proposed maintenance advisor will report any excessive deterioration of load-point reliability within each substation, and require the maintenance optimizer to dynamically re-establish the substation's optimal maintenance activities for meeting the desired reliability with lowest cost during operation.

Hierarchical fuzzy logic is demonstrated to be computationally more efficient than standard type-1 fuzzy logic for handling planned and unplanned operational variations arising from ageing, load factor, and working condition and environment of transformers and circuit breakers. These operational variations are shown to have significant impacts on the maintenance scheduling of offshore substations.

One main contribution of this work is on development of an online platform residing on each offshore substation for providing users with a library of automatic, robust, flexible, modular, expandable and intelligent algorithms for optimizing and implementing condition-based maintenance on offshore power systems, while responding promptly and efficiently to unpredictable operational and weather variations frequently encountered during offshore operations. The platform will also facilitate incorporating other techniques for performance comparison and further development.

CHAPTER 7 CONCLUSIONS AND RECOMMENDATIONS

This chapter concludes the study on optimization and implementation of preventive maintenance schedules in power systems presented in former chapters. Contributions made in this research and the improvements comparing to previous studies in this area are summarized. Some recommendations for future work on the condition-based maintenance scheduling for power systems are presented.

7.1. Conclusions

This thesis reports successful optimization and implementation of maintenance schedules using multi-objective evolutionary algorithms and hierarchical fuzzy logic system. The objectives of this work as defined in Section 1.3 have been fulfilled. The contributions are summarized in the following paragraphs.

7.1.1. Optimization of maintenance schedule

The two-level reliability model in every stage of this work successfully establishes the quantitative relationship between the reliability and costs of inspections and various maintenance activities.

The Markov model in the component-specific level allows predicting the deterioration process of individual component. Compared to the ideal maintenance models in [16, 110], The Markov model in this work increases the accuracy of predicting reliability by incorporating the probabilistic failures undetected by periodic inspections. Furthermore, unlike the conventional homogeneous Markov model with constant transition rates, the strength of this model comes from time- and decision-dependent transition probability/rate between each of the two deterioration states for incorporating the effect of ageing and maintenance. The life curve of individual component demonstrates that the impacts of different inspection frequencies and maintenance schedules on the reliability of individual component are successfully modeled.

The collective effects of maintenance are evaluated in the system-specific level that takes into account the impact of topological and other dependence among multiple components. Network modeling method allows direct simplifying all the series- or parallel-connected configurations of substations. Minimum cut set method can be easily applied either manually or by computer. Furthermore, the ability to handle complex configurations and combination of simultaneous failure events makes it more advantageous to incorporate various failure modes of components, protection and switching actions, and various constraints into the system reliability analysis. The use of a lookup table containing the line outage distribution factors for all transmission lines avoids repeating DC load flow analysis with every line outage event. Using this lookup table, the line whose outage leads to the overloading on another line can be easily and efficiently identified and treated as an event in the minimum cut set of corresponding overloaded line. The Pareto optimal maintenance schedules considering the energy loss due to both total loss of continuity and violation of transfer limit is compared with that only considering the total loss of continuity demonstrating that the load flow constraints between substations in a composite power system (IEEE RTS) are successfully incorporated.

Based on the reliability model, a fast and effective maintenance optimizer, which uses multi-objective evolutionary algorithms, has been developed. Pareto-based multi-objective evolutionary algorithms effectively deal with this combinatorial problem during the search process by evaluating all the potential maintenance schedules in parallel, and treat all the objectives with equal priority for optimization. An efficient and dynamic sharing algorithm based on the population distribution at current generation has been added in generic MOEA, reducing the number of parameters required to be defined by the user through getting rid of the sharing parameter. Higher computational efficiency is obtained by using NSGA II and NSGAII-DE has been employed to further improve the efficiency of optimization. Furthermore, the elitism in NSGA II is further strengthened by adding the optimal solutions that are obtained from optimizing each individual objective into the initial solutions to achieve the most diverse spread of optimal solutions and provide the decision maker more feasible choices. A novel representation of solutions [94, 111] has been improved to significantly reduce the storage space and computational complexity compared to conventional representation methods.

With the increasing awareness concerned with finding a balance between reliability and cost, the objective is to minimize simultaneously the overall operational cost, expected energy not served, and failure cost. Simulations carried out first on various basic substation configurations and then on medium-size power systems (RBTS and IEEE RTS), show that this optimizer is effective in scheduling the inspection frequencies and preventive maintenance schedules, ensuring an appropriate trade-off between reliability and costs. The use of multi-objective evolutionary algorithms simplifies the problem by avoiding the decision maker's subjective preference before optimization. Instead, the Pareto front provides a holistic view of relationships between multiple conflicting objectives. It supplies the decision maker a set of optimal solutions rather than only one, where the decision maker can find his best choice according to his preference. Another important information among all the Pareto-optimal solutions is the most compromised solution. It is extracted by the decision maker to achieve desired operating goals through adjusting the weights to the system reliability or cost.

7.1.2. Implementation of maintenance schedule

A unique adaptive condition-based maintenance advisor using hierarchical fuzzy logic has been developed for tracking the day-to-day operational conditions and accordingly updating reliability indices of components within offshore substation. Compared with the reliability under design/average operational conditions, reliability variations of both individual component and overall substation show the impact of planned and unplanned operational variations has been successfully captured by the maintenance advisor. Using a computationally efficient two-level fuzzy logic system, an innovative fuzzy inference method employing low- and supervisory-level membership functions has been developed. The influence of each unplanned operational variation on the component reliability is captured in each corresponding supervisory-level fuzzy logic unit by producing parametric perturbations to its respective low-level membership function. The strength of this technique comes from its powerful hierarchical structure in handling additional unplanned operational variations and remarkable reduction of rule base compared to the conventional type-1 fuzzy logic.

The ability of maintenance advisor to incorporate updated planned and unplanned operational variations makes it straightforward to cooperate with maintenance optimizer. Thus, an integrated approach consisting of adaptive maintenance advisor multi-objective optimizer is developed for re-estimating the component reliability data according to the new operational variations and re-establishing the optimal maintenance schedules according to the updated reliability data. Simulations conducted on offshore substation show that the Pareto-optimal maintenance schedules obtained under design/average operational conditions become sub-optimal if implemented in the scenarios of new operational conditions. Pareto-optimal maintenance schedules are efficiently and successfully re-established and higher reliability is achieved than the sub-optimal schedules.

7.2. Recommendations

The successful application to the simple test systems and IEEE test systems has proved that this proposed scheme has its potential to be applied to large-scale real-world power systems if given available data. To be applied to real-world problems, there are several investigations that are worth further exploration. These are enumerated as follows:

Future improvement to the reliability model for individual component can be done by using real-world long-term historical data of conditions and maintenance schedule to further elaborate the parameters of Markov model.

Future work can be done involving extensions and modifications of the proposed maintenance optimizer to include more constraints related to limited maintenance resources and manpower. Modification to this optimizer can be made to eliminate the unfeasible schedules during the search process or penalize the violation of constraints in the objective function.

Further improvement to the current maintenance advisor can be made using a more complete data and larger rule base and refining the fuzzy membership functions and fuzzy inference. This improvement may require mass data pertaining to the condition-monitoring of key equipments in offshore substations and optimization technique to find the best suited parameters defining the membership functions.

REFERENCES

1. Wireman, T., *World Class Maintenance Management*. 1990, New York: Industrial Press.
2. Bevilacqua, M. and M. Braglia, *The analytic hierarchy process applied to maintenance strategy selection.* Reliability Engineering & System Safety, 2000. **70**(1): p. 71-83.
3. Waeyenbergh, G. and L. Pintelon, *Maintenance concept development: A case study.* International Journal of Production Economics, 2004. **89**(3): p. 395-405.
4. Mechefske, C.K. and Z. Wang, *Using fuzzy linguistics to select optimum maintenance and condition monitoring strategies.* Mechanical Systems and Signal Processing, 2003. **17**(2): p. 305-316.
5. Mobley, R.K., *An Introduction to Preventive Maintenance*. 2nd ed. 2002, Amsterdam: New York : Butterworth-Heinemann.
6. Endrenyi, J., et al., *The present status of maintenance strategies and the impact of maintenance on reliability*, in *IEEE Transactions on Power Systems*. 2001, IEEE: USA. p. 638-46.
7. Sim, S.H. and J. Endrenyi, *OPTIMAL PREVENTIVE MAINTENANCE WITH REPAIR.* IEEE Transactions on Reliability, 1988. **37**(1): p. 92-96.
8. Sim, S.H. and J. Endrenyi, *A failure-repair model with minimal and major maintenance.* IEEE Transactions on Reliability, 1993. **42**(1): p. 134-40.
9. Jirutitijaroen, P. and C. Singh, *The effect of transformer maintenance parameters on reliability and cost: A probabilistic model.* Electric Power Systems Research, 2004. **72**(3): p. 213-224.

10. Wijnmalen, D.J.D. and J.A.M. Hontelez, *Review of a Markov decision algorithm for optimal inspections and revisions in a maintenance system with partial information.* European Journal of Operational Research, 1992. **62**(1): p. 96-104.

11. Castanier, B., A. Grall, and C. Berenguer, *A condition-based maintenance policy with non-periodic inspections for a two-unit series system.* Reliability Engineering & System Safety, 2005. **87**(1): p. 109-203.

12. Strachan, S.M., et al., *Providing decision support for the condition-based maintenance of circuit breakers through data mining of trip coil current signatures.* IEEE Transactions on Power Delivery, 2007. **22**(1): p. 178-86.

13. Lu, S., Y.-C. Tu, and H. Lu, *Predictive condition-based maintenance for continuously deteriorating systems.* Quality and Reliability Engineering International, 2007. **23**(1): p. 71-81.

14. Scarf, P.A., *On the application of mathematical models in maintenance.* European Journal of Operational Research, 1997. **99**(3): p. 493-506.

15. Endrenyi, J., G.J. Anders, and A.M. Leite da Silva, *Probabilistic evaluation of the effect of maintenance on reliability. An application [to power systems]*, in *IEEE Transactions on Power Systems*. 1998, IEEE: USA. p. 576-83.

16. Amari, S.V. and L. McLaughlin. *Optimal design of a condition-based maintenance model*. 2004. Los Angeles, CA., United states: Institute of Electrical and Electronics Engineers Inc.

17. Marseguerra, M., E. Zio, and L. Podofillini, *Condition-based maintenance optimization by means of genetic algorithms and Monte Carlo simulation.* Reliability Engineering & System Safety, 2002. **77**(2): p. 151-65.

18. Arshad, M. and S.M. Islam. *A novel fuzzy logic technique for power transformer asset management*. 2006. Tampa, FL, United states: Institute of Electrical and Electronics Engineers Inc.

19. Billinton, R. and R.N. Allan, *Reliability Evaluation of Power Systems*. Second ed. 1996, New York: Plenum Press.

20. Kumar, E.V., S.K. Chaturvedi, and A.W. Deshpande, *Maintenance of industrial equipment. Degree of certainty with fuzzy modelling using predictive maintenance.* International Journal of Quality & Reliability Management, 2009. **26**(2): p. 196-211.

21. Arshad, M., S.M. Islam, and A. Khaliq. *Power transformer aging and life extension*. 2004. Piscataway, NJ, USA: IEEE.

22. Muthanna, K.T., et al., *Transformer insulation life assessment.* IEEE Transactions on Power Delivery, 2006. **21**(1): p. 150-6.

23. Anders, G. and B. Kalinowski, *A new look at component maintenance practices and their effect on customer, station and system reliability.* International Journal of Electrical Power & Energy Systems, 2006. **28**(10): p. 679-95.

24. Anders, G.J., et al., *A probabilistic model for evaluating the remaining life of evaluating the remaining life of electrical insulation in rotating machines.* IEEE Transactions on Energy Conversion, 1990. **5**(4): p. 761-7.

25. Meeuwsen, J.J. and W.L. Kling, *Effects of preventive maintenance on circuit breakers and protection systems upon substation reliability.* Electric Power Systems Research, 1997. **40**(3): p. 181-8.

26. Coolen, F.P.A. and R. Dekker, *Analysis of a 2-phase model for optimization of condition-monitoring intervals.* IEEE Transactions on Reliability, 1995. **44**(3): p. 505-511.

27. *IEEE recommended practice for the design of reliable industrial and commercial power systems. (Color Book Series - Gold Book).* IEEE Std 493-1997 [IEEE Gold Book], 1998.

28. Propst, J.E., *Calculating electrical risk and reliability.* IEEE Transactions on Industry Applications, 1995. **31**(5): p. 1197-205.

29. Koval, D.O., *Zone-branch reliability methodology for analyzing industrial power systems.* IEEE Transactions on Industry Applications, 2000. **36**(5): p. 1212-18.

30. Dong, Z., D.O. Koval, and J.E. Propst, *Reliability of various industrial substations.* IEEE Transactions on Industry Applications, 2004. **40**(4): p. 989-994.

31. Propst, J.E. and D.R. Doan, *Improvements in modeling and evaluation of electrical power system reliability.* IEEE Transactions on Industry Applications, 2001. **37**(5): p. 1413-22.

32. da Silva, A.M.L., et al. *Chronological Monte Carlo-based assessment of distribution system reliability*. in *x*. 2006. Piscataway, NJ, USA: IEEE.

33. Billinton, R. and W. Wangdee, *Predicting bulk electricity system reliability performance indices using sequential Monte Carlo simulation.* IEEE Transactions on Power Delivery, 2006. **21**(2): p. 909-17.

34. Endrenyi, J., *Reliability Modeling in Electric Power Systems*. 1978, New York: John Wiley & Sons.

35. Mukerji, R., et al., *Power plant maintenance scheduling: Optimizing economics and reliability.* IEEE Transactions on Power Systems, 1991. **6**(2): p. 476-483.

36. Chen, L. and J. Toyoda, *Optimal generating unit maintenance scheduling for multi-area system with network constraints.* IEEE Transactions on Power Systems, 1991. **6**(3): p. 1168-74.

37. Kralj, B.L. and R. Petrovic, *Optimal preventive maintenance scheduling of thermal generating units in power systems-a survey of problem formulations and solution methods.* European Journal of Operational Research, 1988. **35**(1): p. 1-15.

38. Chin-Tai, C., C. Yi-Wen, and J. Yuan, *On a dynamic preventive maintenance policy for a system under inspection.* Reliability Engineering & System Safety, 2003. **80**(1): p. 41-7.

39. El-Sheikhi, F.A. and R. Billinton. *GENERATING UNIT MAINTENANCE SCHEDULING FOR SINGLE AND TWO INTERCONNECTED SYSTEMS*. 1983. Los Angeles, CA, USA: IEEE.

40. Contaxis, G.C., S.D. Kavatza, and C.D. Vournas, *An interactive package for risk evaluation and maintenance scheduling.* IEEE Transactions on Power Systems, 1989. **4**(2): p. 389-95.

41. Srinivasan, D., et al. *Survey of applications of evolutionary computing to power systems*. 1996. Orlando, FL, USA: IEEE.

42. Goldberg, D.E., *Genetic algorithms in search, optimization, and machine learning* 1989: Reading, Mass. : Addison-Wesley Pub. Co. 412.

43. Herrera, F., *Genetic algorithms and soft computing*, ed. J.L. Verdegay. 1996, Heidelberg Physica-Verlag. 709.

44. Ei-Sharkh, M.Y. and A.A. El-Keib, *An evolutionary programming-based solution methodology for power generation and transmission maintenance scheduling.* Electric Power Systems Research, 2003. **65**(1): p. 35-40.

45. Dahal, K.P., et al. *GA/SA-based hybrid techniques for the scheduling of generator maintenance in power systems*. 2000. Piscataway, NJ, USA: IEEE.

46. Dahal, K.P. and N. Chakpitak, *Generator maintenance scheduling in power systems using metaheuristic-based hybrid approaches.* Electric Power Systems Research, 2007. **77**(7): p. 771-779.

47. Kim, H., Y. Hayashi, and K. Nara. *The performance of hybridized algorithm of GA SA and TS for thermal unit maintenance scheduling*. 1995. New York, NY, USA: IEEE.

48. Kleeman, M.P. and G.B. Lamont. *Solving the aircraft engine maintenance scheduling problem using a multi-objective evolutionary algorithm*. 2005. Berlin, Germany: Springer-Verlag.

49. Tan, K.C., T.H. Lee, and E.F. Khor. *Evolutionary algorithms with goal and priority information for multi-objective optimization*. 1999. Piscataway, NJ, USA: IEEE.

50. Fonseca, C.M. and P.J. Fleming. *Genetic algorithm for multi-objective optimization, formulation, discussion and generalization*. in *the Fifth Int. Conf. Genetic Algorithms*. 1993. San Mateo, CA: Morgan Kaufmann.

51. Deb, N.S.a.K., *Multiobjective function optimization using nondominated sorting genetic algorithms.* Evolutionary Computation, 1995. **2**(3): p. 221-248.

52. Deb, K., et al., *A fast and elitist multiobjective genetic algorithm: NSGA-II.* IEEE Transactions on Evolutionary Computation, 2002. **6**(2): p. 182-97.

53. E. Zitzler, M.L.a.L.T., *SPEA2: Improving the Strength Pareto Evolutionary Algorithm*. Evolutionary Methods for Design, Optimization and Control with Applications to Industrial Problems, ed. D.T. K. Giannakoglou, J. Periaux, P. Papailou and T. Fogarty. 2001, Athens, Greece.

54. Coello, C.A.C., *A comprehensive survey of evolutionary-based multiobjective optimization techniques.* Knowledge and Information Systems, 1999. **1**(3): p. 269-308.

55. Allan, R.N. and M.G. Da Silva, *Evaluation of reliability indices and outage costs in distribution systems.* IEEE Transactions on Power Systems, 1995. **10**(1): p. 413-19.

56. Kjolle, G. and K. Sand, *RELRAD-an analytical approach for distribution system reliability assessment.* IEEE Transactions on Power Delivery, 1992. **7**(2): p. 809-14.

57. Brown, R.E., et al., *Automated primary distribution system design: reliability and cost optimization.* IEEE Transactions on Power Delivery, 1997. **12**(2): p. 1017-22.

58. Mohanta, D.K., P.K. Sadhu, and R. Chakrabarti, *Fuzzy Markov model for determination of fuzzy state probabilities of generating units including the effect of maintenance scheduling.* IEEE Transactions on Power Systems, 2005. **20**(4): p. 2117-2124.

59. L.A.Zadeh, *Fuzzy sets.* Information and Control, 1965. **8**: p. 338-353.

60. Mendel, J.M., *Uncertain Rule-Based Fuzzy Logic Systems: Introduction and New Directions*. 2001: Upper Saddle River, NJ: Prentice-Hall.

61. Lang, B.P. and A. Pahwa, *Power distribution system reliability planning using a fuzzy knowledge-based approach.* IEEE Transactions on Power Delivery, 2000. **15**(1): p. 279-84.

62. Dusmanta Kumar, M., S. Pradip Kumar, and R. Chakrabarti, *Fuzzy reliability evaluation of captive power plant maintenance scheduling incorporating uncertain forced outage rate.* Electric Power Systems Research, 2004. **72**(1): p. 73-84.

63. Mendel, J.M., *Fuzzy logic systems for engineering: a tutorial.* Proceedings of the IEEE, 1995. **83**(3): p. 345-377.

64. Ling, J.-M., C.-E. Lin, and C.-L. Huang, *Probability measure of adequacy assessment using a fuzzy approach.* Electric Power Systems Research, 1995. **33**(1): p. 7-15.

65. Bai, X. and S. Asgarpoor, *Fuzzy-based approaches to substation reliability evaluation.* Electric Power Systems Research, 2004. **69**(2-3): p. 197-204.

66. El-Sayed, M.A.H., T. Seitz, and A. Montebaur. *Fuzzy sets for reliability assessment of electric power distribution systems*. 1994. Lafayette, LA, USA: IEEE.

67. Tomsovic, K., M. Tapper, and T. Ingvarsson, *A fuzzy information approach to integrating different transformer diagnostic methods.* IEEE Transactions on Power Delivery, 1993. **8**(3): p. 1638-46.

68. Tanrioven, M., et al., *A new approach to real-time reliability analysis of transmission system using fuzzy Markov model.* International Journal of Electrical Power & Energy Systems, 2004. **26**(10): p. 821-32.

69. Zadeh, L.A., *The concept of a linguistic variable and its application to approximate reasoning. I.* Information Sciences, 1975. **8**(3): p. 199-249.

70. Tan, W.W. and W. Dongrui, *Genetic learning and performance evaluation of interval type-2 fuzzy logic controllers.* Engineering Applications of Artificial Intelligence, 2006. **19**(8): p. 829-41.

71. Mendel, J.M., R.I. John, and F. Liu, *Interval type-2 fuzzy logic systems made simple.* IEEE Transactions on Fuzzy Systems, 2006. **14**(6): p. 808-21.

72. Mendel, J.M. and D. Wu, *Perceptual reasoning for perceptual computing.* IEEE Transactions on Fuzzy Systems, 2008. **16**(6): p. 1550-1564.

73. Lin, T.Y. and S. Tsumoto. *Qualitative fuzzy sets and granularity*. 2008. Piscataway, NJ, USA: IEEE.

74. Garibaldi, J.M., M. Jaroszewski, and S. Musikasuwan, *Nonstationary fuzzy sets.* IEEE Transactions on Fuzzy Systems, 2008. **16**(4): p. 1072-86.

75. Kanagaraj, N., P. Sivashanmugam, and S. Paramasivam, *A fuzzy logic based supervisory hierarchical control scheme for real time pressure control.* International Journal of Automation and Computing, 2009. **6**(1): p. 88-96.

76. Chopade, P. and M. Bikdash. *Minimizing cost and power loss by optimal placement of capacitor using ETAP*. Auburn, AL, United states: Institute of Electrical and Electronics Engineers Inc.

77. Okuyama, K., et al. *Improvement of reliability of power distribution system by information exchange between dispersed generators*. 2001. Piscataway, NJ, USA: IEEE.

78. Holland, J.H., *Adaptation in natural and artificial systems : an introductory analysis with applications to biology, control, and artificial intelligence*. 1975, Ann Arbor: University of Michigan Press. 183.

79. Abido, M.A., *Multiobjective evolutionary algorithms for electric power dispatch problem.* IEEE Transactions on Evolutionary Computation, 2006. **10**(3): p. 315-329.

80. Fonseca, C.M. and P.J. Fleming, *An overview of evolutionary algorithms in multiobjective optimization.* Evolutionary Computation, 1995. **3**(1): p. 1-16.

81. Abbass, H.A. and R. Sarker, *The Pareto differential evolution algorithm.* International Journal on Artificial Intelligence Tools (Architectures, Languages, Algorithms), 2002. **11**(4): p. 531-52.

82. Xue, F., A.C. Sanderson, and R.J. Graves. *Multi-objective differential evolution and its application to enterprise planning*. 2003. Taipei, Taiwan: Institute of Electrical and Electronics Engineers Inc.

83. Iorio, A.W. and L. Xiaodong. *Solving rotated multi-objective optimization problems using differential evolution*. 2004. Berlin, Germany: Springer-Verlag.

84. Goldberg, D.E. and J. Richardson. *Genetic algorithms with sharing for multimodal function optimization*. 1987. Hillsdale, NJ, USA: Lawrence Erlbaum Associates.

85. Fonseca, C.M. and P.J. Fleming. *Multiobjective genetic algorithms made easy: selection sharing and mating restriction*. 1995. London, UK: IEE.

86. Storn, R. and K. Price, *Diffierential Evolution -A simple and efficient adaptive scheme for global optimization over continuous spaces*. 1995.

87. Zhou, R.C., *Inspection Frequency Optimization and Partial Discharge Monitoring for Condition Based Maintenance OF Substations*, in *Computer & Electrical Engineering Department*. 2005, National University of Singapore: Singapore.

88. Ramakumar, R., *Engineering reliability: fundamentals and applications*. 1993, London: Prentice-Hall International.

89. Brcsok, J., E. Uguesa, and D. Machmur. *Calculation of MTTF values with Markov models for safety instrumented systems*. 2007. Athens, Greece: WSEAS.

90. Papoulis, A. and S.U. Pillai, *Probability, random variables, and stochastic processes*. 2002: McGraw-Hill, Dubuque, Iowa.

91. Fonseca, C.M., *Multiobjective Genetic Algorithms with Application to Control Engineering Problems*, in *Dept. of Automatic Control and Systems Engineering*. 1995, University of Sheffield: UK.

92. Tan, K.C., et al. *MOEA toolbox for computer aided multi-objective optimization*. in *Evolutionary Computation, 2000. Proceedings of the 2000 Congress on*. 2000.

93. Abaza, K.A., S.A. Ashur, and I.A. Al-Khatib, *Integrated pavement management system with a Markovian prediction model.* Journal of Transportation Engineering, 2004. **130**(1): p. 24-33.

94. Morcous, G. and Z. Lounis, *Maintenance optimization of infrastructure networks using genetic algorithms.* Automation in Construction, 2005. **14**(1): p. 129-42.

95. Billinton, R., et al., *A reliability test system for educational purposes-basic results.* IEEE Transactions on Power Systems, 1990. **5**(1): p. 319-25.

96. Herrera, F., M. Lozano, and J.L. Verdegay, *Tackling real-coded genetic algorithms: operators and tools for behavioural analysis.* Artificial Intelligence Review, 1998. **12**(4): p. 265-319.

97. Chen, S.K., T.K. Ho, and B.H. Mao, *Reliability evaluations of railway power supplies by fault-tree analysis.* IET Electric Power Applications, 2007. **1**(2): p. 161-72.

98. Grigg, C., et al., *The IEEE Reliability Test System-1996. A report prepared by the Reliability Test System Task Force of the Application of Probability Methods Subcommittee.* IEEE Transactions on Power Systems, 1999. **14**(3): p. 1010-20.

99. Wenyuan, L., L. Jiping, and Y. Wei, *State enumeration technique combined with a labeling bus set approach for reliability evaluation of substation configuration in power systems.* Electric Power Systems Research, 2007. **77**(5-6): p. 401-6.

100. Yang, F. and C.S. Chang, *Multi-objective Evolutionary Optimization of Maintenance Schedules and Extents for Composite Power Systems.* IEEE Transactions on Power Systems, 2009.

101. Zhu, j., *Optimization of Power System Operation*. 2009: Wiley-IEEE Press. 603.

102. Nighot, R.U., *Incorporating Substation and Switching Station Related Outages in Composite System Reliability Evaluation*, in *Dept. Elect. Engi.* 2003, Univ. Saskatchewan: Saskatoon, Saskatchewan, Canada.

103. Elsayed, E.A., L. Haitao, and C. Ling-Yau, *Maintenance of continuously monitored degrading systems.* European Journal of Operational Research, 2006. **175**(2): p. 821-35.

104. Lu, S., T. Yu-Chen, and H. Lu, *Predictive condition-based maintenance for continuously deteriorating systems.* Quality and Reliability Engineering International, 2007. **23**(1): p. 71-81.

105. Cassady, C.R., et al., *A generic model of equipment availability under imperfect maintenance.* IEEE Transactions on Reliability, 2005. **54**(4): p. 564-571.

106. Ming-Yi, Y., et al., *Cost-Effective Updated Sequential Predictive Maintenance Policy for Continuously Monitored Degrading Systems.* IEEE Transactions on Automation Science and Engineering. **7**(2): p. 257-65.

107. Grall, A., et al., *Continuous-time predictive-maintenance scheduling for a deteriorating system.* IEEE Transactions on Reliability, 2002. **51**(2): p. 141-50.

108. Zhao-xia, W., et al. *Adaptive type-2 fuzzy maintenance advisor for offshore power systems*. in *Systems, Man and Cybernetics, 2009. SMC 2009. IEEE International Conference on*. 2009.

109. Lee, H.M. and C.S. Chang*, Application of Dempster-Shafer's Theory of Evidence for Transformer Incipient Fault Diagnosis,* in *The 8th International Conference on Advances in Power System Control, Operation and Management.* 2009: Hong Kong.

110. Mijailovic, V., *Probabilistic method for planning of maintenance activities of substation components.* Electric Power Systems Research, 2003. **64**(1): p. 53-58.

111. Rong-Ceng, L. *A new method for unit maintenance scheduling based on genetic algorithm*. 2003. Piscataway, NJ, USA: IEEE.

112. Horikawa, S.i., T. Furuhashi, and Y. Uchikawa, *On fuzzy modeling using fuzzy neural networks with the back-propagation algorithm.* IEEE Transactions on Neural Networks, 1992. **3**(5): p. 801-6.

113. Wang, L.X. and J.M. Mendel. *Generating fuzzy rules by learning from examples*. 1991. New York, NY, USA: IEEE.

114. Wang, L.X. and J.M. Mendel. *Back-propagation fuzzy system as nonlinear dynamic system identifiers*. 1992. New York, NY, USA: IEEE.

115. Siler, W. and J.J. Buckley, *Fuzzy expert systems and fuzzy reasoning*. 2005, NJ: Wiley, Hoboken.

APPENDIX A FUZZY LOGIC SYSTEM

Fuzzy Set theory provides a means for representing uncertainties in the real world by resembling the process of human reasoning. It deals with uncertainty by attaching levels of possibility to a number of uncertain categories. Based on that, a fuzzy logic can be synthesized. A fuzzy logic system is a nonlinear mapping of a crisp input vector into a crisp output scalar. Its uniqueness is that it able to simultaneously deal with objective data and subjective knowledge. It has been used with great success in dealing with uncertainty in engineering. This Appendix provides the basic theories for synthesizing a fuzzy logic system.

A.1 Fuzzy sets

A fuzzy set F is defined on a universe of discourse U and it is characterized by a membership function $\mu_F(x)$ (Fig. A.1) which takes on values in the interval. The fuzzy sets overlap with each other and the membership functions provides a measure of the degree of similarity of an element in U to each fuzzy set.

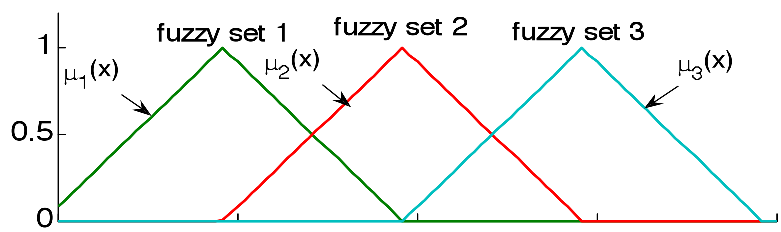

Fig. A.1 Fuzzy Sets

The membership functions can be chosen based on the users' experience or designed by optimization procedures [112-114]. The number of membership functions is up to the designer. Greater resolution is achieved by using more membership functions at the cost of higher computational complexity. The most commonly used shapes of membership functions are triangular, trapezoidal, and Gaussian.

A.2 Fuzzy rules of inference

A fuzzy rule base consists of a collection of IF-THEN rules, which can be expressed as:

$$R^l: \text{ IF } x_1 \text{ is } \mathrm{F}_1^l \text{ and } x_2 \text{ is } \mathrm{F}_2^l \text{ and } \cdots x_p \text{ is } \mathrm{F}_p^l, \text{ THEN } y \text{ is } \mathrm{G}^l.$$

where $l = 1, 2, \ldots, M$, F_i^l and G_i^l are fuzzy sets in X_i and Y_i, respectively. x and y are linguistic variables. The premise of each rule uses the degree of each variable in the relevant fuzzy sets, and the conclusion assigns a membership function to each output. Rules can be provided by experts or can be extracted from numerical data.

A.3 Fuzzy logic system

A fuzzy logic system contains four steps: fuzzifier, rules, inference engine and defuzzifier, as shown in Fig. A. 2. Each of the steps is described in the following sections.

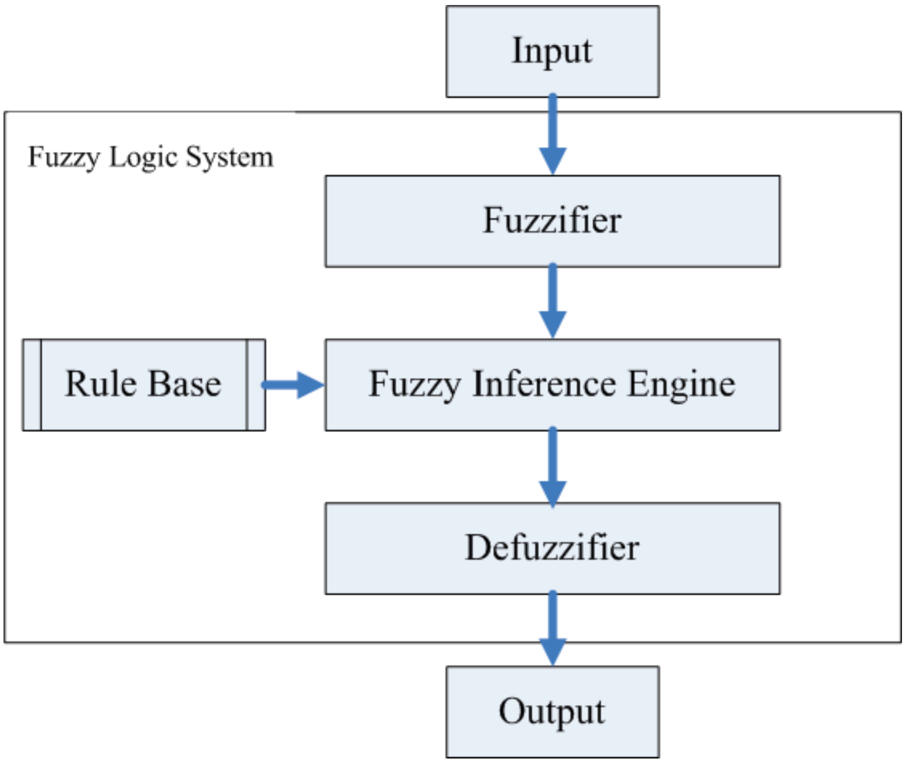

Fig. A. 2 Structure of Fuzzy Logic System

A.3.1 Fuzzifier

This step is to convert the crisp input variable into a set of fuzzy variables by giving the degree to which the input belongs to a linguistic class. For example, a fuzzifier splits the input *x* into three fuzzy levels. Trianglar membership functions are used in this example in Fig. A.3. Suppose the input *x*=12.5, the degree it belongs to the set of "young" is 0.9, and to the set of "mid-age" is 0.1.

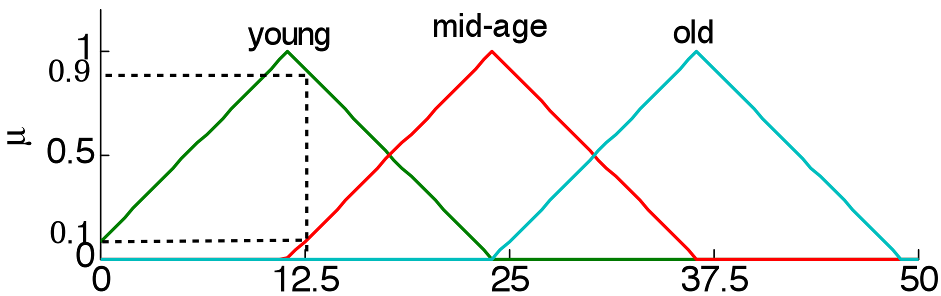

Fig. A. 3 Sample Membership Functions for Input *x*

A.3.2 Inference

The fuzzy inference is to compute the true value for the premise of each rule, namely aggregation, and then apply it to the conclusion part of the rule, namely composition.

1) Aggregation

The true value of the premise of each rule is computed in the aggregation and a fuzzy set is assigned to each output variable. For example, given the two rules as below:

R^1: IF x_1 is *young* and x_2 is *fine weather*, THEN y is *good*.

R^2: IF x_1 is *young* and x_2 is *bad weather*, THEN y is *normal*.

The degree of membership of each input to the respective fuzzy set is calculated as:

$$\begin{aligned} &\mu_{young}(x_1) = 0.6, \\ &\mu_{fine\,weather}(x_2) = 0.3, \\ &\mu_{bad\,weather}(x_2) = 0.8 \end{aligned} \tag{A.1}$$

Hence, the true value of each rule is calculated based on the *min* operator:

$$\begin{aligned} \alpha_1 &= \mu_{young}(x_1) \wedge \mu_{fine\,weather}(x_2) = \min(0.6, 0.3) = 0.3 \\ \alpha_2 &= \mu_{young}(x_1) \wedge \mu_{bad\,weather}(x_2) = \min(0.6, 0.8) = 0.6 \end{aligned} \tag{A.2}$$

Fig. A. 4 gives an example to show how the membership function of each output is determined with triangular membership function.

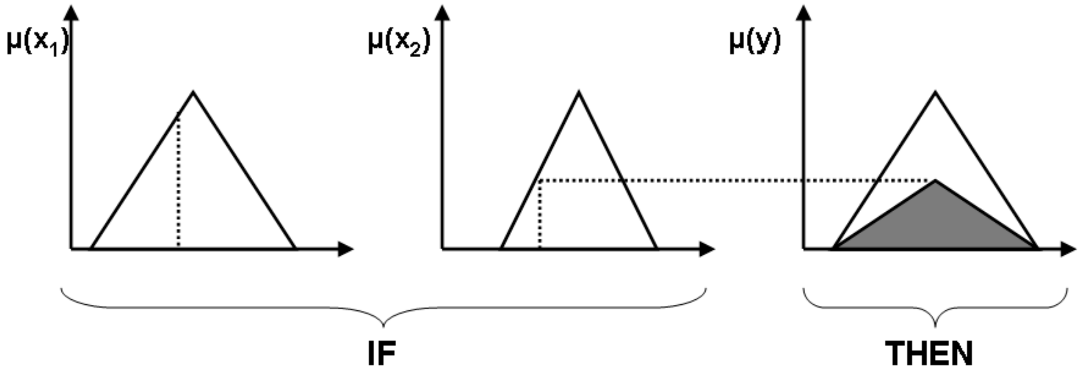

Fig. A.4 Example of Inference Process with Triangular Membership Function

2) Composition

All the fuzzy sets assigned to each output are combined together to form a single fuzzy set. Two operators, *max* and *sum*, are most commonly used in this step. Using the same example as above, in max composition, the combined fuzzy set is formed by taking the pointwise maximum over all of the fuzzy sets for that output variable:

$$\mu(y) = \mu_{good}(y) \vee \mu_{normal}(y) = \max(\mu_{good}(y), \mu_{normal}(y)) \qquad \text{(A.3)}$$

While in sum operation, the combined fuzzy set for each output is constructed by taking pointwise sum over all of the fuzzy sets.

A.3.3 Defuzzifier

This step is to convert the fuzzy linguistic variables to crisp output value. Among many defuzzification methods, Center-of-Area (COA) and Center-of-Maximum (COM) are the mostly common techniques [115]. The COA gives the crisp output value by calculating the center of the area covered by the membership function of that fuzzy rule:

$$Z_{output} = \frac{\sum_{i=1}^{m} \mu_G(z_i) * z_i}{\sum_{i=1}^{m} \mu_G(z_i)} \tag{A.4}$$

where m is the number of segments the universe of discourse is divided into of the output, z_i is the value of the variable at segment *i*, and $\mu_G(z_i)$ represents its membership value in *G*.

The COM is a simplified version of COA. If using COM, only the variable values at which the fuzzy sets have their maximum truth values are chosen to compute the output:

$$Z_{output} = \frac{\sum_{i=1}^{n} z_i}{n} \tag{A.5}$$

where *n* is the number of Z values which have the maximum membership.

APPENDIX B DATA OF SUBSTATIONS

Table B.1 shows the assumed average load demand at each load point

Table B.1 Load at Each Load Point

Configuration	Load point NO.	Load MW
1	1	120
2	1	120
3	1	60
	2	60
4	1	60
	2	60

APPENDIX C DATA OF STUDIED RBTS

Table C.1 Bus Load Data of RBTS

Bus #	Load MW	Bus Load % of System Load
2	30.0	10.81
3	120.0	45.95
4	60.0	21.62
5	30.0	10.81
6	30.0	10.81
	Total 270.0	100.0

Table C.2 Cost Parameters ($\$10^5$)

		Circuit Breaker	Transformer
Inspection		0.001	0.002
Minor Maintenance	D_1	0.008	0.012
	D_2	0.012	0.015
	D_3	0.015	0.02
Major Maintenance	D_1	0.03	0.04
	D_2	0.042	0.055
	D_3	0.06	0.07
Failure		0.4	0.28

APPENDIX D DATA OF STUDIED IEEE RTS

Table D.1 Bus Data of IEEE RTS

Bus #	Bus Type	MW Load	MVAR Load	GL	BL	Sub Area	Base Kv	Zone #
01	2	108	22	0	0	1	138	1
02	2	97	20	0	0	1	138	2
03	1	180	37	0	0	1	138	1
04	1	74	15	0	0	1	138	1
05	1	71	14	0	0	1	138	1
06	1	136	28	0	1.0	1	138	2
07	2	125	25	0	0	1	138	2
08	1	171	35	0	0	1	138	2
09	1	175	36	0	0	1	138	3
10	1	195	40	0	0	1	138	3
11	1	0	0	0	0	1	230	3
12	1	0	0	0	0	1	230	3
13	3	265	54	0	0	2	230	4
14	2	194	39	0	0	2	230	6
15	2	317	64	0	0	2	230	6
16	2	100	20	0	0	2	230	6
17	1	0	0	0	0	2	230	7
18	2	333	68	0	0	2	230	7

19	1	181	37	0	0	2	230	5
20	1	128	26	0	0	2	230	5
21	2	0	0	0	0	2	230	7
22	2	0	0	0	0	2	230	7
23	2	0	0	0	0	2	230	5
24	1	0	0	0	0	2	230	6

Bus Type: 1 - Load Bus (no generation)

2 - Generation or Plant Bus

3 – Swing Bus

MW Load: load real power to be held constant

MVAR Load: load reactive power to be held constant

GL: real component of shunt admittance to ground

BL: imaginary component of shunt admittance to ground

Table D.2 Bus Load Data of IEEE RTS

Bus #	Bus Load	Load		If peak load 10% higher	
	% of System Load	MW	MVAR	MW	MVAR
01	3.8	108	22	118.8	24.2
02	3.4	97	20	106.7	22.0
03	6.3	180	37	198.0	40.7
04	2.6	74	15	81.4	16.5
05	2.5	71	14	78.1	15.4
06	4.8	136	28	149.6	30.8
07	4.4	125	25	137.5	27.5
08	6.0	171	35	188.1	38.5
09	6.1	175	36	192.5	39.6
10	6.8	195	40	214.5	44.0
13	9.3	265	54	291.5	59.4
14	6.8	194	39	213.4	42.9
15	11.1	317	64	348.7	70.4
16	3.5	100	20	110.0	22.0
18	11.7	333	68	366.3	74.8
19	6.4	181	37	199.1	40.7
20	4.5	128	26	140.8	28.6
	Total 100.0	2850	280	3135	638

Table D. 3 Data of Generations at each Bus

Bus #	Unit Type	ID #	PG MW	QG MVAR	Q^{max} MVAR	Q^{min} MVAR	Vs pu
01	U20	1	10	0	10	0	1.035
01	U20	2	10	0	10	0	1.035
01	U76	3	76	14.1	30	-25	1.035
01	U76	4	76	14.1	30	-25	1.035
02	U20	1	10	0	10	0	1.035
02	U20	2	10	0	10	0	1.035
02	U76	3	76	7.0	30	-25	1.035
02	U76	4	76	7.0	30	-25	1.035
07	U100	1	80	17.2	60	0	1.025
07	U100	2	80	17.2	60	0	1.025
07	U100	3	80	17.2	60	0	1.025
13	U197	1	95.1	40.7	80	0	1.020
13	U197	2	95.1	40.7	80	0	1.020
13	U197	3	95.1	40.7	80	0	1.020
14	Sync Cond	1	0	13.7	200	-50	0.980
15	U12	1	12	0	6	0	1.014
15	U12	2	12	0	6	0	1.014
15	U12	3	12	0	6	0	1.014

15	U12	4	12	0	6	0	1.014
15	U12	5	12	0	6	0	1.014
15	U155	6	155	0.05	80	-50	1.014
16	U155	1	155	25.22	80	-50	1.017
18	U400	1	140	137.4	200	-50	1.050

Table D.4 Branch Data

ID #	From Bus	To Bus	L miles	Perm λ_p	Perm Dur	Tran λ_t	R pu	X pu	B pu	Con MVA	LTE MVA	STE MVA	Tr pu
1	01	02	3	.24	16	0.0	0.003	0.014	0.461	175	193	200	0
2	01	03	55	.51	10	2.9	0.055	0.211	0.057	175	208	220	0
3	01	05	22	.33	10	1.2	0.022	0.085	0.023	175	208	220	0
4	02	04	33	.39	10	1.7	0.033	0.127	0.034	175	208	220	0
5	02	06	50	.48	10	2.6	0.050	0.192	0.052	175	208	220	0
6	03	09	31	.38	10	1.6	0.031	0.119	0.032	175	208	220	0
7	03	24	0	.02	768	0.0	0.002	0.084	0	400	510	600	1.015
8	04	09	27	.36	10	1.4	0.027	0.104	0.028	175	208	220	0
9	05	10	23	.34	10	1.2	0.023	0.088	0.024	175	208	220	0
10	06	10	16	.33	35	0.0	0.014	0.061	2.549	175	193	200	0
11	07	08	16	.30	10	0.8	0.016	0.061	0.017	175	208	220	0
12	08	09	43	.4	10	2.3	0.04	0.16	0.04	175	208	220	0

				4			3	5	5				
13	08	10	43	.4 4	10	2.3	0.04 3	0.16 5	0.04 5	175	208	600	0
14	09	11	0	.0 2	768	0.0	0.00 2	0.08 4	0	400	510	600	1.03
15	09	12	0	.0 2	768	0.0	0.00 2	0.08 4	0	400	510	600	1.03
16	10	11	0	.0 2	768	0.0	0.00 2	0.08 4	0	400	510	600	1.01 5
17	10	12	0	.0 2	768	0.0	0.00 2	0.08 4	0	400	510	625	1.01 5
18	11	13	33	.4 0	11	0.8	0.00 6	0.04 8	0.10 0	500	600	625	0
19	11	14	27	.3 9	11	0.7	0.00 5	0.04 2	0.08 8	500	600	625	0
20	12	13	33	.4 0	11	0.8	0.00 6	0.04 8	0.10 0	500	600	625	0
21	12	23	67	.5 2	11	1.6	0.01 2	0.09 7	0.20 3	500	600	625	0
22	13	23	60	.4 9	11	1.5	0.01 1	0.08 7	0.18 2	500	600	625	0
23	14	16	27	.3 8	11	0.7	0.00 5	0.05 9	0.08 2	500	600	625	0
24	15	16	12	.3 3	11	0.3	0.00 2	0.01 7	0.03 6	500	600	625	0

λ_p : permanent outage rate (outages/year)

Dur :	permanent outage duration (hours)
λ_t :	transient outage rate (outages/year)
Con:	continuous rating
LTE:	long-time emergency rating (24 hour)
STE:	short-time emergency rating (15 min)
Tr:	Transformer off-nominal ratio

Table D.5 Cost Parameters ($\$10^5$)

		Circuit Breaker	Bus Bar
Inspection		0.002	0.0018
Minor Maintenance	D_1	0.01	0.012
	D_2	0.015	0.022
	D_3	0.03	0.03
Major Maintenance	D_1	0.03	0.04
	D_2	0.042	0.055
	D_3	0.105	0.12
Failure		0.6	0.85